
UNIVERSITÀ DEGLI STUDI DI TRENTO
Dipartimento di Matematica

DOTTORATO DI RICERCA IN MATEMATICA
XVII CICLO

A thesis submitted for obtaining the degree of Doctor of Philosophy

Galena Georgieva Pelovska

Numerical Investigations
in the Field of
Age-Structured Population Dynamics



ADVISOR:
Prof. Mimmo Iannelli

MARCH 2007

I hear and I forget.

I see and I remember.

I do and I understand.

Ancient Proverb

Acknowledgments

First of all I would like to thank to my father, my sister and the small Cherry who unfortunately are not alive but I am sure they are with me and help me somehow! I thank to the rest of my family, to my great uncle, mum and grandma, to my only love Claude and to the small Duco! Thank you for supporting me in everything through all the long and difficult five years of my PhD studies! I am especially grateful to Any, Dani, Gloria, Maia Martcheva, Maria Lekka, Maria Spassova, Marian, Michela, Milen, Nelly, Vanya Kateva, Vanya Stoyanova, Sonia, Stefi and Zorry for being my real friends! I believe that your true friends are with you in bad and in good! Thank you for everything you have done for me! I also thank to my future mother and father in law, Anita and Norbert for doing their best during the last year!

I would like to thank to my advisor Mimmo Iannelli for leading me in the right direction and for giving me challenging problems to solve! I really do appreciate it! I am thankful to the members of the Commission of my PhD defence, namely Fabio Milner and Elvira Russo! I am proud and pleased for being examined by such famous, but at the same time very nice people! I also thank to the rest of the great group from Napoli, namely Antonella, Eleonora and Giuseppe for being my friends and collaborators! I hope I can see you again soon!

I love you all and I hope you are happy with me!

THANK YOU!

Contents

1	INTRODUCTION TO AGE-STRUCTURED POPULATION DYNAMICS	1
1.1	Linear Age-Structured Models	1
1.2	Nonlinear Age-Structured Models	6
1.3	Age-Structured Diffusion Models	11
1.4	Thesis Organization	13
2	NUMERICAL METHODS FOR THE LOTKA-MCKENDRICK'S EQUATION	17
2.1	Direct Methods (methods, proposed in the literature)	17
2.1.1	First Order Schemes	18
2.1.2	Higher Order Schemes	20
2.2	Methods for the Renewal Equation	21
2.2.1	Methods Based on the Use of Various Quadrature Rules	21
2.2.2	Runge-Kutta Methods	33
2.3	Methods for the Equation with the Age Profile	36
2.4	Test Examples	39
2.5	Numerical Results and Conclusions	44
3	NUMERICAL TREATMENT OF MODELS INCLUDING DIFFUSION AND AGE	51
3.1	Previous Work on the Topic and Connection with Parabolic Problems - STS Algorithm	51
3.2	Modified STS for Age-Structured Problems	55
3.3	Convergence of the Method	58
3.4	Performance on Test Problems	69
3.5	Comparison of Different Approaches	77
3.6	Final Remarks	78
4	HANDLING NONLINEAR AGE-DEPENDENT MODELS	79
4.1	State-of-the-Art of Numerical Methods for Gurtin-MacCamy's Model	80
4.2	Numerical Approximation of a Model of Logistic Growth	91

CONTENTS

4.3	Numerical Approximation of a Model of Cannibalism	107
5	FUTURE RESEARCH	113
	Bibliography	114

CHAPTER 1

INTRODUCTION TO AGE-STRUCTURED POPULATION DYNAMICS

1.1. Linear Age-Structured Models

Populations are made up of individuals whose life cycles, consisting of different states of development, can be described by some significant variables as age, size, sex, etc. Thus, different groups of individuals who have experienced a particular event during the same period of time (cohorts) can be differentiated. This means that when modeling a population it is very important to consider these variables, since the interactions between the different cohorts depend on them as well as on the population structure.

Age is one of the most natural parameters inherent to the living creatures, including humans, and thus many of them have populations structured with respect to age. Evolutionary biologists have been intrigued by the question how natural selection and other evolutionary forces form the way in which fertility and survivorship change with age. Nowadays, age plays a crucial role in fields like demography, ecology, epidemiology, etc.

In the first models of population dynamics all the individuals belonging to a certain population are assumed to be identical. The simplest such model is inspired by the work of Malthus [75] published in 1798. In this model a population is subject to constant **fertility and mortality rates**, β and μ respectively:

$$\begin{cases} \frac{dP(t)}{dt} = (\beta - \mu)P(t) = \alpha P(t) \\ P(0) = P_0 \geq 0 \end{cases}$$

where $P(t)$ is the **total population** at time t and α is the Malthusian parameter that determines the growth of the population. The analytical solution of this model

$$P(t) = P_0 e^{\alpha t}$$

tends to $+\infty$ when $t \rightarrow +\infty$ if $\alpha > 0$. Consequently, the model turns to be unrealistic since we have an exponential growth that is a very rare phenomenon in nature for an infinite time. But even though the model is oversimplified, it gives us a fundamental point in population modeling: *the population growth mechanism is based on the vital rates, namely fertility and mortality, which have to be considered as the most significant terms responsible for the population dynamics.*

Later on, the need of more refined assumptions on the vital rates leads to a model in which the vital rates depend on the age variable. This model is first given by Sharpe and Lotka in [91]. It is an integral formulation of the model, known as Lotka-McKendrick's equation. Lotka-McKendrick's model is analogous to the Malthus' model, i.e. a single population, living isolated is considered. All individuals have no sex, neither size differences, however they are structured by age and the fertility and the mortality functions depend on age as well. Namely, denoting by $p(a, t)$ the **age density** of the population (where $a \in [0, a_+]$, $t \geq 0$ and a_+ is the **maximum age**), we have the following system:

Lotka-McKendrick's equation

$$\begin{cases} \frac{\partial p(a, t)}{\partial t} + \frac{\partial p(a, t)}{\partial a} + \mu(a)p(a, t) = 0, & a \in [0, a_+], t > 0 \\ p(0, t) = \int_0^{a_+} \beta(a)p(a, t) da = B(t), & t > 0 \\ p(a, 0) = p_0(a), & a > 0 \end{cases} \quad (1.1.1)$$

where $B(t) = \int_0^{a_+} \beta(a)p(a, t)da$ is the **total birth rate** (the total number of newborns in one time unit).

This is a well studied model that has been discussed in many works (see for instance [32, 44, 70, 71, 72, 73, 77]). In order to allow the mathematical treatment of (1.1.1) and to deal with a biologically significant case, we need to specify some conditions and particularly we note that we want the maximum age a_+ to be finite since there are no species with infinite life span (i.e. $a \in [0, a_+]$, where $a_+ < +\infty$) and we require that the **survival probability**

$$\pi(a) = e^{-\int_0^a \mu(\tau)d\tau} \quad (1.1.2)$$

vanishes at a_+ . Then we assume:

- $\beta(\cdot)$ is non-negative and belongs to $L^\infty(0, a_+)$;
- $\mu(\cdot)$ is non-negative and belongs to $L^1_{loc}(0, a_+)$;

- $\int_0^{a_+} \mu(\tau) d\tau = +\infty$ (in order survival probability to vanish at a_+);
- $p_0 \in L^1(0, a_+)$, $p_0(a) \geq 0$ a.e. in $[0, a_+]$

If we integrate the governing equation in (1.1.1) along the characteristic lines $a = t + c$, we obtain:

$$p(a, t) = \begin{cases} p_0(a-t) \frac{\pi(a)}{\pi(a-t)}, & a \geq t \\ B(t-a)\pi(a), & a < t \end{cases} \quad (1.1.3)$$

One can immediately see the connection between $p(a, t)$ and $B(t)$. Namely, since the initial value $p_0(a)$ of $p(a, t)$ and the survival probability $\pi(a)$ are known functions, we can easily obtain the solution of the upper model if we know the total birth rate $B(t)$. We have to note the fact that even if the initial age distribution p_0 is continuous, $p(a, t)$ may not be, if the following condition is not satisfied:

$$p_0(0) = \int_0^{a_+} \beta(\sigma) p_0(\sigma) d\sigma \quad (1.1.4)$$

Moreover we have to add another compatibility condition for the differentiability of $p(a, t)$ along the characteristics (see [48]), namely:

$$p'_0(0) + \mu(0)p_0(0) = \int_0^{a_+} \beta(a)[p'_0(a) + \mu(a)p_0(a)]da \quad (1.1.5)$$

Formula (1.1.3) allows us to derive an equation on the birth rate. Actually, using the boundary condition in (1.1.1) and then combining it with (1.1.3), it can be shown (see [44]) that our initial-boundary value problem is equivalent to the following Volterra integral equation of second kind on $B(t)$. Since it shows how a population is renewed when bringing into it the newborn it is called the Renewal equation (or Lotka equation):

Renewal equation

$$B(t) = \begin{cases} F(t) + \int_0^t K(t-a)B(a) da, & t \leq a_+ \\ \int_{t-a_+}^t K(t-a)B(a) da, & t > a_+, \end{cases} \quad (1.1.6)$$

where $F(t)$ and $K(a)$ are given, nonnegative functions:

$$\begin{aligned} K(a) &= \beta(a)\pi(a) \\ F(t) &= \int_t^{a_+} \beta(a)p_0(a-t) \frac{\pi(a)}{\pi(a-t)} da \quad (F(t) = 0 \text{ for } t \geq a_+) \end{aligned}$$

The function K is called **maternity function** and it synthesizes the dynamics of the population, namely it gives the mean number of offspring that are alive. In fact, it is related to the parameter

$$R_0 = \int_0^{a+} \beta(a)\pi(a)da,$$

the so called **net reproduction ratio**, which shows the number of the offspring that an individual is expected to produce during his reproductive period. It is clear from the physical interpretation of R_0 that if $R_0 > 1$ the population is increasing (i.e. more people are being born than are dying), if $R_0 < 1$ the population is decreasing and if $R_0 = 1$ the population is stationary.

The main reason to study the problem in such a way is that many analytical properties of Lotka-McKendrick's model can be investigated via the Renewal equation (1.1.6). In fact, it can be proved that the solution of the renewal equation has the following asymptotic behavior (see for instance [44], [94]):

$$B(t) = b_0 e^{\alpha^* t} (1 + O(t)), \quad (1.1.7)$$

where $b_0 \geq 0$, $\lim_{t \rightarrow \infty} O(t) = 0$ and α^* is the (unique real) solution of the characteristic equation

$$\hat{K}(\lambda) = 1 \quad (1.1.8)$$

Thus, the Lotka characteristic equation (1.1.8) and α^* - the intrinsic Malthusian parameter (already discussed above) determine the growth of the population through the birth rate $B(t)$. They are related to the net reproduction ratio by the following equivalence:

$$\begin{aligned} R_0 > 1 & \quad \text{iff} \quad \alpha^* > 0 \\ R_0 = 1 & \quad \text{iff} \quad \alpha^* = 0 \\ R_0 < 1 & \quad \text{iff} \quad \alpha^* < 0 \end{aligned}$$

A derivation of the age-dependent models described above by using both - matrix algebra and difference equations can be found in [23]. Very interesting examples of constant age-structured populations (populations, whose total size remains constant in time) are presented in [83]. In the same paper sufficient conditions for the birth function to be constant are given and the asymptotic stability of the equilibrium distribution is demonstrated. It is proved that for large times, any distribution of constant size and finite life span tends to the steady state distribution corresponding to its death rate.

Let us now introduce the following variables:

$$\begin{cases} 1) w(a, t) = \frac{p(a, t)}{P(t)} & \text{(age profile)} \\ 2) P(t) = \int_0^{a+} p(a, t) da & \text{(total population)} \end{cases} \quad (1.1.9)$$

These two variables: the age profile which shows how the population is distributed through different ages and the total population, are very important when describing the evolution of the population. By the definition of $w(a, t)$ and $P(t)$ itself, and by differentiating the expression $p(a, t) = w(a, t)P(t)$ and then substituting it in the model (1.1.1) we get the following sets of equations:

Age profile

$$\begin{cases} w_t(a, t) + w_a(a, t) + \mu(a)w(a, t) + w(a, t)\alpha(t) = 0 \\ w(0, t) = \int_0^{a_+} \beta(a)w(a, t)da \\ \int_0^{a_+} w(a, t)da = 1 \\ w(a, 0) = w_0(a) \end{cases} \quad (1.1.10)$$

$$\begin{cases} \frac{d}{dt}P(t) = \alpha(t)P(t) \\ P(0) = P_0 \end{cases} \quad (1.1.11)$$

where:

$$w_0(a) = \frac{p_0(a)}{\int_0^{a_+} p_0(\tau)d\tau}, \quad P_0 = \int_0^{a_+} p_0(\tau)d\tau \quad (1.1.12)$$

and

$$\alpha(t) = \int_0^{a_+} [\beta(\tau) - \mu(\tau)]w(\tau, t)d\tau \quad (1.1.13)$$

where $w_0(a)$ is the initial age profile and $\alpha(t)$ can be treated as the transient Malthusian parameter. One can find the solution $w(a, t)$ of (1.1.10) and $P(t)$ of (1.1.11), then multiply them obtaining $p(a, t)$, i.e. the solution of Lotka McKendrick's equation.

In the models presented above it is assumed that the fertility and the mortality functions depend only on age. Various extensions are known today - for example time dependent vital rates. In fact, improvement of the living conditions and advancement of medical science and technology have led to decreasing the death rate and increasing the expectation of life. Models with vital rates depending on age and time are investigated thoroughly by Inaba [43] and Iannelli [44]. Models, involving migration have also been considered in [44]. Another extension is assuming a population with two sexes. This is a long-standing problem in demography that leads to a theory much more elaborated than the theory for one-sex populations. Such models can be found for example in [33], [46], [47].

1.2. Nonlinear Age-Structured Models

The Lotka McKendrick's model (known also as McKendrick-von Foerster model since von Foerster renewed the interest in it in 1959) is said to be an age-structured version of the Malthus' model. Thus, the main drawback of the latter, namely the exponential growth of the population is a blemish also of the former, unless we follow the growth of the population for a limited time until the assumptions that we have made are satisfied. Hence, we have to consider a nonlinear model, where the exponential growth is replaced by logistic growth or some intra-specific mechanisms such as cannibalism and competition are considered, so we obtain some specific cases.

A general nonlinear model

We assume fertility and mortality depend on a set of N significant variables (**sizes**) which represent different ways of weighing the age distribution

$$\begin{cases} \frac{\partial p}{\partial t} + \frac{\partial p}{\partial a} + \mu(a, S_1(t), \dots, S_N(t))p(a, t) = 0, & a \in [0, a_+], t > 0 \\ p(0, t) = \int_0^{a_+} \beta(a, S_1(t), \dots, S_N(t))p(a, t) da = B(t), & t > 0 \\ p(a, 0) = p_0(a), & a > 0 \\ S_i(t) = \int_0^{a_+} \gamma_i(a)p(a, t)da, & i = 1, \dots, N, \end{cases} \quad (1.2.1)$$

where for $i=1$ and $\gamma(a) = 1$ this is exactly the Gurtin-MacCamy's model introduced in [37]. The reader is referred to [94] for an extensive study on existence and uniqueness of the solution of this specific case and some other analytical results (properties of the steady state) based on a semi-group approach. The relation between the birth and death rates in case of Gurtin-MacCamy populations with constant size is given in [62]. Under some conditions it is proved in [44] that the solution of the general nonlinear model is given by

$$p(a, t) = \begin{cases} p_0(a - t)\Pi(a, t, t; S), & a \geq t \\ B(t - a; S)\Pi(a, t, a; S), & a < t, \end{cases} \quad (1.2.2)$$

where S represents $(S_1(t), S_2(t), \dots, S_N(t))$ and the survival probability is:

$$\Pi(a, t, x; S) = e^{-\int_0^x \mu(a - \sigma, S_1(t - \sigma), \dots, S_N(t - \sigma))d\sigma} \quad (1.2.3)$$

Using the same procedure as in the linear case, i.e. integrating along the characteristic lines, we arrive at the following system of integral equations:

$$\begin{cases} S_i(t) = G_i(t; S) + \int_0^t H_i(t, t-a; S)B(a) da, & t \leq a_+ \\ B(t; S) = F(t; S) + \int_0^t K(t, t-a; S)B(a) da, & t \leq a_+ \\ S_i(t) = \int_{t-a_+}^t H_i(t, t-a; S)B(a) da, & t > a_+ \\ B(t; S) = \int_{t-a_+}^t K(t, t-a; S)B(a) da, & t > a_+, \end{cases} \quad (1.2.4)$$

where

$$\begin{aligned} F(t; S) &= \int_0^{a_+} \beta(a, S_1(t), \dots, S_N(t)) \Pi(a, t, t; S) p_0(a-t) da \\ G(t; S) &= \int_t^{a_+} \gamma_i(a) \Pi(a, t, t; S) p_0(a-t) da \\ K(t, a; S) &= \beta(a, S_1(t), \dots, S_N(t)) \Pi(a, t, a; S) \\ H_i(t, a; S) &= \gamma_i(a) \Pi(a, t, a; S) \end{aligned}$$

Just as in the linear case, knowing the solution of (1.2.4), we can easily find the solution of the nonlinear model (1.2.1) by substituting it in (1.2.2). Existence and uniqueness of the solution of (1.2.1) and some other analytical results for these models can be found in [44].

Of particular interest are the following specific cases:

Logistic growth

$$\begin{cases} \frac{\partial p(a, t)}{\partial t} + \frac{\partial p(a, t)}{\partial a} + \mu_0(a)p(a, t) = 0, & a, t > 0 \\ p(0, t) = R_0 \phi(S(t)) \int_0^{a_+} \beta_0(a)p(a, t) da, & t > 0 \\ p(a, 0) = p_0(a), & a > 0 \\ S(t) = \int_0^{a_+} \gamma(a)p(a, t) da, \end{cases} \quad (1.2.5)$$

where we assume that the age specific mortality $\mu(a) = \mu_0(a)$ depends on age only, while the age specific fertility $\beta(a, S(t))$ depends on age and on a weighted average $S(t)$ of the population density (through the cut-off function $\phi(x)$). In particular we consider

$$\beta(a, x) = R_0 \beta_0(a) \phi(x),$$

with $\phi(x) \geq 0$, $\phi'(x) < 0$, $\phi(0) = 1$, $\phi(+\infty) = 0$ and we assume that the functions $\mu_0(a)$ and $\beta_0(a)$ satisfy the conditions specified for the Lotka-McKendrick's equation. In such case (1.2.5) describes the logistic growth which is one of the most important factors that reduce the growth of the population, namely the fertility is decreased by the crowding effect. A typical example for this mechanism are the corals, i.e. if their density is very high, then the newborns die because of lack of space and hence, the population remains stable.

The solution of this model depends explicitly on the birth rate $B(t)$ (see (1.2.2)), which satisfies the following set of integral equations:

$$\begin{cases} S(t) = G(t) + \int_0^t H(t-a)B(a) da, & t \leq a_+ \\ B(t) = R_0\phi(S(t))[F(t) + \int_0^t K(t-a)B(a)] da, & t \leq a_+ \\ S(t) = \int_{t-a_+}^t H(t-a)B(a) da, & t > a_+ \\ B(t) = \int_{t-a_+}^t K(t-a)B(a) da, & t > a_+ \end{cases} \quad (1.2.6)$$

$$\begin{cases} F(t) = \int_t^{a_+} K(a)\frac{p_0(a-t)}{\pi_0(a-t)}da, & t < a_+, \quad F(t) = 0, t > a_+ \\ G(t) = \int_t^{a_+} H(a)\frac{p_0(a-t)}{\pi_0(a-t)}da, & t < a_+, \quad G(t) = 0, t > a_+ \\ K(a) = \beta_0(a)\pi_0(a), & a \in [0, a_+] \\ H(a) = \gamma(a)\pi_0(a), & a \in [0, a_+] \end{cases}$$

A nonlinear model describing the intra-specific dynamics between juveniles and adults is given as follows:

Cannibalism

$$\begin{cases} \frac{\partial p(a, t)}{\partial t} + \frac{\partial p(a, t)}{\partial a} + \mu_0(a)p(a, t) + m_1\chi_{[0, a^*]}(a)A(t)p(a, t) = 0, & a, t > 0 \\ p(0, t) = R_0 \int_0^{a_+} \beta_0(a)p(a, t)da, & t > 0 \\ p(a, 0) = p_0(a), & a > 0 \\ A(t) = \int_{a^*}^{a_+} p(a, t)da, \end{cases} \quad (1.2.7)$$

where $A(t)$ denotes the number of adults with maturation age a^* and m_1 is the coefficient of attack. The age specific mortality $\mu(a, A(t), J(t)) = \mu_0(a) + m_1\chi_{[0, a^*]}(a)\frac{A(t)}{1 + \theta J(t)}$ is a function

of age, adults and juveniles $J(t) = \int_0^{a^*} p(a, t)da$; θ is the time spent by the predator to eat the prey and $\theta J(t)$ gives the total number of preys. We consider that the fertility $\beta(a, A(t)) = R_0\beta_0(a)\phi(A(t))$ depends on age and on the adult population, where the functions $\mu_0(a)$, $\beta_0(a)$ are the same as in the case of Logistic growth and we assume $\theta = 0$ and $\phi(x) = 1$ for simplicity. Here the decrease of the population growth comes from the predation on the juveniles by the adult population, i.e. the mortality of juveniles increases when the number of adults increases too. Cannibalism can be seen for example among pigs raised in crowded farms. The lack of

water can lead to cannibalism in a rabbit population too.

Equation (1.2.7) can be written in the following integral form:

$$\begin{cases} A(t) = G(t, A) + \int_0^t H(a) e^{-m_1 \int_0^a \chi(a-\sigma)_{[0,a^*]} A(t-\sigma) d\sigma} B(t-a) da \\ B(t) = F(t, A) + R_0 \int_0^t K(a) e^{-m_1 \int_0^a \chi(a-\sigma)_{[0,a^*]} A(t-\sigma) d\sigma} B(t-a) da \\ F(t, A) = R_0 \int_t^{a_+} K(a) \frac{p_0(a-t)}{\pi_0(a-t)} e^{-m_1 \int_0^t \chi(a-\sigma)_{[0,a^*]} A(t-\sigma) d\sigma} da \\ G(t, A) = \int_t^{a_+} H(a) \frac{p_0(a-t)}{\pi_0(a-t)} e^{-m_1 \int_0^t \chi(a-\sigma)_{[0,a^*]} A(t-\sigma) d\sigma} da \end{cases} \quad (1.2.8)$$

$$\begin{cases} H(a) = \gamma(a)\pi_0(a), & a \in [a^*, a_+], & H(a) = 0, & a < a^* \\ K(a) = \beta_0(a)\pi_0(a), & a \in [a^*, a_+], & K(a) = 0, & a < a^* \end{cases}$$

where $\chi(s)_{[0,a^*]}$ is a characteristic function, such that $\chi(s) = 1$ if $s \in [0, a^*]$ and $\chi(s) = 0$ if $s > a^*$.

Competition is another regulatory mechanism that describes the intra-specific dynamics between juveniles and adults and prohibits exponential growth.

Juvenile-Adult Competition

$$\begin{cases} \frac{\partial p(a, t)}{\partial t} + \frac{\partial p(a, t)}{\partial a} + \mu_0(a)p(a, t) + m_1 \chi_{[0,a^*]} J(t)p(a, t) + m_2 \chi_{[a^*, a_+]} A(t)p(a, t) = 0, & a, t > 0 \\ p(0, t) = R_0 \int_{a^*}^{a_+} \beta_0(a) \phi(b_1 J(t) + b_2 A(t)) p(a, t) da, & t > 0 \\ p(a, 0) = p_0(a), & a > 0 \\ J(t) = \int_0^{a^*} p(a, t) da \\ A(t) = \int_{a^*}^{a_+} p(a, t) da, \end{cases} \quad (1.2.9)$$

where a^* is the maturation age and hence $J(t)$ gives the number of juveniles while $A(t)$ is the total number of adults; we assume that $\beta_0(a) = 0$ for $a \leq a^*$; m_1, m_2 represent the impact of juvenile and adult crowding on the mortality: this impact is different for the two classes because we assume that each class has its own niche; b_1, b_2 show the effect of crowding on the fertility rate. We shall study a simplified version of this model, considering the following values of the

parameters: $m_1 \neq 0, m_2 = 0, b_1 = 1, b_2 = 0, \phi(x) = e^{-x^k}, \mu_0(a) = \frac{1}{a_+ - a}, \pi_0(a) = a_+ - a$. Thus, the model of competition can be rewritten in the following integral form:

$$\begin{cases} t \leq a^* \\ B(t) = F(t, J) + R_0 \phi(J(t)) \int_0^t K(a) \Pi(a, t, a) B(t-a) da \\ J(t) = G(t, J) + \int_0^t H(a) \Pi(a, t, a) B(t-a) da \\ A(t) = \int_{a^*}^{a_+} H(a) \frac{p_0(a-t)}{\pi_0(a-t)} \Pi(a, t, t), da \end{cases} \quad (1.2.10)$$

where

$$\begin{cases} K(a) = \beta_0(a) \pi_0(a), a \in [a^*, a_+] & K(a) = 0, a < a^* \\ H(a) = \pi_0(a), a \in [0, a^*], & H(a) = 0, a < a^* \end{cases}$$

and

$$\begin{cases} a^* \leq t \leq a_+ \\ B(t) = R_0 \phi(J(t)) \int_0^t K(a) \Pi(a, t, a) B(t-a) da \\ J(t) = \int_0^t H(a) \Pi(a, t, a) B(t-a) da \\ A(t) = \int_t^{a_+} H(a) \frac{p_0(a-t)}{\pi_0(a-t)} \Pi(a, t, t) da + \int_{a^*}^t H(a) \Pi(a, t, a) B(t-a) da \end{cases} \quad (1.2.11)$$

$$\begin{cases} t \geq a_+ \\ B(t) = R_0 \phi(J(t)) \int_0^{a_+} K(a) \Pi(a, t, a) B(t-a) da \\ J(t) = \int_0^{a_+} H(a) \Pi(a, t, a) B(t-a) da \\ A(t) = \int_{a^*}^{a_+} H(a) \Pi(a, t, a) B(t-a), da \end{cases} \quad (1.2.12)$$

where

$$\Pi(a, t, a) \quad (a < t) = \begin{cases} 1) & e^{-m_1 \int_{t-a}^t J(\sigma) d\sigma}, a \leq a^* \\ 2) & e^{-m_1 \int_{t-a}^{t-a+a^*} J(\sigma) d\sigma} e^{-m_2 \int_{t-a+a^*}^t A(\sigma) d\sigma}, a > a^* \end{cases} \quad (1.2.13)$$

$$\Pi(a, t, t) \quad (t < a) = \begin{cases} 1) & e^{-m_1 \int_0^t J(\sigma) d\sigma}, \quad a - t < a < a^* \\ 2) & e^{-m_1 \int_0^{t-a+a^*} J(\sigma) d\sigma} e^{-m_2 \int_{t-a+a^*}^t A(\sigma) d\sigma}, \quad a - t < a^* < a \\ 3) & e^{-m_2 \int_0^t A(\sigma) d\sigma}, \quad a^* < a - t < a \end{cases} \quad (1.2.14)$$

Competition among members of the same species ("intra-specific competition") is the driving force of evolution and natural selection; the competition for resources such as food, water, territory, and sunlight results in the ultimate survival and dominance of the variation of the species best suited for survival. Intra-specific competition, is illustrated for example by some species of birds and mammals, the males of which set up territories from which all other males of the same species are excluded.

1.3. Age-Structured Diffusion Models

The geographic distribution of a species over its habitat and the associated dynamics of population growth, are inseparably related. Thus, whilst the assumption that populations develop at a single location is good for mathematical purposes, in real life we must accept the spatial dispersal of living organisms. The random-walk problem is adopted as a starting point for the derivation of a model of diffusion of a homogeneous population in which the age-structure in the population is ignored. Later on, scientists trying to create more realistic models, started to take into account both - spatial structure and age structure of the individuals. One of the first who introduced spatial spread in age-dependent populations was Gurtin [36]. Together with MacCamy, they presented age-structured models considering two different diffusion mechanisms, namely random diffusion and movement to avoid crowding (directed diffusion) [38], [39], [74]. In the eighties other authors studied the existence, uniqueness and asymptotic behavior of a solution of different age-dependent diffusion models, either linear or non-linear (see for instance [17], [21], [22], [63], [65], [78]).

We focus our attention on a problem similar to the Lotka-McKendrick's model, but involving the spatial structure of the individuals ([17], [63]). Let $p(a, t, x)$ be the density of a population having age $a \in [0, a_+]$, where a_+ is the maximum age; $t > 0$ denotes time and $x \in (0, 1)$ denotes spatial position. We assume that **the flux of the population** is given by $D \nabla_x p(a, t, x)$, $D > 0$ being **the coefficient of diffusion** (in general it is a function of age and time, but for simplicity we assume it to be constant). Then, following [36], a mathematical model describing

the evolution of the population $p(a, t, x)$ is given by

Dirichlet boundary conditions

$$\begin{cases} 1) p_a + p_t + \mu(a)p = Dp_{xx}, & a \in [0, a_+], \quad t > 0, x \in (0, 1) \\ 2) p(0, t, x) = \int_0^{a_+} \beta(a)p(a, t, x) da = B(t, x), & t > 0, x \in (0, 1) \\ 3) p(a, 0, x) = p_0(a, x), & a \in [0, a_+], x \in (0, 1) \\ 4) p(a, t, 0) = p(a, t, 1) = 0, & a \in [0, a_+], t > 0 \end{cases} \quad (1.3.1)$$

where $p_0(a, x)$ is the initial distribution and $\beta(a)$ and $\mu(a)$ represent the age specific fertility and the age specific mortality respectively. Since homogeneous Dirichlet conditions on the boundaries of the region $(0,1)$ are considered as "extremely inhospitable" (see [22]) in the sense that each individual who reaches the boundary dies, we consider the same model but with Neumann boundary conditions which are imposed to describe a population without immigration or emigration:

Neumann boundary conditions

$$\begin{cases} 1) p_a + p_t + \mu(a)p = Dp_{xx}, & a \in [0, a_+], \quad t > 0, x \in (0, 1) \\ 2) p(0, t, x) = \int_0^{a_+} \beta(a)p(a, t, x) da = B(t, x), & t > 0, x \in (0, 1) \\ 3) p(a, 0, x) = p_0(a, x), & a \in [0, a_+], x \in (0, 1) \\ 4) p_x(a, t, 0) = p_x(a, t, 1) = 0, & a \in [0, a_+], t > 0 \end{cases} \quad (1.3.2)$$

We adopt the assumptions for the fertility and the mortality functions made in Section 1.1 and we want $p_0 \in L^2([0, a_+]; (0, 1))$, $p_0(a, x) \geq 0$ for a.e. $(a, x) \in [0, a_+] \times (0, 1)$. Similarly to the case without diffusion, we add the following compatibility condition to ensure the continuity of $p(a, t, x)$ along the characteristic lines, namely:

$$p_0(0, x) = \int_0^{a_+} \beta(a)p_0(a, x)da, \quad (1.3.3)$$

where $p_0(a, x)$ satisfies the conditions of Dirichlet (1.3.1-4) or Neumann (1.3.2-4). Under these assumptions it is shown (see [17, 63, 65]), that there exists a unique solution $p \in C(0, T; L^2([0, a_+]; (0, 1)))$, verifying the problems above.

Furthermore we consider the variables:

$$\begin{cases} w(a, t, x) = \frac{p(a, t, x)}{P(t)} & \text{(age profile)} \\ P(t) = \int_0^1 \int_0^{a_+} p(a, t, x)dadx & \text{(total population)} \end{cases} \quad (1.3.4)$$

Then, substituting in (1.3.2) we obtain a nonlinear model which is a modified version of our initial-boundary value problem with Neumann conditions:

Age profile (Neumann boundary conditions)

$$\left\{ \begin{array}{l} 1) w_t + w_a + \mu(a)w + w \int_0^1 \int_0^{a+} [\beta(a) - \mu(a)]w(a, t, x)dadx = Dw_{xx}, a \in [0, a_+], t > 0, x \in (0, 1) \\ 2) w(0, t, x) = \int_0^{a+} \beta(a)w(a, t, x)da, t > 0, x \in (0, 1) \\ 3) \int_0^1 \int_0^{a+} w(a, t, x)dadx = 1, t > 0 \\ 4) w(a, 0, x) = w_0(a, x), a \in [0, a_+], x \in (0, 1) \\ 5) w_x(a, t, 0) = w_x(a, t, 1) = 0, a \in [0, a_+], t > 0 \end{array} \right. \quad (1.3.5)$$

$$\left\{ \begin{array}{l} \frac{d}{dt}P(t) = Y(t)P(t) \\ P(0) = P_0 \end{array} \right.$$

where:

$$w_0(a, x) = \frac{p_0(a, x)}{\int_0^1 \int_0^{a+} p_0(a, x)dadx}, \quad P_0 = \int_0^1 \int_0^{a+} p_0(a, x)dadx$$

and

$$Y(t) = \int_0^1 \int_0^{a+} [\beta(a) - \mu(a)]w(a, t, x)dadx$$

This formulation has the advantage that the function w is "smoother" than p ([21], [22]). That's why it is interesting to treat this problem itself, particularly in some developments that will be presented later and obviously, any result obtained for problem (1.3.5) is related to the theory about problem (1.3.2).

1.4. Thesis Organization

The thesis objectives are to gain an insight into the numerical methods in the field of age-structured population dynamics and to design, implement and discuss a large variety of numerical schemes. Some new algorithms are provided, different approaches and techniques are compared and a comprehensive review on similar works in this area is done.

In *Chapter 2* numerical schemes for the Lotka-McKenrick's model are described. In particular, we present and discuss three different approaches for its numerical treatment, namely:

- Direct solving the Lotka-McKendrick's equation as an hyperbolic PDE with a non local boundary condition
- Treating the problem by means of the Renewal equation
- Looking at the equation with the Age profile and splitting the problem into two parts

The advantage of an indirect investigation of model (1.1.1) in terms of the Volterra integral equation of second kind (1.1.6) is that higher order methods can more easily be developed. Of course, the problem with the exponential growth of the birth rate $B(t)$ cannot be avoided, but in a compact time interval we can obtain a high accuracy of the approximation. In order to do that, we apply different quadrature formulas to the integral terms of the renewal equation or we use fourth order Runge-Kutta methods for integral equations.

On the other hand, almost no attention has been paid to the numerical study of equation (1.1.10). The profit of the numerical approach by the equation with the Age profile is not obvious. The reason of this approach is hidden in one of the analytical properties of equation (1.1.10), i.e the boundedness of its solution (see [44]). Hence, by the use of robust low order methods we can obtain both - accuracy and efficiency in a long time interval. Following this idea we apply explicit and implicit second order finite difference schemes and we discuss the obtained results.

During the last years many numerical methods from the first category have been proposed (the method of characteristics has been mostly used) but no approaches via the Renewal equation and the equation with the Age profile have been studied. In this section we recall some of the direct methods for solving the linear problem and we propose different ways to adopt the other two approaches. We compare the numerical schemes in terms of numerical efficiency and accuracy and we discuss their advantages and disadvantages. Most of the results are obtained in collaboration with Mimmo Iannelli [86].

In *Chapter 3* we deal with equations containing both - age and diffusion. Since the models have an hyperbolic and a parabolic part, the method of characteristics can be used. We introduce an improved explicit method, namely Super-Time-Stepping (STS) developed for parabolic problems and we apply its modification for the numerical treatment of the age-structured models with spatial dependence presented above. We explain how the acceleration scheme can be adapted to these models. We compare the two approaches we use in order to approximate the solution of the model with Neumann conditions on the boundary, namely direct methods and methods for the diffusion version of the equation with the Age profile 1.3.5. The modified STS

algorithm was elaborated together with Doychin Boyadzhiev ([85], [87]). We prove convergence of this method in case of Dirichlet boundary conditions and we demonstrate the accuracy and the efficiency of the modified STS comparing it with other classical numerical algorithms of same or higher order, namely the explicit, fully implicit and Crank-Nicolson standard schemes. The convergence of the method applied to the linear model with Neumann boundary conditions and to the nonlinear model 1.3.5 is subject of future studies.

Chapter 4 is devoted to the numerical treatment of the nonlinear age-structured models described above. We start our presentation with a large survey on the methods for Gurtin-MacCamy's equation (1.2.1 with $i=1$ and $\gamma(a) = 1$). We discuss different techniques and we introduce various schemes that have been already used for the numerical approximation of Gurtin-MacCamy's model. In Section 4.2 we deal with the model of Logistic Growth. We present a comparative study about the numerical methods (we compare a first order method along characteristics and the Trapezoidal rule) and their performance for the partial differential equation itself (1.2.5) and its integral reformulation (1.2.6) respectively. Wishing to give an insight on other possibilities to approximate the Logistic Growth equation and to see whether it makes sense to use its integral reformulation as an indirect way for its approximation, we discuss and compare the accuracy and the efficiency of the schemes based on several test examples we propose. Our purpose is to study numerically the behavior of the steady states and to check whether the approximate solution mimics correctly the analytical one. Similar investigations are done in Section 4.3 for a model of Cannibalism. While the leading equation of the model of Logistic Growth is linear, but the boundary condition nonlinear (see 1.2.5), the model of Cannibalism (1.2.7) is nonlinear with linear boundary condition. In [44] it is proved that both models have similar bifurcation graphs but for the model of Cannibalism much less analytical results are available. Taking advantage of the good behavior of the schemes used in Section 4.2, we give an evidence for the presence of bifurcation also in the case of Cannibalism. Results on stability and convergence of the discussed schemes (in case of discontinuous kernels) as well as the numerical treatment of the model of Competition (1.2.9 and 1.2.10) are subject to further studies. Most ideas and results presented in Chapter 4 were elaborated in collaboration with Mimmo Iannelli, Giuseppe Izzo, Eleonora Messina, Elvira Russo and Antonella Vecchio.

Finally, *Chapter 5* is dedicated to the future aspects of the present work. While in the previous chapters we introduced many interesting problems arising in the field of age-structured population dynamics, here we point out several important open issues that are worthy to be investigated and we outline an exemplary plan for their further treatment.

CHAPTER 2

NUMERICAL METHODS FOR THE LOTKA-MCKENDRICK'S EQUATION

In this chapter we consider the Lotka-McKendrick's linear model and we discuss a range of methods for its numerical solution. We take advantage of different analytical approaches to the system, to design different numerical methods and compare them with already existing algorithms. In particular we set up some algorithms inspired by the approach based on Volterra integral equations and we also consider an indirect approach based on the nonlinear system that describes the evolution of the age profile of the population. The results presented in the chapter are published in [86] and are obtained in collaboration with Mimmo Iannelli.

2.1. Direct Methods (methods, proposed in the literature)

Here we describe the method of characteristics and some of the approximation schemes that have been used in connection with problem (1.1.1).

The Method of Characteristics

For a first-order partial differential equation (PDE) the method of characteristics discovers lines (called characteristic lines or characteristics) along which the PDE can be viewed as an ordinary differential equation (ODE). Once the ODE is found it can be solved and transformed into a solution for the original PDE. This technique is known as the Method of Characteristics.

Characteristics are also a powerful tool for gaining qualitative insights into PDEs - finding shock-waves, rarefaction, etc. The direction of the characteristic lines indicates the flow of values through the solution. This kind of knowledge is useful when solving PDEs numerically as well.

We now show how the method of characteristics can be used for the numerical approximation of Lotka-McKendrick's equation. We first introduce some useful notation: let $h > 0$ be the discretization step and $h = \frac{a_+}{N}$, where N is the total number of subintervals in time (since the age of the individuals changes with the same speed as the time passes, we assume that the mesh size in time and in age is equal - see the grid in Figure 2.1), i.e. we have $\{(a_i, t^n) : a_i = ih, i = 0, \dots, M; t^n = nh, n = 0, \dots, N\}$.

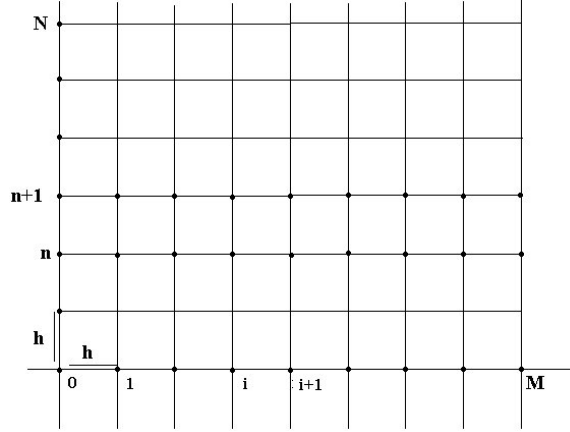


Figure 2.1: The discretization grid

Let p_i^n be an approximation of the solution of (1.1.1) at time level t^n at the grid point a_i , namely an approximation of $p(a_i, t^n)$. Then we approximate the directional derivative $\frac{\partial}{\partial t} + \frac{\partial}{\partial a}$, setting (see the figure above):

$$\left(\frac{\partial}{\partial t} + \frac{\partial}{\partial a} \right) p(a_i, t^n) \approx \frac{p_{i+1}^{n+1} - p_i^n}{h} \quad (2.1.1)$$

Thus, we have the following possible first order schemes:

2.1.1. First Order Schemes

- ◇ explicit Euler scheme: $\frac{p_{i+1}^{n+1} - p_i^n}{h} + \mu_i p_i^n = 0$, i.e. $p_{i+1}^{n+1} = p_i^n(1 - h\mu_i)$, $i, n \geq 0$;
- ◇ implicit Euler scheme: $\frac{p_{i+1}^{n+1} - p_i^n}{h} + \mu_{i+1} p_{i+1}^{n+1} = 0$, i.e. $p_{i+1}^{n+1} = \frac{p_i^n}{(1 + h\mu_{i+1})}$, $i, n \geq 0$;
- ◇ mixed scheme: $\frac{\text{"explicit"} + \text{"implicit"}}{2} = 0$, i.e. $p_{i+1}^{n+1} = \frac{p_i^n(1 - h\mu_i) + \frac{p_i^n}{(1 + h\mu_{i+1})}}{2}$, $i, n \geq 0$;

Moreover we can combine each of these schemes with the first order quadrature rule for the

birth integral:

$$p_0^n = h \sum_{i=1}^N \beta_i p_i^n,$$

where

$$\hat{i} = \begin{cases} i - 1, & \text{for the left-point rule} \\ i, & \text{for the right-point rule} \end{cases}$$

or with the second order trapezoidal rule

$$p_0^n = h \sum_{i=1}^{N-1} \beta_i p_i^n + \frac{h}{2} (\beta_0 p_0^n + \beta_N p_N^n)$$

and the given initial density distribution $p_i^0 = p_0$ in order to obtain a first order algorithm.

Remark: We underline that the combination of first order scheme for the leading equation in (1.1.1) and a second order quadrature rule for the boundary condition of the same model, results in first order algorithm, but the absolute (relative) error in this case is smaller than in the case when the birth integral is approximated with a first order quadrature rule. This fact is explained in details in Sections 4.1 and 4.2.

More details on the effective order of convergence and the stability of the explicit and the implicit Euler schemes can be seen in [48]. A detailed discussion on proving convergence of finite difference methods without requiring the mortality rate $\mu(a)$ to be bounded across all ages is done in the same article. This is a long standing problem since all the proofs of convergence need some derivative of the mortality rate to be bounded, which condition is incompatible with the requirement we impose on the survival probability, namely we want it to vanish at the maximum age (see 1.1.2). Another first order method, especially adapted to the case of finite maximum age can be found in [68]. A numerical scheme for the approximation of the solution of a two-sex version of Lotka-McKendrick's model is presented in [10], while a first order method for a simpler model, in which the mortality rate depends on the size of the total population is proposed in [57].

The procedure described above can be adopted for obtaining higher order schemes.

2.1.2. Higher Order Schemes

The example we present is first proposed by F. Milner and G. Rabbio in [84], namely the Lotka-McKendrick's equation is discretized as follows:

$$\begin{cases} \frac{p_i^n - p_{i-1}^{n-1}}{h} = -\mu_{i-\frac{1}{2}} \frac{p_i^n + p_{i-1}^{n-1}}{2} & 1 \leq i \leq n; \quad 1 \leq n \leq N \\ p_0^n = h \sum_{i=1}^{n-1} \beta_i p_i^n + \frac{h}{2} (\beta_0 p_0^n + \beta_N p_N^n), & 1 \leq n \leq N \\ p_i^0 = p_i, & 0 \leq i \leq N \end{cases}$$

In the same article it is proved that this explicit algorithm converges with second order accuracy. Another finite difference second order method based on the Crank-Nicolson centered scheme is given in [48]. Again Milner and Rabbio [84] use an adaptation of Runge-Kutta fourth order method for ODEs combined with Simpson's formula for the integral terms to obtain the following scheme:

$$\begin{cases} p_{i+1}^{n+1} = p_i^n + \frac{1}{6}[K_1 + 2K_2 + 2K_3 + K_4], & i, n \geq 0 \\ K_1 = hF(t^n, p_i^n) = -h\mu(a_i)p_i^n \\ K_2 = hF(t^n + \frac{h}{2}, p_i^n + \frac{K_1}{2}) = -h\mu(a_i + \frac{h}{2})(p_i^n + \frac{K_1}{2}) \\ K_3 = hF(t^n + \frac{h}{2}, p_i^n + \frac{K_2}{2}) = -h\mu(a_i + \frac{h}{2})(p_i^n + \frac{K_2}{2}) \\ K_4 = hF(t^n + h, p_i^n + K_3) = -h\mu(a_i + h)(p_i^n + K_3) \\ p_0^{n+1} = \frac{h}{(3 - \beta_0 h)} [4\beta_1 p_1^{n+1} + 2\beta_2 p_2^{n+1} + \dots + 2\beta_{N-2} p_{N-2}^{n+1} + 4\beta_{N-1} p_{N-1}^{n+1} + \beta_N p_N^{n+1}] \\ p_i^0 = p(a_i, 0) \end{cases}$$

In the article it is proved that the described scheme converges to fourth order. Another application of Runge-Kutta methods coupled with quadrature formulas to a linear size-structured model (the size of the individuals is considered instead of their age) is described by Angulo and Lopez-Marcos in [7]. There, the authors prove that the scheme converges to order s , where $s \geq 2$ is the order of the Runge-Kutta method.

Projection methods are used by Barr [15] in order to approximate the solution of (1.1.1). A semigroup approach is applied, where the projection method relies on the condition that the subspaces in which the approximation lies, are contained in the domain of the generator of the solution semigroup. Cubic splines are used as basis functions.

Efficient methods for the numerical solution of model (1.1.1) are very important. From the review above one can see that the direct approach has been largely investigated. Our aim is to present more exact and more efficient schemes by taking advantage of already existing numerical methods or to construct new algorithms for the indirect approximation of the solution

of Lotka-McKendrick's equation. Thus, we show an alternative way of treating this problem. This is done in the next two sections, where we deal with the approximation of the Renewal equation (1.1.6) and the equation with the Age profile (1.1.10).

2.2. Methods for the Renewal Equation

In this section we discuss methods involving the Renewal Equation (1.1.6). The numerical approximation of Volterra integral equations has been extensively studied (for example [14],[20],[67]) and to my best knowledge a lot of authors propose various methods for the approximation of $B(t)$ as a solution of the Renewal equation (for example Feller in [31], or Linz in [67]). However nobody uses the relation between equations (1.1.6) and (1.1.1) in order to compare approximation schemes for them in terms of numerical efficiency and accuracy. The objective here is to gain an insight into the numerical methods for Volterra integral equations of second kind (we select and describe some methods in view of their use in connection with the main problem (1.1.1)) and to prove that it makes sense to look for the approximate solution of Lotka-McKendrick's model via the Renewal equation.

2.2.1. Methods Based on the Use of Various Quadrature Rules

We begin our discussion in this section by presenting some intuitively reasonable methods based on a direct application of different quadrature formulas on the integral term of equation (1.1.6). Since we have only one variable t , we discretize a given interval $[0, T]$ as follows

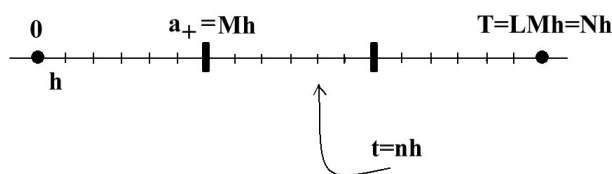


Figure 2.2: Discretization of the interval $[0, T]$

and, in view of the connection with the two variable problem, we take T as a multiple of a_+ so that, for any given step size $h = \frac{a_+}{M}$, we have

$$T = La_+ = LMh = Nh$$

where L , M and N are integers (see Figure 2.2). Then we have the following approximation:

$$\int_0^t K(t-s)B(s)ds \approx \sum_{i=0}^n c_{i,n} K((n-i)h)B(ih), \quad (2.2.1)$$

where $(c_{i,n})$ are the coefficients of the quadrature formula. Thus, if B^n denotes a numerical approximation to the exact solution $B(nh)$, we obtain the following numerical scheme:

$$B^n = F^n + h \sum_{i=0}^n w_{i,n} K_{n-i} B^i, \quad n = l, \dots, N \quad (2.2.2)$$

where:

$$\begin{aligned} w_{i,n} &= \frac{c_{i,n}}{h} \\ F^n &= F(nh) \\ K_i &= K(ih) \end{aligned} \quad (2.2.3)$$

and $B^0 = F^0, B^1, \dots, B^{l-1}$ are given starting values with l depending on the concrete quadrature formula.

In the sequel we present algorithms based on the use of different integration rules (2.2.2).

a) A Hybrid Fourth Order Quadrature Method

We consider a numerical procedure based on the alternate use of different fourth order quadrature rules. Namely we use different versions of (2.2.2), according to the respective steps we perform. Since we want to apply Newton-Cotes type formulas, some adjustment has to be made because these rules involve some restriction on the number of mesh points. Of course we start with

$$B^0 = F^0 \quad (2.2.4)$$

Then, as a first step, we compute B^1 by applying a modified version of the trapezoidal rule given in [12]. Namely, according to the following quadrature formula:

$$\int_{\alpha}^{\beta} f(x) dx \approx \frac{h}{2} [f(\alpha) + f(\beta)] + \frac{h^2}{12} [f'(\alpha) - f'(\beta)] \quad (2.2.5)$$

which is similar to the one of the trapezoidal rule, but it has one complementary term which leads to a higher degree of precision. The numerical scheme that we obtain in this way is more elaborated than (2.2.2). In fact, when (2.2.5) is applied to our equation, in the first step of discretization, we have:

$$B(h) = F(h) + \frac{h}{2} [K(h)B(0) + K(0)B(h)] + \frac{h^2}{12} [Z(0) - Z(h)], \quad (2.2.6)$$

where

$$Z(s) = -K'(h-s)B(s) + K(h-s)B'(s) \quad (2.2.7)$$

Thus we need to approximate $B'(0)$ and $B'(h)$ which can be computed by using the formula:

$$B'(t) = F'(t) + K(0)B(t) + \int_0^t K'(t-a)B(a)da \quad (2.2.8)$$

derived by equation (1.1.6). For $t = 0$ we get:

$$B'(0) = F'(0) + K(0)B(0), \quad (2.2.9)$$

and by applying the trapezoidal rule to the last term of (2.2.8), we obtain:

$$B'(h) \approx F'(h) + K(0)B(h) + \frac{h}{2} [K'(h)B(0) + K'(0)B(h)] \quad (2.2.10)$$

Finally, substituting (2.2.9)-(2.2.10) into (2.2.7)-(2.2.6), and solving for B^1 , we yield

$$B^1 = \frac{F^1 + \frac{h}{2}K_1B^0 + \frac{h^2}{12} \left[-K'_1B^0 + K_1(F'^0 + K_0B^0) - K_0 \left(F'^1 + \frac{h}{2}K'_1B^0 \right) \right]}{1 - \frac{h}{2}K_0 - \frac{h^2}{12}K'_0 + \frac{h^2}{12}K_0^2 - \frac{h^3}{24}K'_0K_0} \quad (2.2.11)$$

After this first step we continue applying (2.2.2) with Simpson's rule:

$$B^n = F^n + \frac{h}{3} [K_nB^0 + 4K_{n-1}B^1 + 2K_{n-2}B^2 + \dots + 2K_2B^{n-2} + 4K_1B^{n-1} + K_0B^n], \quad (2.2.12)$$

jointly with $\frac{3}{8}$ Simpson rule:

$$B^n = F^n + \frac{3h}{8} [K_nB^0 + 3K_{n-1}B^1 + 3K_{n-2}B^2 + 2K_{n-3}B^3 + \dots + 2K_3B^{n-3} + 3K_2B^{n-2} + 3K_1B^{n-1} + K_0B^n] \quad (2.2.13)$$

As a matter of fact formula (2.2.12) requires that n be even, while (2.2.13) needs $n = 3k$, for $k = 1, 2, \dots, q$; moreover each of the described quadrature formulas is fourth order, thus the main idea of our method is to combine these three quadratures in order to obtain a "hybrid" fourth order method. Namely the previous considerations lead to the following algorithm:

- for the first step $n = 1$ we use the modified trapezoidal rule obtaining (2.2.11)
- for $n = 2$ we apply Simpson's rule

$$B^2 = \frac{F^2 + \frac{h}{3} [4K_1B^1 + K_2B^0]}{1 - \frac{h}{3}K_0} \quad (2.2.14)$$

- for $n = 3$ we use $\frac{3}{8}$ Simpson's rule

$$B^3 = \frac{F^3 + \frac{3h}{8} (3K_1B^2 + 3K_2B^1 + K_3B^0)}{1 - \frac{3h}{8}K_0} \quad (2.2.15)$$

- for $n \geq 4$ and even, we use Simpson's rule

$$B^n = F^n + \frac{h}{3} [K_0B^n + 4K_1B^{n-1} + 2K_2B^{n-2} + \dots + 2K_{n-2}B^2 + 4K_{n-1}B^1 + K_nB^0] \quad (2.2.16)$$

- for $n \geq 4$ and odd, we apply $\frac{3}{8}$ Simpson's rule to the last four nodes ($i = n-3, n-2, n-1, n$), and for the rest of them (which are now even number) we use Simpson's rule

$$B^n = F^n + \frac{h}{3} [K_nB^0 + 4K_{n-1}B^1 + 2K_{n-2}B^2 + \dots + 2K_5B^{n-5} + 4K_4B^{n-4} + K_3B^{n-3}] + \frac{3h}{8} [K_3B^{n-3} + 3K_2B^{n-2} + 3K_1B^{n-1} + K_0B^n] \quad (2.2.17)$$

One can use the $\frac{3}{8}$ Simpson's rule on the points ($i = 0, 1, 2, 3$) and Simpson's rule over the rest of the interval, but this combination leads to a method that can show unstable error growth. Therefore the upper version is preferable for computational purposes (see [67] for details). Since the accuracy of the approximate solution depends on the numerical integration, then for more accurate methods better integration rules must be used. The "hybrid" fourth order method that we presented is better than the "pure" modified trapezoidal rule because by using modified trapezoidal rule only at the first interval we lessen the truncation error induced by the complex calculations that we need for applying the method to the whole interval. Moreover, Simpson's and $\frac{3}{8}$ Simpson's rules have better theoretical error estimates than the modified trapezoidal rule which is another benefit.

The procedure above is applicable for $t \leq a_+$. Furthermore, in the case when $t > a_+$, we have

$$B^n = F^n + \int_{t^n - a_+}^{t^n} K(t^n - a)B(a)da = \int_0^{a_+} K(a)B(t^n - a)da \quad (2.2.18)$$

We note that in this case the length of the interval on which we integrate is always a_+ which implies the use of the previous formulas is even simpler and we are not going to discuss it in details.

Stability and convergence analysis of a similar method to the one we described can be found in [67]. The difference with our algorithm is that Linz proposes Block-by-block fourth order methods (that are in fact a generalization of the implicit Runge-Kutta methods for ODEs) as

an efficient way for finding the starting values of the method, namely B^0 and B^1 . This means that as a first step it is needed a system of two additional equations to be solved and then the respective quadrature rules to be applied. The way we proceed, is to compute B^1 directly approximating it by another fourth order quadrature formula.

b) Using Lobatto Points - Fifth Order Method

In the previous method we used a grid where all the points were equally spaced. Now we use a non-uniform mesh with Lobatto points, which are symmetric. The whole interval $[0, a_+]$ can be divided as follows:



Figure 2.3: Lobatto's partition

We have q "big" subintervals and each of them is partitioned into another three parts - one "middle" and two "small" as follows:

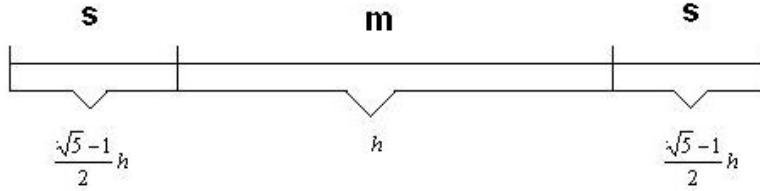


Figure 2.4: "Big's" interval partition

Where:

h - the length of the "middle" part "m" of one "big" interval;

$\frac{\sqrt{5}-1}{2}h$ - the length of the "small" part "s" of one "big" interval;

$h\sqrt{5} = H = \frac{t_{3q} - t_0}{q}$ - the length of one "big" interval

Namely, we have partitioned the whole interval $[0, a_+]$ using the rule:

$$\begin{aligned}
 t_0 &= 0 \\
 t_1 &= t_0 + \frac{\sqrt{5}-1}{2}h \\
 t_2 &= t_0 + \frac{\sqrt{5}+1}{2}h \\
 t_3 &= t_0 + h\sqrt{5} \\
 t_4 &= t_1 + h\sqrt{5} \\
 t_5 &= t_2 + h\sqrt{5} \\
 &\vdots \\
 t_i &= t_{i-3} + h\sqrt{5}, \text{ for } i = 6, \dots, 3q-1 \\
 &\vdots \\
 t_{3q} &= a_+
 \end{aligned} \tag{2.2.19}$$

Let $i = 3k$ ($k = 1, 2, \dots, q$ as shown on Figure 2.3). Then, in connection with the both partitions we consider the following quadrature formulas:

★ In each "big" subinterval we use the 4-point Lobatto quadrature formula

$$\int_{t_0}^{t_i} \phi(t) dt \approx \frac{h\sqrt{5}}{24} [2\phi_0 + 10\phi_1 + 10\phi_2 + 4\phi_3 + 10\phi_4 + 10\phi_5 + 4\phi_6 + \dots + 4\phi_{i-3} + 10\phi_{i-2} + 10\phi_{i-1} + 2\phi_i], \tag{2.2.20}$$

where $\phi_i = \phi(t_i)$.

★ For one "s" subinterval we have two possibilities:

- *forward formula*:

$$\int_{t_i}^{t_{i+1}} \phi(t) dt \approx \frac{h\sqrt{5}}{24} [v_0\phi_{i-3} + v_1\phi_{i-2} + v_2\phi_{i-1} + v_3\phi_i + v_4\phi_{i+1}] \tag{2.2.21}$$

- *backward formula*:

$$\int_{t_{i-1}}^{t_i} \phi(t) dt \approx \frac{h\sqrt{5}}{24} [v_4\phi_{i-1} + v_3\phi_i + v_2\phi_{i+1} + v_1\phi_{i+2} + v_0\phi_{i+3}] \tag{2.2.22}$$

★ For one "s + m" subinterval we again have two cases, namely:

- *forward formula*:

$$\int_{t_i}^{t_{i+2}} \phi(t) dt \approx \frac{h\sqrt{5}}{24} [w_0\phi_{i-2} + w_1\phi_{i-1} + w_2\phi_i + w_3\phi_{i+1} + w_4\phi_{i+2}] \tag{2.2.23}$$

- *backward formula*:

$$\int_{t_{i-2}}^{t_i} \phi(t) dt \approx \frac{h\sqrt{5}}{24} [w_4\phi_{i-2} + w_3\phi_{i-1} + w_2\phi_i + w_1\phi_{i+1} + w_0\phi_{i+2}] \tag{2.2.24}$$

Formulas (2.2.21),..., (2.2.24) are extrapolation formulas with errors compatible with the error of the Lobatto's rule (2.2.20). Their weights are listed in Table 1:

Table 1: Values of v_j and w_j			
v_0	-0.119473775300143	w_0	-0.261114561800008
v_1	0.449194269498781	w_1	2.636919426949720
v_2	-1.682104898799400	w_2	-4.293250516799280
v_3	5.607462045101100	w_3	15.945123359449500
v_4	2.378359213500060	w_4	3.338885438199970

We note that the given formulas are not applicable in the intervals $[t_0, t_1]$ and $[t_0, t_2]$ since we do not have a sufficient number of nodes in order to use them. To initiate the algorithm we need to provide the first six B^i ($i = 1, \dots, 6$). We obtain these values as the solution of a linear system that we set up as follows:

For $i = 0$, i.e. $B^0 = B(0) = F(0)$

For $i = 1$ we present the current integral as a difference of the following two integrals:

$$\int_{t_0}^{t_1} \phi(t) dt = \int_{t_0}^{t_3} \phi(t) dt - \int_{t_1}^{t_3} \phi(t) dt \quad (2.2.25)$$

or we have:

$$B(t_1) = F(t_1) + \int_0^{t_1} K(t_1 - s) B(s) ds = F^1 + \int_0^{t_3} K(t_3 - s) B(s) ds - \int_{t_1}^{t_3} K(t_3 - s) B(s) ds \quad (2.2.26)$$

So for the first integral we use Lobatto's rule (2.2.20) and for the second integral - formula (2.2.24) obtaining:

$$B^1 \approx F^1 + \frac{h\sqrt{5}}{24} [2K_0^1 B^0 + (10 - w_4)K_1^1 B^1 + (10 - w_3)K_2^1 B^2 + (2 - w_2)K_3^1 B^3 - w_1 K_4^1 B^4 - w_0 K_5^1 B^5], \quad (2.2.27)$$

where we have used the notation $K_i^j = K(t_j - t_i)$.

For $i = 2$ we proceed in an analogous way:

$$\int_{t_0}^{t_2} \phi(t) dt = \int_{t_0}^{t_3} \phi(t) dt - \int_{t_2}^{t_3} \phi(t) dt \quad (2.2.28)$$

Consequently, to the first integral we apply Lobatto's rule (2.2.20) and to the second one - backward formula (2.2.22), providing:

$$B^2 \approx F^2 + \frac{h\sqrt{5}}{24} [2K_0^2 B^0 + 10K_1^2 B^1 + (10 - v_4)K_2^2 B^2 + (2 - v_3)K_3^2 B^3 - v_2 K_4^2 B^4 - v_1 K_5^2 B^5 - v_0 K_6^2 B^6] \quad (2.2.29)$$

For $i = 3$ we can use the Lobatto's rule (2.2.20):

$$B^3 \approx F^3 + \frac{h\sqrt{5}}{24}[2K_0^3B^0 + 10K_1^3B^1 + 10K_2^3B^2 + 2K_3^3B^3] \quad (2.2.30)$$

For $i = 4$ we do the following:

$$\int_{t_0}^{t_4} \phi(t)dt = \int_{t_0}^{t_3} \phi(t)dt + \int_{t_3}^{t_4} \phi(t)dt \quad (2.2.31)$$

and thus we use the Lobatto's rule (2.2.20) for the first integral and the forward formula (2.2.21) for the second one:

$$B^4 \approx F^4 + \frac{h\sqrt{5}}{24}[(2 + v_0)K_0^4B^0 + (10 + v_1)K_1^4B^1 + (10 + v_2)K_2^4B^2 + (2 + v_3)K_3^4B^3 + v_4K_4^4B^4] \quad (2.2.32)$$

For $i = 5$ we split the integral as follows:

$$\int_{t_0}^{t_5} \phi(t)dt = \int_{t_0}^{t_3} \phi(t)dt + \int_{t_3}^{t_5} \phi(t)dt \quad (2.2.33)$$

and so we can apply the Lobatto's rule (2.2.20) to the first one and the forward formula (2.2.23) to the second integral, obtaining:

$$B^5 \approx F^5 + \frac{h\sqrt{5}}{24}[2K_0^5B^0 + (10 + w_0)K_1^5B^1 + (10 + w_1)K_2^5B^2 + (2 + w_2)K_3^5B^3 + w_3K_4^5B^4 + w_4K_5^5B^5] \quad (2.2.34)$$

For $i = 6$ we use Lobatto's rule (2.2.20) two times and we get:

$$B^6 \approx F^6 + \frac{h\sqrt{5}}{24}[2K_0^6B^0 + 10K_1^6B^1 + 10K_2^6B^2 + 4K_3^6B^3 + 10K_4^6B^4 + 10K_5^6B^5 + 2K_6^6B^6] \quad (2.2.35)$$

Thus we obtain a system of six equations (2.2.27), (2.2.29), (2.2.30), (2.2.32), (2.2.34) and (2.2.35). This system is with dominating diagonal and there are well known, fast converging methods for solving such kind of systems (Gaussian elimination, Seidel iteration, etc.).

In other words, we have to observe the following procedure:

- To start the process we solve a system with the six unknowns, namely: $B^1, B^2, B^3, B^4, B^5, B^6$
- For B^{3k+1} , where $k = 2, \dots, q-1$, we use k times Lobatto's rule (2.2.20) and one time the forward formula (2.2.21).
- For B^{3k+2} , where $k = 2, \dots, q-1$, we use k times Lobatto's rule (2.2.20) and one time the forward formula (2.2.23).
- For B^{3k} , where $k = 3, \dots, q$, we directly apply Lobatto's rule (2.2.20) k times.

Thus we complete the process in the case when $t \leq a_+$.

In the other case, i.e. when $t > a_+$, the integral equation takes the form

$$B(t) = \int_{t-a_+}^t K(t-a)B(a) da, \quad t > a_+$$

i.e. all the integrals should be calculated on an interval with length a_+ . As the application of the used formulas is not trivial we shall discuss it in details, namely:

Let us present all the mesh points after $a_+ = 3q$ as $3q + p$, where $p = 1, 2, \dots$. Thus, we have the following three cases:

- $p = 1, 4, 7, 10, \dots$

Then we proceed as follows

$$\begin{aligned} B^{3q+p} &= \int_{t_p}^{t_{3q+p}} K(t_{3q+p} - a)B(a)da = \int_{t_p}^{t_{p+2}} K(t_{p+2} - a)B(a)da + \\ &\quad + \int_{t_{p+2}}^{t_{3q+p-1}} K(t_{3q+p-1} - a)B(a)da + \int_{t_{3q+p-1}}^{t_{3q+p}} K(t_{3q+p} - a)B(a)da \end{aligned}$$

Splitting the integral in such a way we can apply the backward formula (2.2.24) to the first integral, Lobatto's rule (2.2.20) to the second one and the forward formula (2.2.21) to the last of them.

- $p = 2, 5, 8, 11, \dots$

Then we obtain:

$$\begin{aligned} B^{3q+p} &= \int_{t_p}^{t_{3q+p}} K(t_{3q+p} - a)B(a)da = \int_{t_p}^{t_{p+1}} K(t_{p+1} - a)B(a)da + \\ &\quad + \int_{t_{p+1}}^{t_{3q+p-2}} K(t_{3q+p-2} - a)B(a)da + \int_{t_{3q+p-2}}^{t_{3q+p}} K(t_{3q+p} - a)B(a)da \end{aligned}$$

Proceeding like that, we can consecutively apply the backward formula (2.2.22), Lobatto's rule (2.2.20) and the forward formula (2.2.23) respectively.

- $p = 3, 6, 9, 12, \dots$

So we have:

$$B^{3q+p} = \int_{t_p}^{t_{3q+p}} K(t_{3q+p} - a)B(a)da$$

and this implies we can directly use Lobatto's rule (2.2.20).

Lobatto formulas belong to the class of Gauss-Legendre formulas which in general are open formulas because the end points of the interval are not involved in the set of the chosen nodes. However, in the construction of Volterra equations solvers, it is often desirable to include either

one or both end points in the set of abscissas (nodes) t_i and then to choose the remaining points in such a way that the degree of precision is as large as possible. One such choice was done in our case.

Interesting analytical results about the described procedure can be found in [20], [50].

c) Error Analysis: Convergence of the Approximate Solution

The nature of the algorithms described above and the results given further intuitively lead us to the thought that, in general, if the integral in (1.1.6) is approximated by a quadrature rule having certain order of accuracy, then the approximate solution computed in this way has the same order of accuracy. Following Linz [67] we shall prove that this conjecture is true.

First of all we assume:

$$\begin{aligned} a) & F(t) \text{ is a continuous function in } 0 \leq t \leq T; \\ b) & \text{ the kernel } K(s) \text{ for } s = t - a \text{ is bounded and } \max_{0 \leq s \leq a_+} |K(s)| \leq L \end{aligned} \quad (2.2.36)$$

Under these conditions it is shown (for example [20], [44], [67]) that (1.1.6) has a unique solution. The analysis of the numerical methods utilizes these assumptions and holds only when they are satisfied.

Let us consider the set of values:

$$\varepsilon^n = B^n - B(nh), \quad n = 0, 1, 2, \dots \quad (2.2.37)$$

which we will call the discretization error and we are interested in the behavior of this discretization error as a function of the stepsize h .

Definition 1. A method of the form (2.2.2) is said to be a **convergent approximation method** if

$$\lim_{h \rightarrow 0} \left(\max_{0 \leq n \leq N} |\varepsilon^n| \right) = 0 \quad (2.2.38)$$

Definition 2. If, for all $h > 0$, there exists a number $M < \infty$, independent of h , such that

$$\max_{0 \leq n \leq N} |\varepsilon^n| = Mh^p, \quad (2.2.39)$$

and if p is the largest number for which such an inequality holds, then p is called **the order of convergence** of the method.

Definition 3. Let B be the solution of (1.1.6). Then the function

$$\delta(h, t^n) = \int_0^{t^n} K(t^n - a)B(a) - h \sum_{i=0}^n w_{i,n} K(t^n - t^i)B(t^i) \quad (2.2.40)$$

is **the local consistency error** for (1.1.6).

The local consistency error is a measure of the accuracy with which, in the context of a given equation, the numerical integration rule represents the integral.

Definition 4. Let L be a class of equations of the form (1.1.6). If for every equation in L

$$\lim_{h \rightarrow 0} \max_{0 \leq n \leq N} |\delta(h, t^n)| = 0 \quad (2.2.41)$$

then the approximation method (2.2.2) is said to be **consistent** with (1.1.6) for the class of equations L . If for every equation in L , there exists a constant \mathbf{C} (independent of h , but generally dependent on B and K) such that

$$\max_{0 \leq n \leq N} |\delta(h, t^n)| \leq Ch^p, \quad (2.2.42)$$

then the method is said to be **consistent of order p** in L .

Before proceeding with the statement and the proof of the main convergence theorem, we need the following results:

Lemma 1.

$$1 + A \left[1 + (1 + A) + (1 + A)^2 + \dots + (1 + A)^{n-l} \right] = (1 + A)^{n-l+1}, \quad A > 0, \quad n \geq l \quad (2.2.43)$$

Proof: We shall prove the statement by mathematical induction.

For $n=l$ we obviously have: $1 + A = 1 + A$. We assume

$$1 + A \left[1 + (1 + A) + (1 + A)^2 + \dots + (1 + A)^{n-l-1} \right] = (1 + A)^{n-l}, \quad A > 0, \quad n \geq l$$

and we want to prove (2.2.43).

$$\begin{aligned} 1 + A \left[1 + (1 + A) + \dots + (1 + A)^{n-l} \right] &= 1 + A \left[1 + (1 + A) + \dots + (1 + A)^{n-l-1} \right] + \\ &+ A(1 + A)^{n-l} = (1 + A)^{n-l} + A(1 + A)^{n-l} = (1 + A)^{n-l+1}, \end{aligned}$$

which completes the proof.

Theorem 1. Let the sequence $\xi^0, \xi^1 \dots$ satisfy

$$|\xi^n| \leq A \sum_{i=0}^{n-1} |\xi^i| + B^n, \quad n = l, l+1, \dots, \quad (2.2.44)$$

where

$$A > 0, \quad |B^n| \leq B, \quad \sum_{i=0}^{l-1} |\xi^i| \leq \eta. \quad (2.2.45)$$

Then

$$|\xi^n| \leq (1 + A)^{n-l} (B + A\eta), \quad n = l, l+1, \dots, \quad (2.2.46)$$

Proof: In order to prove this theorem, we shall again use an inductive argument.

For $n=l$ we have:

$$|\xi^l| \leq A \sum_{i=0}^{l-1} |\xi^i| + B^l \leq A\eta + B \quad (2.2.47)$$

Consequently (2.2.46) holds ($n-l=l-l=0$, thus the first multiplier in (2.2.46) is equal to 1). We assume the equality is satisfied for n . We want to prove it is valid for $n+1$.

$$\begin{aligned} |\xi^{n+1}| &\leq A \sum_{i=0}^n |\xi^i| + B^{n+1} = A \sum_{i=0}^{l-1} |\xi^i| + A \sum_{i=l}^n |\xi^i| + B^{n+1} = \\ &= A \sum_{i=0}^{l-1} |\xi^i| + A \left[|\xi^l| + |\xi^{l+1}| + \dots + |\xi^n| \right] + B^{n+1} \leq \\ &\leq (A\eta + B) + A \left[(A\eta + B)(1 + A) + (A\eta + B)(1 + A)^2 + \dots + (A\eta + B)(1 + A)^{n-l} \right] = \\ &= (A\eta + B) \left[1 + A \left(1 + (1 + A) + (1 + A)^2 + \dots + (1 + A)^{n-l} \right) \right] = \\ &= (\text{Lemma 1}) \quad (A\eta + B)(1 + A)^{n+1-l} \end{aligned}$$

Thus, Theorem 1 is proved. From (2.2.46) it follows that if $A = hK, t^n = nh$, then

$$|\xi^n| \leq (1 + A)^{n-l} (B + A\eta) \leq (1 + Kh)^{\frac{t^n}{h}-l} (B + hK\eta) \leq (B + hK\eta) e^{Kt^n}, \quad (2.2.48)$$

$$\text{since } (1 + Kh)^{\frac{t^n}{h}-l} = \frac{(1 + Kh)^{\frac{t^n}{h}}}{(1 + Kh)^l} \leq \left[(1 + Kh)^{\frac{1}{h}} \right]^{t^n} \leq e^{Kt^n}.$$

The main convergence theorem follows by a simple application of this preliminary result.

Theorem 2. Consider the approximate solution of (1.1.6) by (2.2.2) and assume that

- (i) the solution $B(t)$ of (1.1.6) and the kernel $K(t-a)$ are such that the approximation method is consistent of order p with (1.1.6);
- (ii) the weights satisfy

$$\sup_{i,n} |w_{i,n}| \leq W < \infty;$$

- (iii) the starting errors $B^n - B(t^n)$, $n = 0, \dots, l-1$ go to 0 as $h \rightarrow 0$. Since l is fixed, this implies that

$$\lim_{h \rightarrow 0} \sum_{n=0}^{l-1} |B^n - B(t^n)| = 0.$$

Then the method is a convergent approximation method of order at least p .

Proof: Putting $t = t^n$ in (1.1.6) and subtracting from (2.2.2), we get for $n = l, l+1, \dots$

$$|\varepsilon^n| = h \sum_{i=0}^n w_{i,n} \left[K(t^n - t^i) B^i - K(t^n - t^i) B(t^i) \right] - \delta(h, t^n)$$

Using the condition (2.2.36 -b) and assumption (ii), and choosing $h < \frac{1}{WL}$, we have

$$|\varepsilon^n| \leq \frac{hWL}{1-hWL} \sum_{i=0}^{n-1} |\varepsilon^i| + \frac{|\delta(h, t^n)|}{1-hWL}$$

Then, applying Theorem 1 and (2.2.48) we yield

$$|\varepsilon^n| \leq \frac{1}{1-hWL} \left[\max_{t \leq i \leq n} |\delta(h, t^i)| + hWL \sum_{i=0}^{l-1} |B^n - B(t^n)| \right] e^{\frac{WLt^n}{1-hWL}} \quad (2.2.49)$$

Since by assumption both the starting errors and the local consistency error go to zero when $h \rightarrow 0$, it follows that

$$\lim_{h \rightarrow 0} |\varepsilon^n| = 0 \quad \text{and} \quad |\varepsilon^n| = O(\max |\delta(h, t^i)|),$$

and the proof is complete. \square

2.2.2. Runge-Kutta Methods

Another way to solve equation (1.1.6) is by using Runge-Kutta-Type methods, which have been developed in the mid-1960s. The idea of these methods is the following:

Let us consider the discretization mesh as given in Figure 2.2 and let us rewrite equation (1.1.6) in the consequent form

$$B(t) = F(t) + \int_0^{t_n} K(t-s)B(s) ds + \int_{t_n}^t K(t-s)B(s) ds = F_n(t) + \int_{t_n}^t K(t-s)B(s) ds, \quad t \in [0, T], \quad (2.2.50)$$

where $F_n(t)$ is called *lag (tail) term* and

$$F_n(t) = F(t) + \int_0^{t_n} K(t-s)B(s) ds, \quad n = 0, \dots, N-1 \quad (2.2.51)$$

Moreover, we define

$$h\Phi_n(t) = \int_{t_n}^t K(t-s)B(s) ds, \quad t \in [t_n, T], \quad n = 0, \dots, N-1 \quad (2.2.52)$$

Here $\Phi_n(t)$ is *the increment function* (with respect to the subinterval $[t_n, t_{n+1}]$).

A Runge-Kutta method is based on two approximation processes:

- an approximation scheme for the increment function $\Phi_n(t)$. The resulting discrete increment function, denoted by $\tilde{\Phi}_n(t)$ is called *Volterra-Runge-Kutta (VRK) formula*.

- an approximation scheme for the lag term $F_n(t)$. The discrete lag term is denoted by $\tilde{F}_n(t)$ and will be referred to as *lag term formula*.

Thus, we obtain an approximation of equation (2.2.50) at $t = t_{n+1} = t_n + h$:

$$B^{n+1} = \tilde{F}_n(t_n + h) + h\tilde{\Phi}_n(t_n + h), \quad n = 0, \dots, N-1 \quad (2.2.53)$$

We shall call this equation a *VRK method* if both the VRK formula and the lag term has been specified.

Definition 2.2.2.1 An *m-stage* Volterra-Runge-Kutta formula for equation (1.1.6) has the form

$$\tilde{\Phi}_n(t) = \sum_{i=1}^m b_i K(t_n + e_i h, t_n + c_i h) Y_i^n \quad (2.2.54)$$

with Y_i^n given by

$$Y_i^n = \tilde{F}_n(t_n + \theta_i h) + h \sum_{j=1}^m a_{i,j} K(t_n + d_{i,j} h, t_n + c_j h) Y_j^n, \quad i = 1, \dots, m \quad (2.2.55)$$

Here, the vectors $\theta = (\theta_i)$, $c = (c_i)$, $e = (e_i)$, $b = (b_i)$, and the square matrices $A = (a_{i,j})$, $D = (d_{i,j})$ are given.

Definition 2.2.2.2 (a) A VRK formula is of **Pouzet type** (*PVRK formula*) if:

$$d_{i,j} = c_i = \sum_{j=1}^m a_{i,j}, \quad e_i = 1, \quad \theta_i = c_i \quad i, j = 1, \dots, m \quad (2.2.56)$$

i.e. if its VRK formula is characterized by the symbolic diagram (the "Butcher array" for ODE's)

c	A
	b^T

Written explicitly, an *m-stage* PVRK formula is given by

$$\begin{aligned} Y_i^n &= \tilde{F}_n(t_n + c_i h) + h \sum_{j=1}^m a_{i,j} K(t_n + c_i h, t_n + c_j h) Y_j^n, \\ &\quad i = 1, \dots, m \\ B^{n+1} &= \tilde{F}_n(t_n + h) + h \sum_{i=1}^m b_i K(t_n + h, t_n + c_i h) Y_i^n, \\ &\quad n = 0, \dots, N-1 \end{aligned} \quad (2.2.57)$$

(b) A VRK formula is of **Beltyukov type** (*BVRK formula*) if

$$d_{i,j} = d_j = e_j, \quad \theta_i = c_i \quad i, j = 1, \dots, m \quad (2.2.58)$$

Thus, the VRK part of a Beltyukov method is characterized by the diagram

d	c	A
		b^T

Hence, an m -stage BVRK formula has the following form:

$$\begin{aligned}
 Y_i^n &= \tilde{F}_n(t_n + c_i h) + h \sum_{j=1}^m a_{i,j} K(t_n + d_j h, t_n + c_j h) Y_j^n, \\
 &\quad i = 1, \dots, m \\
 B^{n+1} &= \tilde{F}_n(t_n + h) + h \sum_{i=1}^m b_i K(t_n + d_i h, t_n + c_i h) Y_i^n, \\
 &\quad n = 0, \dots, N-1
 \end{aligned} \tag{2.2.59}$$

Many and various Runge-Kutta-Methods can be constructed - of different types, orders and different number of stages (see for example [19], [20]). In the following we present an explicit, 4-stage and fourth order VRK formula of Pouzet type (it is analogues to the fourth order one that is most used for ODE's) where its Butcher's array and Pouzet conditions can be seen in [20].

The scheme of the method is the consequent one

$$\begin{aligned}
 Y_1^n &= \tilde{F}^n(t_n) \\
 Y_2^n &= \tilde{F}^n(t_n + \frac{h}{2}) + \frac{h}{2} [K(t_n + \frac{h}{2}, t_n) Y_1^n] \\
 Y_3^n &= \tilde{F}^n(t_n + \frac{h}{2}) + \frac{h}{2} [K(t_n + \frac{h}{2}, t_n + \frac{h}{2}) Y_2^n] \\
 Y_4^n &= \tilde{F}^n(t_n + h) + h [K(t_n + h, t_n + \frac{h}{2}) Y_3^n] \\
 B^{n+1} &= \tilde{F}^n(t_n + h) + \frac{h}{6} [K(t_n + h, t_n) Y_1^n + 2K(t_n + h, t_n + \frac{h}{2}) Y_2^n + \\
 &\quad + 2K(t_n + h, t_n + \frac{h}{2}) Y_3^n + K(t_n + h, t_n + h) Y_4^n]
 \end{aligned} \tag{2.2.60}$$

Up to now, we have described the approximation of the VRK formula. In order to complete the VRK method we have to specify the lag term formula (2.2.51).

The second term on the right hand side of this formula can be approximated by different quadrature rules involving both intermediate and step points. In our concrete case we have used quadrature rules which include only step points - Modified Trapezoidal rule, Simpson's rule and $\frac{3}{8}$ Simpson's rule since each of them is of fourth order and they all have already been discussed in the same chapter. Some other techniques can be found in the book of Brunner and van der Houwen [20].

In the case $t > a_+$ we apply the same algorithm considering that:

$$B(t) = \int_{t-a_+}^t K(t-s) B(s) ds = \int_0^t K(t-s) B(s) ds \tag{2.2.61}$$

where $K(t - s) = 0$ for $t - s < 0$ or $t - s > 1$.

One of the first who made real efforts to develop a theory on the numerical approximation of Volterra integral equations was Pouzet. His primary interest laid in explicit Runge-Kutta methods, and his work resulted in a variety of algorithms, such as the one presented above. In addition to his work many other authors showed considerable interest in explicit and implicit Runge-Kutta methods and various modifications (see for instance [13], [16], [19], [20], [42] and the references therein).

Convergence and stability analysis of explicit Runge-Kutta methods are similar to what we already discussed. The selection of the parameters assures local consistency and establishes the order of the method. Theorem 2 can then be used to prove convergence.

2.3. Methods for the Equation with the Age Profile

In this section we consider equation (1.1.10) and we present numerical algorithms for it. We take advantage of the numerical schemes developed for Gurtin-MacCamy's model (see Chapter 4) in order to apply them (or their adaptation) to the equation with the Age Profile. We want to approximate the model with a second order explicit and implicit methods. This implies that we have to use a second order method for the approximation of the integral terms. For example this could be the trapezoidal rule which is a second order accurate. It requires an evaluation of the integrated function at the right endpoint a_+ of the interval. This represents a problem for the model (1.1.10) since $\lim_{a \rightarrow a_+} \mu(a) = \infty$. To avoid this problem we make the following substitution

$$v(a, t) = \frac{w(a, t)}{\pi(a)} \quad (2.3.1)$$

and we assume that

$$\sup_{a \in [0, a_+]} \mu(a)\pi(a) \leq \mu^* < \infty \quad (2.3.2)$$

Following [46], we need the product above to be bounded, because without this condition we have intrinsic problems with the order of convergence of the numerical methods.

After the substitution (2.3.1), (1.1.10) transforms into

$$\begin{cases} 1) v_t(a, t) + v_a(a, t) = -v(a, t)A(t) \\ 2) v(0, t) = \int_0^{a_+} \beta(a)\pi(a)v(a, t)da \\ 3) \int_0^{a_+} \pi(a)v(a, t)da = 1 \\ 4) v(a, 0) = \pi^{-1}(a)w_0(a) = v_0(a) \end{cases} \quad (2.3.3)$$

where we have denoted

$$A(t) = \int_0^{a^+} [\beta(\tau) - \mu(\tau)] \pi(\tau) v(\tau, t) d\tau \quad (2.3.4)$$

The penalty condition $\int_0^{a^+} \pi(a) v(a, t) da = 1$ could be dropped and we can approximate the first two equations only. Since that condition is automatically satisfied for the solution of 1), 2), 4) and if $V_i^n \approx v(a_i, t^n)$ with any order, then 3) will be satisfied for V_i^n with the same order. Numerical method of first order where the scheme automatically satisfies the algebraic condition is created in [76].

Let us consider the same discretization grid as in Section 2.1 and let V_i^n be an approximation of $v(a_i, t^n)$. Then, we propose an explicit second order RK scheme combined with the use of trapezoidal rule and midpoint rule as follows:

$$\begin{cases} V_{i+1}^{n+1} = V_i^n + K_2, & i = 0, \dots, M-1; n \geq 0 \\ K_1 = -hA^n V_i^n, & i, n \geq 0 \\ K_2 = -A^{n+\frac{1}{2}}(V_i^n + \frac{K_1}{2}), & i, n \geq 0 \end{cases} \quad (2.3.5)$$

where A^n , given by:

$$A^n = \frac{h}{2} [(\beta_0 - \mu_0) \pi_0 V_0^n + 2 \sum_{i=1}^{M-1} (\beta_i - \mu_i) \pi_i V_i^n + (\beta_M - \mu_M) \pi_M V_M^n] \quad (2.3.6)$$

is an approximation of $A(t)$ defined at t^n and we have assumed that $\mu_M \pi_M$ is a finite number. The approximation of $A(t)$ at time $t^{n+\frac{1}{2}}$ will be further defined.

By these formulas we find the solution at the new time level t^{n+1} at the grid points a_1, \dots, a_M . For the boundary points we apply the trapezoidal rule:

$$V_0^{n+1} = \frac{h}{(2 - h\beta_0\pi_0)} [2\beta_1\pi_1 V_1^{n+1} + 2\beta_2\pi_2 V_2^{n+1} + \dots + 2\beta_{M-1}\pi_{M-1} V_{M-1}^{n+1} + \beta_M\pi_M V_M^{n+1}] \quad (2.3.7)$$

Concerning $A^{n+\frac{1}{2}}$, we can notice that the second multiplier in the third equation in (2.3.5) is in fact an approximation of our solution for time $(t^n + \frac{h}{2})$, found by making a half step of Euler's method for ODE's. It implies we know all the "inner" points at level $(t^n + \frac{h}{2})$. Thus, we can use the midpoint rule in order to calculate the integral at this time level:

$$A^{n+\frac{1}{2}} = h \sum_{i=0}^{M-1} (V_i^n + \frac{K_1}{2}) (\beta_{i+\frac{1}{2}} - \mu_{i+\frac{1}{2}}) \pi_{i+\frac{1}{2}} \quad (2.3.8)$$

Now putting together (2.3.5), (2.3.6), (2.3.7), (2.3.8) we complete our method.

This procedure is applicable to second order RK schemes, but it may be adapted also for higher

order RK schemes. Relative algorithms differ in the way of calculation the values of $A(t^n + c_i h)$, for $c_i \in Q$. In fact, to find $A^{n+\frac{1}{2}}$, we have not used extrapolations (as in [2]) but another quadrature formula of the same order which is much better since otherwise we need "starting points" to initiate the procedure which increases the computational time and cost. Other methods to solve numerically problem (2.3.3) can be inspired by similar works on Gurtin MacCamy's equation which is presented in Chapter 4 of the present work.

The next method we propose is an implicit second order method (Box method) that has been first presented in 1991 by Fairweather and Lopez-Marcos. Its consistency, stability and convergence are studied in [29].

The method is based on the following second order approximations:

$$\frac{V_i^{n+1} - V_i^n}{h} + \frac{V_{i-1}^{n+1} - V_{i-1}^n}{h} \approx 2 \frac{\partial v}{\partial t}(a_{i-\frac{1}{2}}, t^{n+\frac{1}{2}}) + O(h^2) \quad (2.3.9)$$

$$\frac{V_i^{n+1} - V_{i-1}^{n+1}}{h} + \frac{V_i^n - V_{i-1}^n}{h} \approx 2 \frac{\partial v}{\partial a}(a_{i-\frac{1}{2}}, t^{n+\frac{1}{2}}) + O(h^2) \quad (2.3.10)$$

$$\frac{V_{i-1}^{n+1} + V_{i-1}^n}{2} + \frac{V_i^{n+1} + V_i^n}{2} \approx 2v(a_{i-\frac{1}{2}}, t^{n+\frac{1}{2}}) + O(h^2) \quad (2.3.11)$$

Substituting with these formulas in ((2.3.3)-1) we obtain:

$$\frac{h}{2} A^{n+\frac{1}{2}} V_{i-1}^{n+1} + [\frac{h}{2} A^{n+\frac{1}{2}} + 2] V_i^{n+1} = 2V_{i-1}^n - \frac{h}{2} A^{n+\frac{1}{2}} (V_{i-1}^n + V_i^n) \quad \text{for } i = 1, \dots, M \quad (2.3.12)$$

These equations can be rewritten in the following form

$$\begin{aligned} b(1)V_0^{n+1} + c(1)V_1^{n+1} &= d(1) \\ b(2)V_1^{n+1} + c(2)V_2^{n+1} &= d(2) \\ &\dots\dots\dots \\ b(M)V_{M-1}^{n+1} + c(M)V_M^{n+1} &= d(M), \end{aligned} \quad (2.3.13)$$

where the coefficients $b(i)$, $c(i)$ and $d(i)$ for $i = 1, \dots, M$ are given by

$$\begin{aligned} b(i) &= \frac{h}{2} A^{n+\frac{1}{2}} \\ c(i) &= 2 + \frac{h}{2} A^{n+\frac{1}{2}} \\ d(i) &= 2V_{i-1}^n - \frac{h}{2} A^{n+\frac{1}{2}} (V_{i-1}^n + V_i^n) \end{aligned} \quad (2.3.14)$$

and the approximation of $A(t)$ at $t^{n+\frac{1}{2}}$ time level is the following one:

$$A^{n+\frac{1}{2}} = \frac{h}{2} \left[\frac{V_0^n + V_0^{n+1}}{2} (\beta_0 - \mu_0) \pi_0 + \sum_{i=1}^{M-1} (V_i^n + V_i^{n+1}) (\beta_i - \mu_i) \pi_i + \frac{V_M^n + V_M^{n+1}}{2} (\beta_M - \mu_M) \pi_M \right] \quad (2.3.15)$$

Thus, we have a system of M equations that involves $M+1$ unknowns. In order to solve it we add the following equation arising from ((2.3.3)-2):

$$V_0^{n+1} = \frac{h}{2} [\beta_0 \pi_0 V_0^{n+1} + 2\beta_1 \pi_1 V_1^{n+1} + 2\beta_2 \pi_2 V_2^{n+1} + \dots + 2\beta_{M-1} \pi_{M-1} V_{M-1}^{n+1} + \beta_M \pi_M V_M^{n+1}] \quad (2.3.16)$$

Or, rewriting it in a suitable form we have

$$a(0)V_0^{n+1} + a(1)V_1^{n+1} + \dots + a(M)V_M^{n+1} = 0, \quad (2.3.17)$$

where $a(0) = 1 - \frac{h}{2}\beta_0\pi_0$, $a(i) = -h\beta_i\pi_i$ for $i = 1, \dots, M-1$, $a(M) = -\frac{h}{2}\beta_M\pi_M$.

Consequently, when joining (2.3.13) and (2.3.17) we obtain a system of $M+1$ equations with $M+1$ unknowns. To solve this system we use a forward and a backward substitution.

To start the process we take $V_i^{n+1} = V_i^n$ as an initial approximation. Then, we substitute it in (2.3.15) and afterwards we solve the system (2.3.13) - (2.3.17). Thus, we find a new approximation to V_i^{n+1} which is better than the previous one. This iterative procedure continues until we obtain the required accuracy for the discrete approximation of $v(a, t)$ at the new time level $n+1$. It means that we have resolved the nonlinearity by means of an iteration with needed tolerance (in our case h^3 because of the second order accuracy of the applied algorithm). A description of a variation of the box method (an explicit extrapolated box scheme) and its application to the Gurtin-MacCamy problem can be found in [30].

2.4. Test Examples

In this section we shall introduce two test examples in order to compare obtained approximate solutions and evaluate the method's efficiency.

We assume the maximum age $a_+ = 1$; the mortality $\mu(a) = \frac{1}{1-a}$ so that the survival probability is $\pi(a) = 1 - a$. The initial values are chosen in such a way that compatibility condition (1.1.4) is satisfied which provides continuity of the solution.

Example 1: In the first example we assume $\beta(a) = 2$. Then we have the net reproduction ratio $R = \int_0^{a_+} \beta(a)\pi(a)da = 1$, so we obtain $\alpha^* = 0$ (see [44]) that is the intrinsic Malthusian parameter which determines the population growth via the birth rate $B(t)$. Substituting with $\alpha^* = 0$ in equation (1.1.7) we see that in this first case the population remains stable.

We have chosen the following initial conditions:

$$p_0(a) = \begin{cases} (1-2a)^3(1-a), & a \in [0, \frac{1}{2}] \\ 31(2a-1)^3(1-a), & a \in [\frac{1}{2}, 1] \end{cases} \quad (2.4.1)$$

In order to skip troubles with the unboundedness of $\mu(a_+)$, we set

$$u(a, t) = \frac{p(a, t)}{\pi(a)} \quad (2.4.2)$$

or for $u_0(a)$ we have

$$u_0(a) = \begin{cases} (1 - 2a)^3, & a \in [0, \frac{1}{2}] \\ 31(2a - 1)^3, & a \in [\frac{1}{2}, 1] \end{cases} \quad (2.4.3)$$

Considering (2.3.1) and formulas (1.1.12) and (1.1.13) we can calculate $v_0(a)$ for the profile:

$$v_0(a) = \begin{cases} 2(1 - 2a)^3, & a \in [0, \frac{1}{2}] \\ 62(2a - 1)^3, & a \in [\frac{1}{2}, 1] \end{cases} \quad (2.4.4)$$

It follows that for the functions $F(t)$ and $K(a)$ we have:

$$\begin{aligned} K(a) &= 2(1 - a) \\ F(t) &= 2 \int_t^1 (1 - a)u_0(a - t)da, \quad t \in [0, 1] \\ F(t) &= 0, \quad t > 1 \end{aligned} \quad (2.4.5)$$

Then substituting with that data into the integral equation (1.1.6) and differentiating it two times in t we obtain the following differential equation in the interval $t \in [0, 1]$:

$$B''(t) - 2B'(t) + 2B(t) = 2u_0(1 - t) \quad (2.4.6)$$

with initial conditions:

$$\begin{aligned} B(0) &= 2 \int_0^1 (1 - a)u_0(a)da = 1 \\ B'(0) &= -2 \int_0^1 u_0(a)da + 2B(0) = -6 \end{aligned}$$

Furthermore, for $t \geq 1$ we get the following delay differential equation:

$$B''(t) - 2B'(t) + 2B(t) = 2B(t - 1) \quad (2.4.7)$$

To obtain the solution of (2.4.6) and (2.4.7) we have developed a solver for delay equations by using Mathematica. More precisely, we have

$$B(t) = -216e^t \cos(t) + 396e^t \sin(t) + 31(7 - 6t - 12t^2 - 8t^3), \quad t \in [0, \frac{1}{2}]$$

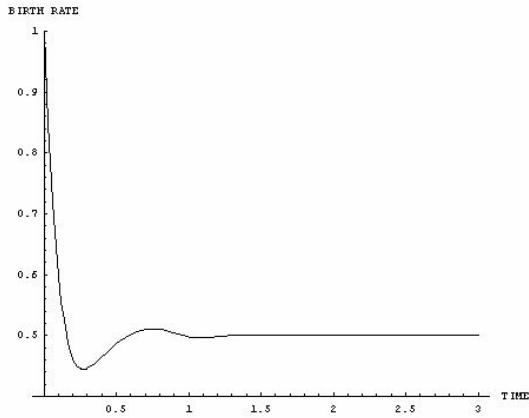
$$\begin{aligned} B(t) &= [(-216 + 768e^{\frac{1}{2}} \sin(\frac{1}{2})) \cos(t) + (396 - 768e^{\frac{1}{2}} \cos(\frac{1}{2})) \sin(t)]e^t - \\ &\quad - 7 + 6t + 12t^2 + 8t^3, \quad t \in [\frac{1}{2}, 1] \end{aligned}$$

$$B(t) = [m \cos(t) + n \sin(t)]e^t + [p \sin(t) - q \cos(t)]te^t + 31(15 - 6t - 12t^2 - 8t^3), \quad t \in [1, 1.5]$$

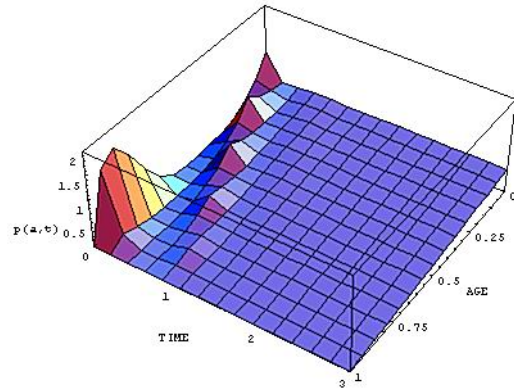
where m, n, p, q are the following suitable constants:

$$\begin{aligned} p &= \frac{216 \cos(1) + 396 \sin(1)}{e}; & q &= \frac{396 \cos(1) - 216 \sin(1)}{e} \\ m &= c + q - [q \cos(1) - p \sin(1)] \sin(1) + 36 \frac{10 \cos(1) - 38 \sin(1)}{e} \\ n &= d - p + [q \cos(1) - p \sin(1)] \cos(1) + 36 \frac{38 \cos(1) + 10 \sin(1)}{e} \end{aligned}$$

For $t > 1,5$ we can take $B(t) \approx 0,5$ since $B(t)$ tends to the constant value 0,5 (see Figure 2.5a).



(a) The birth rate $B(t)$, $\beta(a) = 2$



(b) The age density $p(a, t)$, $\beta(a) = 2$

Figure 2.5: Case without exponential growth, $\alpha^* = 0$, calculated at $t \in [0, 3]$

Obviously $p(a, t)$ does not grow exponentially (see Figure 2.5b) or we are in the banal case where the solution of Lotka-McKendrick's equation is bounded. However, we are much more interested in the case with the exponential growth.

Example 2: In this example we assume $\beta(a) = 6$ in order to obtain exponential population growth, i.e. we have $R = \int_0^{a+} \beta(a)\pi(a)da = 3$, which implies $\alpha^* > 0$ and therefore the birth rate $B(t)$ increases exponentially (see 1.1.7).

In this case we have the following initial conditions:

$$p_0(a) = \begin{cases} (1 - 2a)^3(1 - a), & a \in [0, \frac{1}{2}] \\ \frac{13}{3}(2a - 1)^3(1 - a), & a \in [\frac{1}{2}, 1] \end{cases} \quad (2.4.8)$$

Considering substitutions (2.4.2) and (2.3.1) for $u_0(a)$ and $v_0(a)$ we obtain:

$$u_0(a) = \begin{cases} (1 - 2a)^3, & a \in [0, \frac{1}{2}] \\ \frac{13}{3}(2a - 1)^3, & a \in [\frac{1}{2}, 1] \end{cases} \quad (2.4.9)$$

$$v_0(a) = \begin{cases} 6(1 - 2a)^3, & a \in [0, \frac{1}{2}] \\ 26(2a - 1)^3, & a \in [\frac{1}{2}, 1] \end{cases} \quad (2.4.10)$$

For the functions $F(t)$ and $K(a)$ we have:

$$\begin{aligned} K(a) &= 6(1 - a) \\ F(t) &= 6 \int_t^1 (1 - a)u_0(a - t)da, \quad t \in [0, 1] \\ F(t) &= 0, \quad t > 1 \end{aligned} \quad (2.4.11)$$

Proceeding as in Example 1 we obtain the following differential equation in the interval $[0, 1]$:

$$B''(t) - 6B'(t) + 6B(t) = 6u_0(1 - t) \quad (2.4.12)$$

with initial conditions:

$$\begin{aligned} B(0) &= 6 \int_0^1 (1 - a)u_0(a)da = 1 \\ B'(0) &= -6 \int_0^1 u_0(a)da + 6B(0) = 2 \end{aligned}$$

Furthermore, for $t \geq 1$ we get the following differential delay equation:

$$B''(t) - 6B'(t) + 6B(t) = 6B(t - 1) \quad (2.4.13)$$

Running our solver we can obtain the exact solution of (2.4.12) and (2.4.13) for a long period of time but here we give the solution of these equations only in the interval $[0, 2]$, namely

- in $[0, \frac{1}{2}]$:

$$B(t) = \frac{-663 + ae^{(3-\sqrt{3})t} + be^{(3+\sqrt{3})t} - 858t - 468t^2 - 312t^3}{9},$$

where

$$a = 336 + 190\sqrt{3}, \quad b = 336 - 190\sqrt{3}$$

-in $[\frac{1}{2}, 1]$:

$$\begin{aligned} B(t) &= B_1(t) + B_2(t) \\ B_1(t) &= \frac{1}{9m} \left(ae^{3+\frac{\sqrt{3}}{2}+(3-\sqrt{3})t} - be^{\frac{3}{2}+\sqrt{3}+(3-\sqrt{3})t} + ce^{\frac{3}{2}+(3+\sqrt{3})t} + de^{3+\frac{\sqrt{3}}{2}+(3+\sqrt{3})t} \right) \\ B_2(t) &= 17 + 22t + 12t^2 + 8t^3 \end{aligned}$$

where

$$\begin{aligned} a &= 2(168 + 95\sqrt{3}), \quad b = 64(12 + 7\sqrt{3}) \\ c &= 64(-12 + 7\sqrt{3}), \quad d = 336 - 190\sqrt{3}, \quad m = e^{3+\frac{\sqrt{3}}{2}} \end{aligned}$$

- in $[1, \frac{3}{2}]$:

$$\begin{aligned} B(t) &= \frac{1}{9} e^{-3-\sqrt{3}-\sqrt{3}t} [B_1(t) + B_2(t)] \\ B_1(t) &= a e^{\frac{3(1+\sqrt{3}+2t)}{2}} + b e^{3+\sqrt{3}+3t} + c e^{3+\sqrt{3}+3t+2\sqrt{3}t} + d e^{\frac{3+\sqrt{3}(6+4\sqrt{3})t}{2}} \\ B_2(t) &= 2 e^{(3+2\sqrt{3})t} (m + nt) + e^{2\sqrt{3}+3t} (p - qt) - 39 e^{3+\sqrt{3}(1+t)} (33 + 38t + 12t^2 + 8t^3) \end{aligned}$$

where

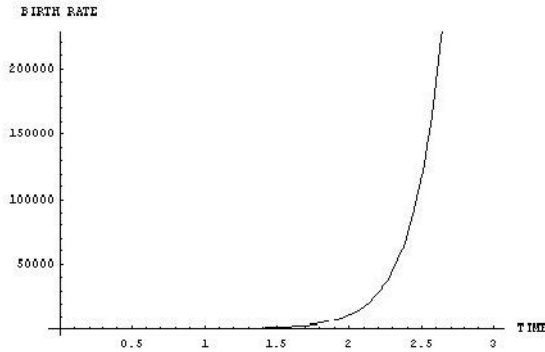
$$\begin{aligned} a &= -64 (12 + 7\sqrt{3}), \quad b = 2 (168 + 95\sqrt{3}), \quad c = (336 - 190\sqrt{3}), \\ d &= 64 (-12 + 7\sqrt{3}), \quad m = 1305 - 761\sqrt{3}, \quad n = 3 (-95 + 56\sqrt{3}) \\ p &= 2610 + 1522\sqrt{3}, \quad q = 6 (95 + 56\sqrt{3}) \end{aligned}$$

- in $[\frac{3}{2}, 2]$:

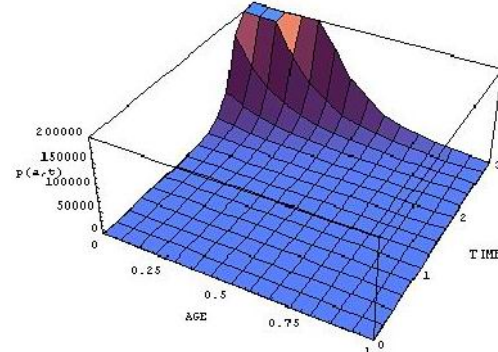
$$\begin{aligned} B(t) &= \frac{1}{9} e^{\frac{-3(9+\sqrt{3})}{2}-\sqrt{3}t} [B_1(t) + B_2(t) + B_3(t)] \\ B_1(t) &= a e^{\frac{3(9+\sqrt{3}+2t)}{2}} - b e^{12+2\sqrt{3}+3t} + c e^{12+\sqrt{3}+3t+2\sqrt{3}t} + d e^{\frac{27}{2}+\frac{3\sqrt{3}}{2}+3t+2\sqrt{3}t} \\ B_2(t) &= -32 e^{9+3t+2\sqrt{3}t} (l + kt) + 32 e^{3(3+\sqrt{3}+t)} (m + nt) + 2 e^{\frac{21+\sqrt{3}+(6+4\sqrt{3})t}{2}} (p + qt) \\ B_3(t) &= e^{\frac{21}{2}+\frac{5\sqrt{3}}{2}+3t} (v - wt) + 9 e^{\frac{3(9+\sqrt{3})}{2}+\sqrt{3}t} (33 + 38t + 12t^2 + 8t^3) \end{aligned}$$

where

$$\begin{aligned} a &= 2 (168 + 95\sqrt{3}), \quad b = 64 (12 + 7\sqrt{3}), \quad c = 64 (-12 + 7\sqrt{3}) \\ d &= (336 - 190\sqrt{3}), \quad l = 171 - 98\sqrt{3}, \quad k = 6 (-7 + 4\sqrt{3}) \\ m &= -171 - 98\sqrt{3}, \quad n = 6 (7 + 4\sqrt{3}), \quad p = 1305 - 761\sqrt{3} \\ q &= 3 (-95 + 56\sqrt{3}), \quad v = 2610 + 1522\sqrt{3}, \quad w = 6 (95 + 56\sqrt{3}) \end{aligned}$$



(a) The birth rate $B(t)$, $\beta(a) = 6$

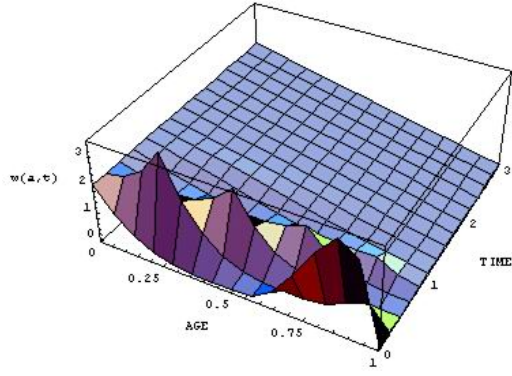


(b) The age density $p(a, t)$, $\beta(a) = 6$

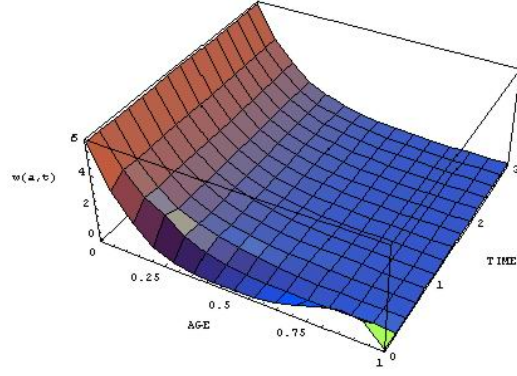
Figure 2.6: The exponential growth when $\alpha^* > 0$, calculated at $t \in [0, 3]$

The basic difference with the previous case is that $B(t)$ grows exponentially and consequently the age density of the population $p(a, t)$ too, which can be seen from the figures above.

As it was already mentioned the age profile $w(a, t)$ remains bounded no matter if $p(a, t)$ grows exponentially or not. On the figure below the exact age profile at $t \in [0, 3]$ is drawn.



(a) The age profile for $\beta(a)=2$



(b) The age profile for $\beta(a)=6$

Figure 2.7: The boundedness of the age profile, calculated at $t \in [0, 3]$

In order to obtain the solution $w(a, t)$ of (1.1.10), we have used formula (1.1.9) to calculate $p(a, t)$ and (1.1.11), (1.1.12) and (1.1.13) for the whole population $P(t)$. In the case $\beta(a) = 6$, by substituting with the given data in (1.1.13) we have obtained

$$\alpha(t) = \int_0^1 (5 - 6a)v(a, t)da \quad (2.4.14)$$

Then we have used the value of $\alpha(t)$ in order to find the solution $P(t)$ of (1.1.11) as follows

$$P(t) = P_0 e^{\int_0^t \alpha(s)ds} \quad (2.4.15)$$

We have obtained $P_0 = \frac{1}{6}$ and we have approximated both integrals in (2.4.14) and (2.4.15) by the trapezoidal rule since it is of order compatible to the order of accuracy of the algorithms developed for equation (2.3.3).

2.5. Numerical Results and Conclusions

In the following we give different results for the algorithms described above. In all tests we compute the effective order of convergence of the schemes by the well-known formula

$$\alpha = \frac{\ln\left(\frac{E_h}{E_{\frac{h}{2}}}\right)}{\ln(2)}, \quad (2.5.1)$$

where E_h is the absolute error defined by

$$E_h = \begin{cases} E_p = \max_{n \geq 1, j \geq 0} |p_j^n - p(a_j, t^n)|, & \text{for the age density} \\ E_w = \max_{n \geq 1, j \geq 0} |w_j^n - w(a_j, t^n)|, & \text{for the age profile} \\ E_B = \max_{n \geq 1} |B^n - B(t^n)|, & \text{for the birth integrals} \end{cases} \quad (2.5.2)$$

The maximum relative error can be calculated in a similar manner:

$$E_{prel} = \max_{n \geq 1, j \geq 0} \frac{|p_j^n - p(a_j, t^n)|}{p(a_j, t^n)} \quad (2.5.3)$$

In the tables below we list the following results:

- In *Table 2* we show results for the absolute maximum error E_h of the different methods. In the first three columns we give E_B for the Hybrid (H), Lobatto (L) and Runge-Kutta (RK) methods for the integral equation respectively. In the next two columns E_w for the Box (Box) and Runge-Kutta (RK) methods for the equation with the age profile respectively. Finally, in the last two columns we give E_p for the Box (Box) and Runge-Kutta (RK) methods for the Lotka-McKendrick's equation respectively. The results are for the case $\beta(a) = 2$ and calculated at $t = 1$.
- In *Table 3* results for the same methods (structured in the same order) are listed. We consider the case $\beta(a) = 6$ calculated at $t = 1$.
- In *Table 4a* values of the maximum absolute error E_p are given. They are found by means of each of the already mentioned methods. The results are arranged in the same order as in the previous tables. We calculate E_p only for the case $\beta(a) = 6$. The results are for time $t = 1, 2, 3$ and total number of intervals $N = 60$.
- In *Table 4b* the maximum relative error E_{prel} obtained by means of all the methods is shown. The results reported here are calculated at time $t = 1, 2$ and with total number of time intervals $N = 60$. They are arranged in the same order as in *Table 4a*.
- In *Table 5* a comparison of the maximum absolute error for $p(a, t)$ found by application of the Box method to the Lotka-MacKendrick's equation and to the equation with the age profile is done. The same comparison, but for $w(a, t)$ is also shown.
- In *Table 6* we show the effective order of convergence of all the methods.
- In *Table 7* we give the CPU time (in seconds) needed to calculate $p(a, t)$ by the different methods applied to the equations we discussed. The experiments are done at different times, namely $t = 1, 2, 5, 7$ and with different number of intervals $N = 300$ and $N = 600$.

Table 2: Maximum absolute error for all methods, $\beta(a) = 2$

h	$E_B(H)$	$E_B(L)$	$E_B(RK)$	$E_w(\text{Box})$	$E_w(RK)$	$E_p(\text{Box})$	$E_p(RK)$
$\frac{1}{30}$	5.02E-006	3.69E-007	1.13E-005	7.61E-003	1.43E-002	4.34E-003	3.31E-003
$\frac{1}{60}$	2.68E-007	7.32E-009	1.72E-006	1.91E-003	3.31E-003	1.11E-003	9.66E-004
$\frac{1}{120}$	1.47E-008	9.23E-010	2.36E-007	4.79E-004	7.91E-004	2.76E-004	2.59E-004
$\frac{1}{240}$	8.42E-010	1.32E-010	3.02E-008	1.19E-004	1.93E-004	6.93E-005	6.71E-005

Table 3: Maximum absolute error for all methods, $\beta(a) = 6$

h	$E_B(H)$	$E_B(L)$	$E_B(RK)$	$E_w(\text{Box})$	$E_w(RK)$	$E_p(\text{Box})$	$E_p(RK)$
$\frac{1}{30}$	1.35E-002	4.61E-004	3.18E-002	1.66E-002	1.79E-002	2.297	2.73E-001
$\frac{1}{60}$	9.25E-004	9.95E-006	4.83E-003	4.46E-003	4.69E-003	5.69E-001	6.79E-002
$\frac{1}{120}$	6.07E-005	9.16E-007	6.64E-004	1.11E-003	1.25E-003	1.42E-001	1.69E-002
$\frac{1}{240}$	3.89E-006	1.14E-007	8.69E-005	2.78E-004	3.22E-004	3.55E-002	4.24E-003

Table 4a: Maximum absolute error E_p for all methods, $\beta(a) = 6$

t	$E_p^B(H)$	$E_p^B(L)$	$E_p^B(RK)$	$E_p^w(\text{Box})$	$E_p^w(RK)$	$E_p(\text{Box})$	$E_p(RK)$
1	9.25E-004	8.20E-006	3.47E-003	0.135	0.610	0.569	6.79E-002
2	0.137	1.87E-003	0.675	42.398	171.167	121.49	7.86
3	19.446	0.322	112.07	7976.302	21454.825	20474.186	909.378

Table 4b: Maximum relative error E_{prel} for all methods, $\beta(a) = 6$

t	$E_{prel}^B(H)$	$E_{prel}^B(L)$	$E_{prel}^B(RK)$	$E_{prel}^w(\text{Box})$	$E_{prel}^w(RK)$	$E_{prel}(\text{Box})$	$E_{prel}(RK)$
1	2.78E-006	1.12E-007	5.52E-005	1.43E-003	1.29E-002	6.01E-003	1.09E-003
2	5.62E-006	1.97E-007	1.09E-004	3.88E-003	2.29E-002	1.11E-002	2.34E-003

Table 5: Box method: maximum absolute error

h	$p(a, t)$ by $w(a, t)$	$p(a, t)$	$w(a, t)$ by $p(a, t)$	$w(a, t)$
$\frac{1}{30}$	5.51E-001	2.297	1.92E-002	1.66E-002
$\frac{1}{60}$	1.36E-001	5.69E-001	4.88E-003	4.46E-003
$\frac{1}{120}$	3.37E-002	1.42E-001	1.23E-003	1.11E-003
$\frac{1}{240}$	8.40E-003	3.55E-002	3.09E-004	2.78E-004

Table 6: Effective order of convergence for the different methods

h	$\frac{h}{2}$	$\alpha_B(H)$	$\alpha_B(L)$	$\alpha_B(RK)$	$\alpha_w(Box)$	$\alpha_w(RK)$	$\alpha_p(Box)$	$\alpha_p(RK)$
$\frac{1}{30}$	$\frac{1}{60}$	3.86	5.23	2.71	2.01	1.83	2.00	1.98
$\frac{1}{60}$	$\frac{1}{120}$	3.93	3.44	2.86	2.00	1.91	2.00	2.01
$\frac{1}{120}$	$\frac{1}{240}$	3.96	3.00	2.93	2.00	1.95	2.00	1.99

Table 7: $CPU = \sigma$ time (in seconds) needed to calculate $p(a, t)$ by all methods

t/N	$\sigma_p^B(H)$	$\sigma_p^B(L)$	$\sigma_p^B(RK)$	$\sigma_p^w(Box)$	$\sigma_p^w(RK)$	$\sigma_p(Box)$	$\sigma_p(RK)$
1/300	0.015	0.016	0.016	0.047	0.015	0.024	0.062
2/300	0.016	0.031	0.029	0.094	0.057	0.047	0.15
5/300	0.041	0.078	0.071	0.20	0.12	0.12	0.41
7/300	0.062	0.104	0.096	0.26	0.18	0.17	0.63
1/600	0.031	0.047	0.047	0.20	0.078	0.094	0.31
2/600	0.062	0.094	0.094	0.41	0.18	0.19	0.59
5/600	0.15	0.23	0.19	0.84	0.51	0.48	1.55
7/600	0.21	0.33	0.28	1.16	0.75	0.69	2.11

From Table 2 we see that all the methods give good results because of the small values of the solution when $\beta(a) = 2$. However, as we already mentioned the more interesting case is the one with exponential growth when the solution increases very fast. From Table 3 we can see that the errors E_p are much larger than the errors E_B . Since both functions $p(a, t)$ and $B(t)$ grow with an equal rate (see Figure 2.6), this means that the fourth and fifth order methods (H),(RK) and (L) that we have applied to the Renewal equation are more accurate than the second and fourth order (Box) and (RK) methods (applied to Lotka-McKendrick's equation) in the case of exponential growth. Of course the accuracy of these methods is relative to a compact time interval in which all calculations are done. Concerning the age profile, we can see that the second order methods (Box) and (RK) work well in both cases, i.e. $\beta(a) = 2$ and $\beta(a) = 6$, because of the boundedness of the solution $w(a, t)$ (see Figure 2.7). We can also notice that the difference between the errors $E_w(Box)$ and $E_w(RK)$ is very slight even though the Box method is an implicit method and the Runge-Kutta is an explicit method. It follows that when dealing with the equation with the age profile we can apply explicit methods and obtain almost the same accuracy as when using implicit schemes, but gain numerical efficiency (see Table 7). However the main advantage when calculating $w(a, t)$ is that the error remains stable in a long time interval and thus we can apply different methods without losing accuracy.

In Table 4a we see a comparison of the absolute error E_p found by all the algorithms at different times. A fast growth of this error related to the large values of the solution (at $t = 3, a = 0$

the exact solution $p(0, 3) \approx 1259062.86067$) can be observed. In Table 4b we report the relative error E_{prel} of the respective methods. Considering the results given there the reader can see that the large values of the absolute error at time $t = 3$ in Table 4a are due to the large values of the solution but not because of lack of convergence of some of the methods. Of course the smallest errors are $E_p^B(L)$ since Lobatto's method is a fifth order method (and the other methods are of order ≤ 4). If we compare all the fourth order methods, i.e $E_p^B(H)$, $E_p^B(L)$ and $E_p(RK)$ we see that the worst results are for $E_p(RK)$ while the Runge-Kutta and especially the Hybrid methods developed for the integral equation are much more precise. The error accumulated by some of the second order methods increases so fast that at $t = 3$ it blows up. The most inaccurate is $E_p^w(RK)$ in comparison with $E_p(Box)$ and $E_p^w(Box)$. One can explain it with the bigger number of approximations we need to do in order to calculate $p(a, t)$ by means of $w(a, t)$ (see (2.4.14) and (2.4.15)) and of course with the explicitness of the scheme. While in the case of the age profile the difference between an explicit and an implicit method was not so important for the numerical accuracy, here we can see very well the need of applying implicit schemes instead of explicit ones, namely $E_p^w(Box)$ is much smaller than $E_p^w(Box)$. It is clear that finding $p(a, t)$ by $w(a, t)$ when using an implicit scheme is better than the direct calculation of $p(a, t)$ by the same scheme (since $w(a, t)$ is bounded and $p(a, t)$ grows exponentially - see Table 5). It follows that in this case a reasonable decision in terms of numerical accuracy could be to use a high order explicit methods for the integral equation or implicit methods for the equation with the age profile.

Let us now consider the case when we try to approximate $w(a, t)$ by means of $p(a, t)$. Some results are given in Table 5. What we see is that there is almost no difference between the respective errors (see $w(a, t)$ by $p(a, t)$ and $w(a, t)$). The difference comes from the fact that the equation with the age profile is nonlinear which means it is more difficult (and time consuming as well) to develop numerical schemes for than for the linear Lotka-McKendrick's equation. That's why if we need to approximate $w(a, t)$ we can simply do it by treating equation (1.1.1). Our comments can be confirmed by Figure 2.8. In case a), we have drawn the absolute error at $t = 2$ and with $N = 20$ for all the second order methods as follows:

- dashed line: Box method applied to the equation with the age profile;
- thick line: Box method applied to the Lotka-McKendrick's equation;
- thin line: RK method applied to the equation with the age profile;

While the thick and the thin lines are "almost" coinciding, the dashed line is much beneath them which confirms the better accuracy of the Box method for the age profile.

In case b) we have the following graphics:

- dashed thin line: Lobatto's method for the integral equation;
- thin line: Hybrid method for the integral equation;
- thick line: RK method for the integral equation;

- dashed thick line: RK method for the Lotka-McKendrick's equation.

From the plots below we see that the first three lines are much below the dashed thick line (the dashed thin line "almost" coincides with the x-axes), which implies the methods for the integral equation are much more precise than the fourth order Runge-Kutta method applied to the Lotka-McKendrick's equation.

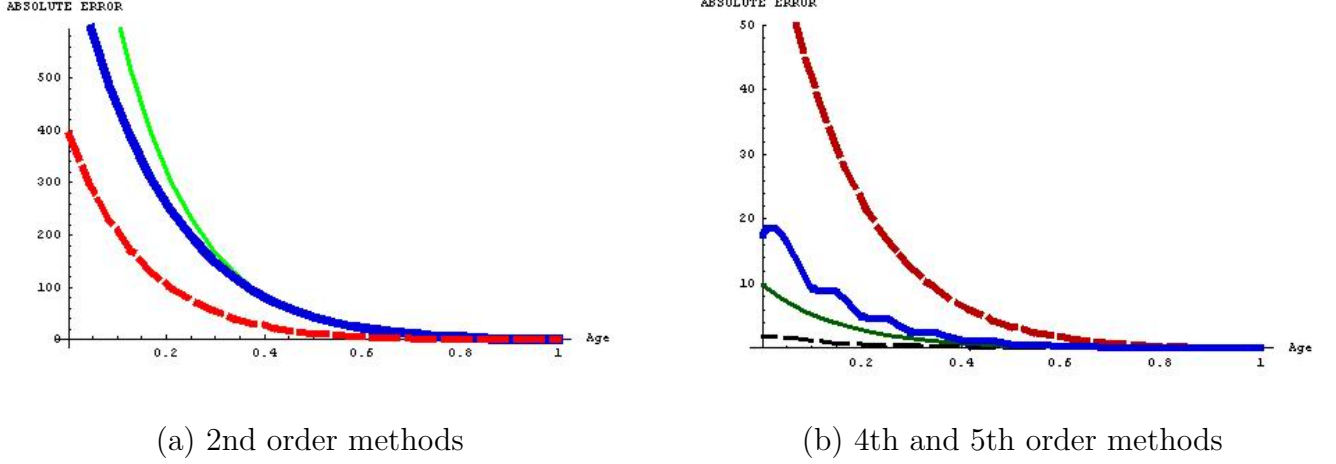


Figure 2.8: Absolute error for $\beta(a) = 6$, $N = 20$ calculated at $t = 2$

Results about the effective order of convergence of the methods can be found in Table 6. The effective order of convergence $\alpha_B(H)$, $\alpha_w(Box)$, $\alpha_w(RK)$ and $\alpha_p(Box)$ coincides with the theoretical order of convergence of the respective methods. In the case of Lobatto's method we do not see fifth order of effective convergence because of the lack of regularity of our test example, i.e. it does not have the needed number of continuous derivatives in order to apply a fifth order method. $\alpha_p(RK) \approx 2$ instead of 4, for the same reason and because of the fact that the test example we use does not satisfy compatibility condition (1.1.5). Both methods were tested with proper test examples and they showed Lobatto fifth and Runge-Kutta fourth order of effective convergence respectively. However, we could not specify why $\alpha_B(RK) \approx 3$ instead of its theoretical rate of convergence 4.

Finally, concerning the numerical efficiency of the methods we can conclude by the results listed in Table 7 that the fastest are the methods for the integral equation since we solve a single variable problem. The most "expensive" as CPU time is the Runge-Kutta method for Lotka-McKendrick's equation. From all the second order methods the slowest is the implicit Box method applied to the equation with age profile. But considering the fact that the given CPU time is in seconds, we can say the difference between $CPU_p^w(Box)$, $CPU_p^w(RK)$ and $CPU_p(Box)$ is not that big.

CHAPTER 3

NUMERICAL TREATMENT OF MODELS INCLUDING DIFFUSION AND AGE

While in Chapter 1 we discussed the numerical treatment of models, including only age, in this chapter we deal with the age-structured problems with spatial dependence presented in Section 1.3. We introduce an improved explicit method, namely Super-Time-Stepping (STS) developed for parabolic problems and we use its modification for the numerical treatment of our models. We explain how the acceleration scheme can be adapted to the age-dependent models. We prove convergence of the method in case of Dirichlet boundary conditions and we demonstrate the accuracy and the efficiency of the modified STS comparing it with other numerical algorithms of same or higher order, namely the explicit, fully implicit and Crank-Nicolson standard schemes. All results are contained in [85] and [87].

3.1. Previous Work on the Topic and Connection with Parabolic Problems - STS Algorithm

During the last years, when modeling how populations change in time, it has been common to take into account not only the age structure of the species, but also their distribution in space. One of the first who introduced spatial spread in age-dependent populations was Gurtin [36]. Later on many other authors have investigated the analytical aspects of various age-structured models with linear or nonlinear diffusion (for instance [17], [21], [22], [63], [74], [78]). Concerning the numerical treatment of the models arising in the field of population dynamics, numerical methods for models including only age or space structure, have been studied extensively (see [86, 90, 92] and the references cited therein). Much less research work has been done on models

that include both - age and space. In the works of Kim [52], Kim-Park [54] and Milner [81], nonlinear models with nonlinear diffusion are treated. They propose and analyze some mixed numerical algorithms combining finite difference methods along the characteristic lines and finite element methods in the spatial variables. In the case of linear fertility and mortality functions, Lopez and Trigiante [68] have developed a finite difference scheme for an age-dependent model with Dirichlet boundary conditions and linear population flux. Ayati [11] proposes a numerical method for a nonlinear model with nonlinear diffusion which allows the use of variable time steps and independent age and time discretization.

In the following we propose a variation of the standard explicit scheme for the heat equation adapted for solving age-dependent population models with linear spatial diffusion. One of the main ideas we use is that along characteristics in the age-time direction the models presented in the previous chapter (Section 1.3) can be viewed as parabolic differential equations. The super-time-stepping (STS) algorithm that we employ is an acceleration method for explicit schemes for parabolic problems. The method is almost 30 years old and has been first introduced by Gentzsch [34], [35]. STS relaxes the condition of stability at the end of every time step that is imposed for the normal explicit scheme and demands stability at the end of every super-step, where a super-step consists of K sub-steps. It implies that we can take larger time steps and consequently the total number of steps is reduced speeding up the computations, compared with the standard explicit scheme.

Adopting the assumptions for the fertility and the mortality functions, made in Section 1.1 (see 1.1.2 and the assumptions below it) and considering the problems with the mortality at the end-point a_+ explained in Section 2.3, we make the following substitution:

$$\begin{aligned} u(a, t, x) &= \frac{p(a, t, x)}{\pi(a)} \\ v(a, t, x) &= \frac{w(a, t, x)}{\pi(a)} \end{aligned}$$

and then plugging the new variables u and v into equations (1.3.1), (1.3.2) and (1.3.5) respectively, we obtain:

$$\begin{cases} 1) u_t + u_a = Du_{xx}, & a \in [0, a_+], t > 0, x \in (0, 1) \\ 2) u(0, t, x) = \int_0^{a_+} \beta(a)\pi(a)u(a, t, x) da = B(t, x), & t > 0, x \in (0, 1) \\ 3) u(a, 0, x) = u_0(a, x), & a \in [0, a_+], x \in (0, 1) \\ 4) u(a, t, 0) = u(a, t, 1) = 0 \quad or \quad u_x(a, t, 0) = u_x(a, t, 1) = 0, & a \in [0, a_+], t > 0 \end{cases} \quad (3.1.1)$$

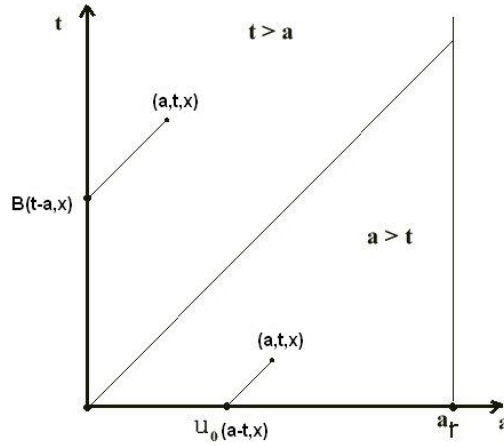
$$\left\{ \begin{array}{l} 1) v_t + v_a + v \int_0^1 \int_0^{a_+} [(\beta(a) - \mu(a))\pi(a)]v(a, t, x)dadx = Dv_{xx}, \quad a \in [0, a_+], t > 0, x \in (0, 1) \\ 2) v(0, t, x) = \int_0^{a_+} \beta(a)\pi(a)v(a, t, x)da, \quad t > 0, x \in (0, 1) \\ 3) \int_0^1 \int_0^{a_+} v(a, t, x)\pi(a)dadx = 1, \quad t > 0 \\ 4) v(a, 0, x) = v_0(a, x), \quad a \in [0, a_+], x \in (0, 1) \\ 5) v_x(a, t, 0) = v_x(a, t, 1) = 0, \quad a \in [0, a_+], t > 0 \end{array} \right. \quad (3.1.2)$$

Written in this way, the qualitative features of the discussed models are preserved but there is no more problem with their numerical treatment (see Section 2.3). Because of this reason in the sequel we shall apply numerical schemes on equations (3.1.1) and 3.1.2) and once knowing their approximate solution $u(a, t, x)$ and $v(a, t, x)$ respectively, we will multiply it by $\pi(a)$ in order to yield results for $p(a, t, x)$ and $w(a, t, x)$ respectively.

We now give the connection between (3.1.1) and the heat equation and we present the super-time-stepping method for parabolic equations. Let us make the following substitution

$$\gamma(s, x) = u(a_0 + s, t_0 + s, x), \quad (3.1.3)$$

where (a_0, t_0) is a certain point of the characteristic line $t = a + s$ (or $a = t + s$) as shown on the figure below.



Thus, we obtain:

$$\left\{ \begin{array}{l} \gamma_s = u_a + u_t = Du_{xx}(a_0 + s, t_0 + s, x) = D\gamma_{xx} \\ \gamma(s, 0) = \gamma(s, 1) = 0 \quad or \quad \gamma_x(s, 0) = \gamma_x(s, 1) = 0 \\ \gamma(0, x) = u(a_0, t_0, x), \end{array} \right. \quad (3.1.4)$$

where if $a_0 > t_0$, then $u(a_0 + s, t_0 + s, x) = u_0(a, x)$ and $u(a_0 + s, t_0 + s, x) = B(t, x)$ vice versa (see the figure above). This means that along the characteristic lines we can write the governing equation in (3.1.1) as:

$$\gamma_t = D\gamma_{xx}, \quad t > 0, x \in (0, 1) \quad (3.1.5)$$

coupled with Dirichlet or Neumann boundary conditions:

$$\gamma(t, 0) = \gamma(t, 1) = 0 \quad \text{or} \quad \gamma_x(t, 0) = \gamma_x(t, 1) = 0, \quad t > 0 \quad (3.1.6)$$

and initial conditions:

$$\gamma(0, x) = \gamma_0(x), \quad x \in (0, 1) \quad (3.1.7)$$

Consequently an approximation of this problem by a standard Euler explicit scheme is given by

$$\begin{cases} 1) \gamma_i^{n+1} = \frac{D\tau}{h^2} \gamma_{i-1}^n + (1 - \frac{2D\tau}{h^2}) \gamma_i^n + \frac{D\tau}{h^2} \gamma_{i+1}^n, & i = 1, \dots, M-1; n = 0, \dots, N-1 \\ 2) \gamma_0^{n+1} = 0 \quad \text{or} \quad \gamma_0^{n+1} = (1 - \frac{2D\tau}{h^2}) \gamma_0^n + \frac{2D\tau}{h^2} \gamma_1^n, & n = 0, \dots, N-1 \\ 3) \gamma_M^{n+1} = 0 \quad \text{or} \quad \gamma_M^{n+1} = \frac{2D\tau}{h^2} \gamma_{M-1}^n + (1 - \frac{2D\tau}{h^2}) \gamma_M^n, & n = 0, \dots, N-1 \\ 4) \gamma(0, x) = \gamma_0(x), \end{cases} \quad (3.1.8)$$

where τ is the step size in time; h is the mesh size in space; by γ_i^{n+1} we have denoted an approximation of the exact solution $\gamma(s, x)$ at the mesh point (t^{n+1}, x_i) and for the end points $i = 0$ and $i = M$ we have employed a central-difference approximation (with a "fictitious" point) (see [90, 92]) in case of Neumann boundary conditions. Rewriting the scheme in a suitable way, we get:

$$\begin{cases} \gamma^{n+1} = A\gamma^n, & n = 0, \dots, N-1 \\ \gamma^0 = \gamma_0, \end{cases} \quad (3.1.9)$$

where A is an $(M-1) \times (M-1)$ symmetric, tri-diagonal, positive definite matrix [92] and γ^n denotes a column vector with $M-1$ elements.

Even though this scheme is computationally simple, it has a serious drawback - the scheme is stable if the time step is very small, namely $\tau \leq \frac{2}{\lambda_{max}}$ (λ_{max} is the biggest eigenvalue of the matrix A). This is the so called Courant-Friedrichs-Lewy condition (CFL), which in our case is: $\tau \leq \frac{h^2}{2D}$. Aiming to overcome this drawback and to increase the efficiency of the method by a slight modification in the code while keeping the accuracy at the same time we use the STS method for parabolic problems (see [6], [34]) whose idea is to require stability only at the end of a super-step ΔT , consisting of K sub-steps $\tau_1, \tau_2, \dots, \tau_K$ with different length. These inner steps have no particular approximation properties and can be chosen explicitly in such a way

that stability is ensured over the super-step

$$\Delta T = \sum_{k=1}^K \tau_k \quad (3.1.10)$$

Consequently the method can be associated with Runge-Kutta type methods with K stages. Alexiades [6] uses the optimality properties of some modified Chebishev polynomials to give the following formula for τ_k :

$$\tau_k = \tau((-1 + \nu) \cos(\frac{(2k-1)\pi}{2K}) + 1 + \nu)^{-1}, \quad k = 1, \dots, K \quad (3.1.11)$$

where τ is the time step for the explicit scheme, calculated in such a way that the CFL (stability) condition is satisfied; ν is a number in the interval $(0, \frac{\lambda_{min}}{\lambda_{max}}]$ with λ_{min} and λ_{max} being the smallest and the biggest eigenvalues respectively of the matrix A in (3.1.9).

From the equation above it can be shown [6] that:

$$\Delta T \rightarrow K^2 \tau \quad as \quad \nu \rightarrow 0$$

Analyzing this result we can conclude that for ν being close to 0 the super-step ΔT is K times faster than an explicit time step, i.e. the length of the time interval covered when executing K explicit steps $K\tau$ is K times shorter than a super-step, consisting of K sub-steps. Hence, by a proper choice of K and ν , STS can accelerate an explicit scheme for parabolic equations up to K times. In [6] it is shown that for each choice of K the standard explicit scheme (3.1.8-1), applied to equation (3.1.5), coupled with Dirichlet boundary conditions is stable and accurate for larger ν (< 1). But the larger the damping factor ν is, shorter ΔT becomes, trading accuracy for speed. When ν is small, the method is faster but less accurate which can be expected, since the time steps become larger. The same subordination can also be seen by our experiments.

3.2. Modified STS for Age-Structured Problems

Inspired by the approach described above, we note that the age of species changes at the same rate as the time passes, so we assume the step size in age identical to the step size in time and along the characteristic lines, we have the following numerical grid:

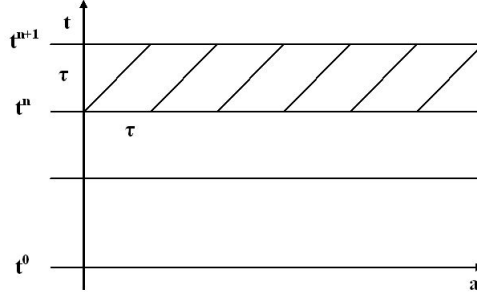


Figure 3.1: Along the characteristics

where $\tau > 0$ is the age and time discretization parameter and $\tau = \frac{a_+}{N}$ (N is the total number of subintervals in time). Let $h = \frac{1}{M}$ is the discretization step in space where M is the number of subintervals in space. Let $L = \frac{M}{a_+}$ be the number of discrete age steps. Then for each time level $t^n = n\tau$, $n = 0, \dots, N$ we have the following grid: $\Gamma = \{(a^j, x_i) : a^j = j\tau, j = 0, \dots, L; x_i = ih, i = 0, \dots, M\}$. Let the discrete function U_i^j be an approximation of the solution of (3.1.5) at time level t^n at grid point (a^j, x_i) and \hat{U}_i^{j+1} - at time level t^{n+1} at grid point (a^{j+1}, x_i) . Then we approximate the directional derivative $\frac{\partial}{\partial t} + \frac{\partial}{\partial a}$, setting

$$\left(\frac{\partial}{\partial t} + \frac{\partial}{\partial a}\right) u(a^j, t^n, x_i) \approx \frac{\hat{U}_i^{j+1} - U_i^j}{\tau} \quad (3.2.1)$$

and the Laplace operator

$$U_{xx} = \frac{U_{i-1}^j - 2U_i^j + U_{i+1}^j}{h^2} \quad (3.2.2)$$

Thus, an approximation of problem (3.1.1) (analogous to the one we applied to the heat equation) is as follows (see Figure 3.1):

$$\begin{cases} 1) \hat{U}_i^{j+1} = \frac{D\tau}{h^2} U_{i-1}^j + (1 - \frac{2D\tau}{h^2}) U_i^j + \frac{D\tau}{h^2} U_{i+1}^j, & i = 1, \dots, M-1; j = 0, \dots, L-1 \\ 2) \hat{U}_0^{j+1} = 0 \quad or \quad \hat{U}_0^{j+1} = (1 - \frac{2D\tau}{h^2}) U_0^j + \frac{2D\tau}{h^2} U_1^j, & j = 0, \dots, L-1 \\ 3) \hat{U}_M^{j+1} = 0 \quad or \quad \hat{U}_M^{j+1} = \frac{2D\tau}{h^2} U_{M-1}^j + (1 - \frac{2D\tau}{h^2}) U_M^j, & j = 0, \dots, L-1 \end{cases} \quad (3.2.3)$$

Proceeding as in the case without age-structure we rewrite (3.2.3) in the form

$$\hat{U}^{j+1} = AU^j, \quad j = 0, \dots, L-1 \quad (3.2.4)$$

where A is again an $(M-1) \times (M-1)$ symmetric, tri-diagonal, positive definite matrix.

At the initial time $t = 0$ we consider $U_i^j = \frac{p_0(a^j, x_i)}{\pi(a^j)}$, $j = 0, \dots, L$, $i = 0, \dots, M$ and for the

boundary condition (3.1.1-2) we apply the trapezoidal rule, obtaining

$$\hat{U}_i^0 = \tau \sum_{j=1}^{L-1} \beta_j \pi(a_j) \hat{U}_i^j + \frac{\tau}{2} [\beta_0 \pi(a_0) \hat{U}_i^0 + \beta_L \pi(a_L) \hat{U}_i^L], \quad i = 0, \dots, M \quad (3.2.5)$$

The previous description concerns a uniform grid (see Figure 3.1). Wishing to adapt STS to the age-structured problems, we consider a mesh as shown in Figure 3.2, which shows how one super-step looks like.

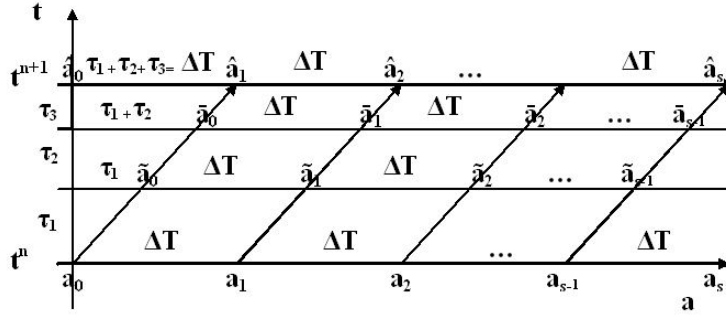


Figure 3.2: One super-time-step with $K = 3$ intermediate steps

The vertical and horizontal axes present the time and the age distributions respectively; τ_k , $k = 1, \dots, K$ are the inner-time-steps (on the graph we have drawn one super-step, consisting of three sub-steps). The first difference with STS for parabolic problems is that when stepping in time, we move also in age. Another particularity is that we have to calculate the solution at the boundary points as well. Because of these reasons, for the implementation of the modified STS scheme we proceed as follows: first we choose the value of ν and the number of intermediate steps, K ; then we calculate τ_k , $k = 1, \dots, K$, the length of ΔT and $s = \frac{a_+ K}{\Delta T}$ the number of age-nodes (see Figure 3.2), which depends on the choice of K . To initialize the procedure, we consider the discrete solution identical to the analytical solution at time $T=0$. Next we start using sub-steps τ_k , $k = 1, \dots, K$ in time. Since we have multiple age nodes at each time level, we re-number the "inner" age-nodes in a convenient way (as shown on Figure 3.2) and we calculate the discrete solution at the k^{th} inner time level $k = 1, \dots, K - 1$ as follows:

$$\begin{cases} \hat{U}_i^j = \frac{D\tau_k}{h^2} U_{i-1}^j + (1 - \frac{2D\tau_k}{h^2}) U_i^j + \frac{D\tau_k}{h^2} U_{i+1}^j, & i = 1, M-1; j = 0, \dots, s-1 \\ \hat{U}_0^j = \hat{U}_M^j = 0, & j = 0, \dots, s-1 \quad \text{or} \\ \hat{U}_0^j = (1 - \frac{2D\tau_k}{h^2}) U_0^j + \frac{2D\tau_k}{h^2} U_1^j, \hat{U}_M^j = \frac{2D\tau_k}{h^2} U_{M-1}^j + (1 - \frac{2D\tau_k}{h^2}) U_M^j, & j = 0, \dots, s-1 \end{cases} \quad (3.2.6)$$

where U_i^j is the discrete solution at the $(k-1)^{st}$ time level and we consider it as known. One can see that within one super-step, we do not use the value of the discrete solution at the boundary

points and that's why we do not calculate it. Another specification is that the discrete solution at the inner time levels has no particular approximation properties and consequently we do not output it. We use the approximation only at the end inner time-level K corresponding to time level t^{n+1} , found by formula (3.2.3), but with time step τ_K , i.e. $\tau = \tau_K$. At this level we calculate the solution at the boundary point as well, by formula (3.2.5) and time step ΔT . The described procedure is repeated for each super-step and continues until we reach the end of the time interval.

In the nonlinear case (3.1.2), we proceed in an analogous way. The only difference here is that we need to approximate the double integral in the first equation with a proper quadrature formula, namely we use the trapezoidal rule. Since we employ an explicit scheme, its application is trivial. The modified STS procedure is also easy to use once we have developed it for the linear model. The difficulty comes from the fact that for the nonlinear problem no theoretical results are available. This implies that we cannot determine the upper bound for the parameter ν , but the results show that this is not a real obstacle since we can choose ν as a suitable number in the interval $(0, 1)$ [5] and apply the modified STS also in this case. The good performance of STS-like algorithms for degenerate nonlinear parabolic problems is given in [27]. A method for an automatic time-step selection for STS applied to a Stefan-like problem, is proposed in [66]. While with a proper choice of K and ν , STS can accelerate an explicit scheme for parabolic equations up to K times (3.1.12), in our case, as we do steps in time and in age, modified STS can speed up the explicit scheme up to K^2 times. If we consider also the fact that by the STS modification, we calculate the boundary condition much less frequently (we calculate it only at the end of each super-step) in comparison with the explicit scheme, this means the acceleration is even bigger.

3.3. Convergence of the Method

We shall show in this Section that under certain conditions on regularity of the coefficients of (3.1.1), the approximate solution defined by the modified STS converges to u , uniformly in ΔT , as $\Delta T \rightarrow 0$.

Let us first note that the formula of integration by parts

$$f(\Delta T) - f(0) = \Delta T f'(0) + \int_0^{\Delta T} (\Delta T - s) f''(s) ds$$

is equivalent to

$$f'(0) = \frac{f(\Delta T) - f(0)}{\Delta T} - \frac{1}{\Delta T} \int_0^{\Delta T} (\Delta T - s) f''(s) ds \quad (3.3.1)$$

Using that formula and equation (3.1.1-1) it can be shown that

$$\frac{u(a + \Delta T, t + \Delta T, x) - u(a, t, x)}{\Delta T} = D \frac{\partial^2 u(a, t, x)}{\partial x^2} + \frac{1}{\Delta T} \int_0^{\Delta T} (\Delta T - s) \frac{\partial^2 u}{\partial \xi^2}(a + s, t + s, x) ds, \quad (3.3.2)$$

where we have considered the directional derivative in the characteristic direction $\xi = \frac{1}{\sqrt{2}}(1, 1)$:

$$\frac{\partial}{\partial \xi} = \left(\frac{\partial}{\partial t}, \frac{\partial}{\partial a} \right) \cdot \xi$$

Thus, for $0 \leq i \leq M$, $0 \leq j \leq N_s$, $0 \leq n \leq N_t$ (N_s and N_t represent the number of subintervals in age and time respectively; $N_t = TN_s$ (since for simplicity we assume $a_+ = 1$) and we use the notation introduced in Section 3.2, replacing the step-size τ in age and time by ΔT) we have

$$\frac{\hat{u}_i^{j+1} - u_i^j}{\Delta T} - D \frac{\partial^2 u_i^j}{\partial x_i^2} = \frac{1}{\Delta T} \int_0^{\Delta T} (\Delta T - s) \frac{\partial^2 u}{\partial \xi^2}(a^j + s, t^n + s, x_i) ds, \quad (3.3.3)$$

which can be rewritten in the following form

$$\hat{u}_i^{j+1} = u_i^j + D \Delta T \frac{\partial^2 u_i^j}{\partial x_i^2} + \int_0^{\Delta T} (\Delta T - s) \frac{\partial^2 u}{\partial \xi^2}(a^j + s, t^n + s, x_i) ds \quad (3.3.4)$$

Let us now introduce the approximation error ε , defined by

$$\begin{cases} \varepsilon_i^j = u(a^j, t^n, x_i) - U_i^j = u_i^j - U_i^j, \\ \hat{\varepsilon}_i^{j+1} = u(a^{j+1}, t^{n+1}, x_i) - \hat{U}_i^{j+1} = \hat{u}_i^{j+1} - \hat{U}_i^{j+1}, \end{cases} \quad (3.3.5)$$

for $0 \leq i \leq M$, $0 \leq j \leq N_s$, $0 \leq n \leq N_t$.

For readers' convenience we give the definition of some norms, associated with ε :

$$\begin{aligned} \|\varepsilon_i\|_{l^1} &= \Delta T \sum_{j=0}^{N_s} |\varepsilon_i^j|, \\ \|\varepsilon\|_{l^1}^\infty &= \Delta T \max_{0 \leq i \leq M} \sum_{j=0}^{N_s} |\varepsilon_i^j|, \\ \|\varepsilon\|_{l^\infty}^\infty &= \max_{0 \leq i \leq M} \max_{0 \leq j \leq N_s} \{|\varepsilon_i^j|\}, \end{aligned} \quad (3.3.6)$$

Here is the result about the convergence of the modified STS:

Theorem 1. *Let the solution $u(a, t, x)$ of (3.1.1) with conditions of Dirichlet on the boundary be continuously differentiable for $(a, t, x) \in (0, a_+) \times (0, T) \times (0, 1)$ and its derivatives are bounded. Then, there exists a constant $C > 0$ (independent of ΔT and depending on the norms indicated below), such that*

$$\begin{aligned} a) \|\varepsilon\|_l^\infty &\leq C \left(\|\tilde{\beta}\|_{L^\infty} + \left\| \frac{\partial u}{\partial t} \right\|_{L^\infty} + \left\| \frac{\partial u}{\partial a} \right\|_{L^\infty} + \left\| \frac{\partial^2 u}{\partial \xi^2} \right\|_{L^\infty} \right) \Delta T, \\ b) \|\varepsilon\|_l^\infty &\leq C \left(\|\tilde{\beta}\|_{L^\infty} + \left\| \frac{\partial u}{\partial t} \right\|_{L^\infty} + \left\| \frac{\partial u}{\partial a} \right\|_{L^\infty} + \left\| \frac{\partial^2 u}{\partial \xi^2} \right\|_{L^\infty} \right) \Delta T, \end{aligned} \quad (3.3.7)$$

where with $\tilde{\beta}$ we have denoted the function $\tilde{\beta}(a) = \beta(a)\pi(a)$.

Proof:

1) If $i > K$

Let us consider K intermediate steps within one super-step (see Figure 3.2). Then, after one step in time ΔT , we have the following more convenient form of the modified STS scheme:

$$\begin{aligned} \hat{U}_i^{j+1} &= c_K(U_{i-K}^j + U_{i+K}^j) + c_{K-1}(U_{i-K+1}^j + U_{i+K-1}^j) + \dots \\ &\quad + c_1(U_{i-1}^j + U_{i+1}^j) + c_0(U_i^j), \quad i = 1, \dots, M-1, j = 0, \dots, N_s-1 \end{aligned} \quad (3.3.8)$$

where c_k , $k = 0, \dots, K$ are **positive** (and **bounded**) coefficients which can be obtained explicitly by formula (3.3.10) given below. Subtracting (3.3.8) from (3.3.4) we obtain, for $i = 1, \dots, M-1, j = 0, \dots, N_s-1, 0 \leq n \leq N_t-1$ the following error equation:

$$\begin{aligned} \hat{\varepsilon}_i^{j+1} &= \hat{u}_i^{j+1} - \hat{U}_i^{j+1} = \\ &= u_i^j + D\Delta T \frac{\partial^2 u_i^j}{\partial x_i^2} + \int_0^{\Delta T} (\Delta T - s) \frac{\partial^2 u}{\partial \xi^2}(a^j + s, t^n + s, x_i) ds - c_K(U_{i-K}^j + U_{i+K}^j) - \\ &\quad - c_{K-1}(U_{i-K+1}^j + U_{i+K-1}^j) - \dots - c_i(U_0^j + U_{2i}^j) - \dots - c_1(U_{i-1}^j + U_{i+1}^j) - c_0(U_i^j) \end{aligned}$$

We add and subtract the exact solution in mesh points $(a^j, t^n, x_{i-K}), (a^j, t^n, x_{i+K}), (a^j, t^n, x_{i-K+1}), (a^j, t^n, x_{i+K-1}), \dots, (a^j, t^n, x_0)$, multiplied by proper coefficients and thus, we obtain:

$$\begin{aligned} \hat{\varepsilon}_i^{j+1} &= u_i^j + D\Delta T \frac{\partial^2 u_i^j}{\partial x_i^2} + \int_0^{\Delta T} (\Delta T - s) \frac{\partial^2 u}{\partial \xi^2}(a^j + s, t^n + s, x_i) ds + c_K(\varepsilon_{K+i}^j + \varepsilon_{i-K}^j) + \\ &\quad + c_{K-1}(\varepsilon_{i+K-1}^j + \varepsilon_{i-K+1}^j) + \dots + c_i(\varepsilon_{2i}^j + \varepsilon_0^j) + \dots + c_1(\varepsilon_{i-1}^j + \varepsilon_{i+1}^j) + c_0(\varepsilon_i^j) - \\ &\quad - c_K(u_{i-K}^j + u_{i+K}^j) - c_{K-1}(u_{i-K+1}^j + u_{i+K-1}^j) - \dots - c_i(u_0^j + u_{2i}^j) - \dots \\ &\quad - c_1(u_{i-1}^j + u_{i+1}^j) - c_0(u_i^j) \end{aligned}$$

Using Taylor expansions we have:

$$u_{i+k}^j = u(a^j, t^n, x_i + kh) = u_i^j + kh \frac{\partial u_i^j}{\partial x_i} + \frac{k^2 h^2}{2!} \frac{\partial^2 u_i^j}{\partial x_i^2} + \frac{k^3 h^3}{3!} \frac{\partial^3 u_i^j}{\partial x_i^3} + O(h^4)$$

$$u_{i-k}^j = u(a^j, t^n, x_i - kh) = u_i^j - kh \frac{\partial u_i^j}{\partial x_i} + \frac{k^2 h^2}{2!} \frac{\partial^2 u_i^j}{\partial x_i^2} - \frac{k^3 h^3}{3!} \frac{\partial^3 u_i^j}{\partial x_i^3} + O(h^4)$$

which implies:

$$u_{i+k}^j + u_{i-k}^j = 2u_i^j + k^2 h^2 \frac{\partial^2 u_i^j}{\partial x_i^2} + O(h^3)$$

Hence we see that:

$$\begin{aligned} \varepsilon_i^{j+1} &= u_i^j + D\Delta T \frac{\partial^2 u_i^j}{\partial x_i^2} + \int_0^{\Delta T} (\Delta T - s) \frac{\partial^2 u}{\partial \xi^2}(a^j + s, t^n + s, x_i) ds + c_K(\varepsilon_{i+K}^j + \varepsilon_{i-K}^j) + \\ &\quad + c_{K-1}(\varepsilon_{i+K-1}^j + \varepsilon_{i-K+1}^j) + \dots + c_i(\varepsilon_{2i}^j + \varepsilon_0^j) + \dots + c_1(\varepsilon_{i-1}^j + \varepsilon_{i+1}^j) + c_0(\varepsilon_i^j) - \\ &\quad - c_K(2u_i^j + K^2 h^2 \frac{\partial^2 u_i^j}{\partial x_i^2}) - c_{K-1}(2u_i^j + (K-1)^2 h^2 \frac{\partial^2 u_i^j}{\partial x_i^2}) - \dots \\ &\quad - c_1(2u_i^j + h^2 \frac{\partial^2 u_i^j}{\partial x_i^2}) - c_0(u_i^j) + O(h^3) = \\ &= u_i^j + D\Delta T \frac{\partial^2 u_i^j}{\partial x_i^2} + \int_0^{\Delta T} (\Delta T - s) \frac{\partial^2 u}{\partial \xi^2}(a^j + s, t^n + s, x_i) ds + c_K(\varepsilon_{i+K}^j + \varepsilon_{i-K}^j) + \\ &\quad + c_{K-1}(\varepsilon_{i+K-1}^j + \varepsilon_{i-K+1}^j) + \dots + c_i(\varepsilon_{2i}^j + \varepsilon_0^j) + \dots + c_1(\varepsilon_{i-1}^j + \varepsilon_{i+1}^j) + \\ &\quad + c_0(\varepsilon_i^j) - h^2(K^2 c_K + (K-1)^2 c_{K-1} + \dots c_1) \frac{\partial^2 u_i^j}{\partial x_i^2} - \\ &\quad - (2c_K + 2c_{K-1} + \dots 2c_1 + c_0)u_i^j + O(h^3) \end{aligned} \quad (3.3.9)$$

We shall give some results about the coefficients (3.3.8) of the method: the coefficients c_l^k , $l = 0, \dots, k$ at the t^k intermediate time level $k = 1, \dots, K$ can be obtained by the following recursive formulas

$$\begin{aligned} c_0^k &= (1 - 2\sigma_k)c_0^{k-1} + 2\sigma_k c_1^{k-1}, \\ c_l^k &= \sigma_k(c_{l-1}^{k-1} + c_{l+1}^{k-1}) + (1 - 2\sigma_k)c_l^{k-1}, \quad l = 1, \dots, k-1, \\ c_k^k &= \sigma_k c_{k-1}^{k-1}, \end{aligned} \quad (3.3.10)$$

where $\sigma_k = \frac{D\tau_k}{h^2}$; c_l^{k-1} , $l = 0, \dots, k-1$ are the (non-zero) coefficients of the previous $(k-1)^{\text{st}}$ intermediate time level and $c_l^{k-1} = 0$ for $l \geq k$, i.e. if a super-step consists of K sub-steps, then for each sub-step k , $k = 1, \dots, K$ we calculate the discrete solution by using formula (3.3.10), where all c_l^k , $l = 0, \dots, k$ are dependent on the coefficients c_l^{k-1} , $l = 0, \dots, k-1$ of the $(k-1)^{\text{st}}$ sub-step as shown above and to initiate this procedure we assume that at the beginning $c_0^0 = 1$, $c_l^0 = 0$, $l \geq 1$. Under these conditions the following statements hold:

Proposition 1. *At each (also intermediate) time level t^k , we have:*

$$2c_k^k + 2c_{k-1}^k + \dots + 2c_1^k + c_0^k = 1, \quad k = 1, \dots, K \quad (3.3.11)$$

Proof: We will prove this statement by mathematical induction. Let $k = 1$, then using formula (3.3.10) we yield

$$\begin{aligned} c_0^1 &= 1 - 2\sigma_1 \\ c_1^1 &= \sigma_1 \end{aligned}$$

i.e. $2c_1^1 + c_0^1 = 1$. Let us assume that the equality holds for the first $k - 1$ intermediate steps; we shall show it is valid for the k^{th} sub-step. Using again (3.3.10) we obtain

$$\begin{aligned}
 c_0^k + 2c_1^k + \dots + 2c_k^k &= (1 - 2\sigma_k)c_0^{k-1} + 2\sigma_k c_1^{k-1} + 2\sigma_k c_{k-1}^{k-1} + 2\sigma_k \sum_{l=1}^{k-1} (c_{l-1}^{k-1} + c_{l+1}^{k-1}) + \\
 &\quad + 2(1 - 2\sigma_k) \sum_{l=1}^{k-1} c_l^{k-1} = \\
 &= (1 - 2\sigma_k)c_0^{k-1} + 2\sigma_k c_1^{k-1} + 2\sigma_k c_{k-1}^{k-1} + 2\sigma_k \sum_{l=0}^{k-2} c_l^{k-1} + 2\sigma_k \sum_{l=2}^k c_l^{k-1} + 2(1 - 2\sigma_k) \sum_{l=1}^{k-1} c_l^{k-1} = \\
 &= (1 - 2\sigma_k)c_0^{k-1} + 2\sigma_k \sum_{l=1}^{k-1} c_l^{k-1} + 2\sigma_k c_0^{k-1} + 2\sigma_k \sum_{l=1}^{k-1} c_l^{k-1} + 2\sigma_k c_k^{k-1} + 2 \sum_{l=1}^{k-1} c_l^{k-1} - 4\sigma_k \sum_{l=1}^{k-1} c_l^{k-1} = \\
 &= c_0^{k-1} + 2 \sum_{l=1}^{k-1} c_l^{k-1} + 2\sigma_k c_k^{k-1} = c_0^{k-1} + 2 \sum_{l=1}^{k-1} c_l^{k-1} = 1,
 \end{aligned}$$

where we have used that since c_l^{k-1} , $l = 0, \dots, k - 1$ are the coefficients of level $k - 1$, then $c_l^{k-1} = 0$ for $l \geq k$.

Proposition 2. *At each time level t^k , we have:*

$$k^2 c_k^k + (k - 1)^2 c_{k-1}^k + \dots + c_1^k = \frac{D(\tau_1 + \tau_2 + \dots + \tau_k)}{h^2}, \quad k = 1, \dots, K$$

In particular, for the last sub-level $k = K$, this sum is exactly $\frac{D\Delta T}{h^2}$ (since a super-step ΔT consists of K sub-steps).

Proof: The proof of Proposition 2 is analogous to that of Proposition 1. In order to verify it, we shall again use mathematical induction, adopting the notation we introduced above. Let $k = 1$, then we obtain the following result for the coefficients of (3.3.8):

$$c_1^1 = \sigma_1 = \frac{D\tau_1}{h^2}$$

We assume the equality holds for $k - 1$ intermediate steps, using (3.3.10) we shall verify it for the k^{th} sub-step:

$$\begin{aligned}
 k^2 c_k^k + (k - 1)^2 c_{k-1}^k + \dots + c_1^k &= \sigma_k k^2 c_{k-1}^{k-1} + \sigma_k \sum_{l=1}^{k-1} l^2 (c_{l-1}^{k-1} + c_{l+1}^{k-1}) + (1 - 2\sigma_k) \sum_{l=1}^{k-1} l^2 c_l^{k-1} = \\
 &= \sigma_k \left[1^2 c_0^{k-1} + 2^2 c_1^{k-1} + (1^2 + 3^2) c_2^{k-1} + \dots + \left((k - 3)^2 + (k - 1)^2 \right) c_{k-2}^{k-1} + \right. \\
 &\quad \left. + \left((k - 2)^2 + k^2 \right) c_{k-1}^{k-1} \right] + (1 - 2\sigma_k) \sum_{l=1}^{k-1} l^2 c_l^{k-1} = \\
 &= 2\sigma_k \left[c_1^{k-1} + 2^2 c_2^{k-1} + 3^2 c_3^{k-1} + \dots + (k - 2)^2 c_{k-2}^{k-1} + (k - 1)^2 c_{k-1}^{k-1} \right] + \\
 &\quad + \sigma_k \left[c_0^{k-1} + 2c_1^{k-1} + 2c_2^{k-1} + 2c_3^{k-1} + \dots + 2c_{k-2}^{k-1} + 2c_{k-1}^{k-1} \right] + (1 - 2\sigma_k) \sum_{l=1}^{k-1} l^2 c_l^{k-1}
 \end{aligned}$$

Using the result obtained in Proposition 1, we have:

$$\begin{aligned} k^2 c_k^k + (k-1)^2 c_{k-1}^k + \dots + c_1^k &= \sigma_k + \sum_{l=1}^{k-1} l^2 c_l^{k-1} = \sigma + \frac{D(\tau_1 + \tau_2 + \dots + \tau_{k-1})}{h^2} = \\ &= \frac{D(\tau_1 + \tau_2 + \dots + \tau_k)}{h^2} = \frac{D\Delta T}{h^2} \end{aligned}$$

and thus, we finish the proof.

Remark: We underline that in the sequel by c_l , $l = 0, \dots, K$ we have denoted the coefficients of the last K^{th} level of each super-step and that's why we have skipped their upper index.

Substituting with these results into the error equation (3.3.9), we readily obtain:

$$\begin{aligned} \varepsilon_i^{j+1} &= \int_0^{\Delta T} (\Delta T - s) \frac{\partial^2 u}{\partial \xi^2}(a^j + s, t^n + s, x_i) ds + c_K(\varepsilon_{i+K}^j + \varepsilon_{i-K}^j) + c_{K-1}(\varepsilon_{i+K-1}^j + \varepsilon_{i-K+1}^j) + \\ &+ \dots + c_i(\varepsilon_{2i}^j + \varepsilon_0^j) + \dots + c_1(\varepsilon_{i-1}^j + \varepsilon_{i+1}^j) + c_0(\varepsilon_i^j) + O(h^3) \end{aligned} \quad (3.3.12)$$

We take the absolute values of (3.3.12) to deduce that:

$$\begin{aligned} |\varepsilon_i^{j+1}| &= \left| \int_0^{\Delta T} (\Delta T - s) \frac{\partial^2 u}{\partial \xi^2}(a^j + s, t^n + s, x_i) ds \right| + |c_K(\varepsilon_{i+K}^j + \varepsilon_{i-K}^j)| + \\ &+ |c_{K-1}(\varepsilon_{i+K-1}^j + \varepsilon_{i-K+1}^j)| + \dots + |c_i(\varepsilon_{2i}^j + \varepsilon_0^j)| + \dots + |c_1(\varepsilon_{i-1}^j + \varepsilon_{i+1}^j)| + \\ &+ |c_0(\varepsilon_i^j)| + O(h^3) \leq \\ &\leq \int_0^{\Delta T} |(\Delta T - s) \frac{\partial^2 u}{\partial \xi^2}(a^j + s, t^n + s, x_i)| ds + |c_K||\varepsilon_{i+K}^j + \varepsilon_{i-K}^j| + \\ &+ |c_{K-1}||\varepsilon_{i+K-1}^j + \varepsilon_{i-K+1}^j| + \dots + |c_i||\varepsilon_{2i}^j + \varepsilon_0^j| + \dots + |c_1||\varepsilon_{i-1}^j + \varepsilon_{i+1}^j| + \\ &+ |c_0||\varepsilon_i^j| + O(h^3) \leq \\ &\leq \sup_{s \in [0, \Delta T]} \left\{ \left| \frac{\partial^2 u}{\partial \xi^2}(a^j + s, t^n + s, x_i) \right| \right\} \frac{\Delta T^2}{2} + |c_K||\varepsilon_{i+K}^j + \varepsilon_{i-K}^j| + \\ &+ |c_{K-1}||\varepsilon_{i+K-1}^j + \varepsilon_{i-K+1}^j| + \dots + |c_i||\varepsilon_{2i}^j + \varepsilon_0^j| + \dots + |c_1||\varepsilon_{i-1}^j + \varepsilon_{i+1}^j| + \\ &+ |c_0||\varepsilon_i^j| + O(h^3) \leq \\ &\leq C_1 \Delta T^2 + \max_{1 \leq i \leq M-1} |\varepsilon_i^j| (| \underbrace{2c_K + \dots + 2c_1 + c_0}_1 |) + O(h^3) = \\ &= C_1 \Delta T^2 + \max_{1 \leq i \leq M-1} |\varepsilon_i^j| + O(h^3) \end{aligned} \quad (3.3.13)$$

Concerning $n = 0$ we see that

$$\varepsilon_i^j = u_0(a^j, x_i) - u_0(a^j, x_i) = 0, \quad (3.3.14)$$

while for the approximation of the newborn ($j = 0$) we have

$$\hat{\varepsilon}_i^0 = \int_0^{a_+} \tilde{\beta}(a^{j+1})u(a^{j+1}, t^{n+1}, x_i)da - \left(\Delta T \sum_{j=0}^{N_s-1} \tilde{\beta}_{j+1} \hat{U}_i^{j+1} + \frac{\Delta T}{2} \tilde{\beta}_0 \hat{U}_i^0 \right) \quad (3.3.15)$$

Using the standard error estimate for the trapezoidal rule, an immediate consequence is

$$|\hat{\varepsilon}_i^0| \leq \Delta T^2 \|\tilde{\beta}\|_{L^\infty} C_2 \left(\left\| \frac{\partial u}{\partial t} \right\|_{L^\infty} + \left\| \frac{\partial u}{\partial a} \right\|_{L^\infty} \right), \quad (3.3.16)$$

where C_2 does not depend on ΔT or u .

From (3.3.13) and (3.3.16) it follows that:

$$\max_{1 \leq i \leq M-1} |\hat{\varepsilon}_i^{j+1}| \leq \max_{1 \leq i \leq M-1} |\varepsilon_i^j| + C_1 \Delta T^2 + O(h^3) \quad (3.3.17)$$

and

$$\max_{1 \leq i \leq M-1} |\hat{\varepsilon}_i^0| \leq C_2 \Delta T^2 \quad (3.3.18)$$

Consequently, multiplying (3.3.17) and (3.3.18) by ΔT and summing on j , $j = 0, \dots, N_s$, we obtain:

$$\|\hat{\varepsilon}\|_{l^1}^\infty \leq \|\varepsilon\|_{l^1}^\infty + C^* \Delta T^2, \quad (3.3.19)$$

where C^* depends on $\left(\left\| \frac{\partial u}{\partial t} \right\|_{L^\infty}, \left\| \frac{\partial u}{\partial a} \right\|_{L^\infty}, \left\| \frac{\partial^2 u}{\partial \xi^2} \right\|_{L^\infty}, \|\tilde{\beta}\|_{L^\infty}, T \text{ and } a_+ \right)$. Substituting this relation into itself n times and using (3.3.14), we see that

$$\|\varepsilon\|_{l^1}^\infty \leq C^* \Delta T, \quad (3.3.20)$$

which is exactly part a) of Theorem 1.

In order to derive the $\|\cdot\|_{l^\infty}^\infty$ estimate, we use (3.3.17) and (3.3.18) to see that:

$$\max_{0 \leq j \leq N_s} \max_{1 \leq i \leq M-1} |\hat{\varepsilon}_i^j| \leq \max_{0 \leq j \leq N_s} \max_{1 \leq i \leq M-1} |\varepsilon_i^j| + C_3 \Delta T^2,$$

and then using the same iterative procedure as in case a), we obtain the second part of the proof:

$$\|\varepsilon\|_{l^\infty}^\infty \leq C^{**} \Delta T \quad (3.3.21)$$

2a) If $i \leq K \leq 2i$

In this case, it can easily be checked that we can present the modified STS scheme at time level t^{n+1} in the following form:

$$\begin{aligned} \hat{U}_i^{j+1} = & c_K (U_{i+K}^j - U_{i-(2i-K)}^j) + c_{K-1} (U_{i+(K-1)}^j - U_{i-(2i-K+1)}^j) + \dots + c_{i+1} (U_{i+(i+1)}^j - U_{i-(i-1)}^j) + \\ & + c_i (U_{i+i}^j - U_{i-i}^j) + c_{i-1} (U_{i+(i-1)}^j + U_{i-(i-1)}^j) + \dots + c_1 (U_{i+1}^j + U_{i-1}^j) + c_0 (U_i^j), \\ & i = 1, \dots, M-1, j = 0, \dots, N_s-1, \end{aligned} \quad (3.3.22)$$

where c_l , $l = 0, \dots, K$ are the same coefficients as in case 1. Subtracting (3.3.22) from (3.3.4) we obtain, for $i = 1, \dots, M-1, j = 0, \dots, N_s-1, n = 0, \dots, N_t-1$, the following error equation

$$\begin{aligned} \hat{\varepsilon}_i^{j+1} = & u_i^j + D\Delta T \frac{\partial^2 u_i^j}{\partial x_i^2} + I - c_K(U_{i+K}^j - U_{i-(2i-K)}^j) - c_{K-1}(U_{i+(K-1)}^j - U_{i-(2i-K+1)}^j) - \dots \\ & - c_{i+1}(U_{i+(i+1)}^j - U_{i-(i-1)}^j) - c_i(U_{i+i}^j - U_{i-i}^j) - \dots - c_1(U_{i+1}^j + U_{i-1}^j) - c_0 U_i^j, \end{aligned} \quad (3.3.23)$$

where we have used the notation $I = \int_0^{\Delta T} (\Delta T - s) \frac{\partial^2 u}{\partial \xi^2}(a^j + s, t^n + s, x_i) ds$. We add and subtract the exact solution in mesh points (a^j, t^n, x_{i+K}) , (a^j, t^n, x_{i-K}) , (a^j, t^n, x_{i+K-1}) , \dots , (a^j, t^n, x_0) , multiplied by proper coefficients and thus, we obtain

$$\hat{\varepsilon}_i^{j+1} = \varepsilon_1 - \varepsilon_2, \quad (3.3.24)$$

where

$$\begin{aligned} \varepsilon_1 = & u_i^j + D\Delta T \frac{\partial^2 u_i^j}{\partial x_i^2} + I + c_K(\varepsilon_{i+K}^j - \varepsilon_{i-(2i-K)}^j) + c_{K-1}(\varepsilon_{i+(K-1)}^j - \varepsilon_{i-(2i-K+1)}^j) + \\ & + \dots + c_{i+1}(\varepsilon_{i+(i+1)}^j - \varepsilon_{i-(i-1)}^j) + c_i(\varepsilon_{i+i}^j - \varepsilon_{i-i}^j) + \dots + c_1(\varepsilon_{i+1}^j + \varepsilon_{i-1}^j) + c_0 \varepsilon_i^j \end{aligned} \quad (3.3.25)$$

$$\begin{aligned} \varepsilon_2 = & c_K(u_{i+K}^j - u_{i-(2i-K)}^j) + c_{K-1}(u_{i+(K-1)}^j - u_{i-(2i-K+1)}^j) + \dots \\ & + c_{i+1}(u_{i+(i+1)}^j - u_{i-(i-1)}^j) + c_i(u_{i+i}^j - u_{i-i}^j) + \dots + c_1(u_{i+1}^j + u_{i-1}^j) + c_0 u_i^j \end{aligned} \quad (3.3.26)$$

Proceeding as in the previous case, i.e. using Taylor expansions and simplifying afterwards, we readily obtain:

$$\begin{aligned} \varepsilon_2 = & u_i^j [c_0 + 2c_1 + \dots + 2c_i] + 2ih \frac{\partial u_i^j}{\partial x_i} [c_{i+1} + c_{i+2} + \dots + c_K] + \\ & + h^2 \frac{\partial^2 u_i^j}{\partial x_i^2} [c_1 + 2^2 c_2 + \dots + i^2 c_i] + 2ih^2 \frac{\partial^2 u_i^j}{\partial x_i^2} [1c_{i+1} + 2c_{i+2} + \dots + (K-i)c_K] + \\ & + \frac{2ih^3}{3!} \frac{\partial^3 u_i^j}{\partial x_i^3} [(i^2 + 3.1^2)c_{i+1} + (i^2 + 3.2^2)c_{i+2} + \dots + (i^2 + 3.(K-i)^2)c_K] + O(h^4) \end{aligned}$$

We add and subtract the expression $2u_i^j[c_{i+1} + c_{i+2} + \dots + c_K]$ and using the fact that the solution of (3.1.1) (Dirichlet boundary conditions) is identically 0 at the boundary points $x = 0$ and $x = 1$, we only add $2u_0^j[c_{i+1} + c_{i+2} + \dots + c_K]$.

We also use the formulas:

- $2u_0^j[c_{i+1} + c_{i+2} + \dots + c_K] =$
 $= 2[c_{i+1} + c_{i+2} + \dots + c_K] \left[u_i^j - ih \frac{\partial u_i^j}{\partial x_i} + \frac{i^2 h^2}{2!} \frac{\partial^2 u_i^j}{\partial x_i^2} - \frac{i^3 h^3}{3!} \frac{\partial^3 u_i^j}{\partial x_i^3} + O(h^4) \right]$
- $u_i^j[c_0 + 2c_1 + \dots + 2c_i] + 2u_i^j[c_{i+1} + c_{i+2} + \dots + c_K] = u_i^j$ (see Proposition 1)

Thus, we arrive to the following result

$$\begin{aligned}
 \varepsilon_2 &= u_i^j - 2u_i^j[c_{i+1} + c_{i+2} + \dots + c_K] + \\
 &+ 2[c_{i+1} + c_{i+2} + \dots + c_K] \left[u_i^j - ih \frac{\partial u_i^j}{\partial x_i} + \frac{i^2 h^2}{2!} \frac{\partial^2 u_i^j}{\partial x_i^2} - \frac{i^3 h^3}{3!} \frac{\partial^3 u_i^j}{\partial x_i^3} \right] + \\
 &+ 2ih \frac{\partial u_i^j}{\partial x_i} [c_{i+1} + c_{i+2} + \dots + c_K] + h^2 \frac{\partial^2 u_i^j}{\partial x_i^2} [c_1 + 2^2 c_2 + \dots + i^2 c_i] + \\
 &+ 2ih^2 \frac{\partial^2 u_i^j}{\partial x_i^2} [1c_{i+1} + 2c_{i+2} + \dots + (K-i)c_K] + \\
 &+ \frac{ih^3}{3} \frac{\partial^3 u_i^j}{\partial x_i^3} [(i^2 + 3.1^2)c_{i+1} + (i^2 + 3.2^2)c_{i+2} + \dots + (i^2 + 3.(K-i)^2)c_K] + O(h^4) = \\
 &= u_i^j + h^2 \frac{\partial^2 u_i^j}{\partial x_i^2} [c_1 + 2^2 c_2 + \dots + i^2 c_i] + \\
 &+ h^2 \frac{\partial^2 u_i^j}{\partial x_i^2} [(i+1)^2 c_{i+1} + (i+2)^2 c_{i+2} + \dots + K^2 c_K] - \\
 &- h^2 \frac{\partial^2 u_i^j}{\partial x_i^2} [1^2 c_{i+1} + 2^2 c_{i+2} + \dots + (K-i)^2 c_K] + \\
 &+ ih^3 \frac{\partial^3 u_i^j}{\partial x_i^3} [1^2 c_{i+1} + 2^2 c_{i+2} + \dots + (K-i)^2 c_K] + O(h^4)
 \end{aligned}$$

Using the result obtained in Proposition 2 and the fact that since $u_0^j = 0$, it follows $\frac{\partial^2 u_0^j}{\partial x_0^2} = 0$, we get

$$\begin{aligned}
 \varepsilon_2 &= u_i^j + D\Delta T \frac{\partial^2 u_i^j}{\partial x_i^2} - h^2 [1^2 c_{i+1} + 2^2 c_{i+2} + \dots + (K-i)^2 c_K] \left[\frac{\partial^2 u_0^j}{\partial x_0^2} + ih \frac{\partial^3 u_0^j}{\partial x_0^3} + O(h^2) \right] + \\
 &+ ih^3 [1^2 c_{i+1} + 2^2 c_{i+2} + \dots + (K-i)^2 c_K] \left[\frac{\partial^3 u_0^j}{\partial x_0^3} + O(h) \right] + O(h^4) = \\
 &= u_i^j + D\Delta T \frac{\partial^2 u_i^j}{\partial x_i^2} + O(h^4)
 \end{aligned} \tag{3.3.27}$$

Combining this result with (3.3.25), we yield

$$\begin{aligned}
 \hat{\varepsilon}_i^{j+1} &= \varepsilon_1 - \varepsilon_2 = u_i^j + D\Delta T \frac{\partial^2 u_i^j}{\partial x_i^2} + I + c_K(\varepsilon_{i+K}^j - \varepsilon_{i-(2i-K)}^j) + \\
 &+ c_{K-1}(\varepsilon_{i+(K-1)}^j - \varepsilon_{i-(2i-K+1)}^j) + \dots + c_{i+1}(\varepsilon_{i+(i+1)}^j - \varepsilon_{i-(i-1)}^j) + \\
 &+ c_i(\varepsilon_{i+i}^j - \varepsilon_{i-i}^j) + \dots + c_1(\varepsilon_{i+1}^j + \varepsilon_{i-1}^j) + c_0 \varepsilon_i^j - [u_i^j + D\Delta T \frac{\partial^2 u_i^j}{\partial x_i^2} + O(h^4)] = \\
 &= \int_0^{\Delta T} (\Delta T - s) \frac{\partial^2 u}{\partial \xi^2}(a^j + s, t^n + s, x_i) ds + c_K(\varepsilon_{i+K}^j - \varepsilon_{i-(2i-K)}^j) + \\
 &+ c_{K-1}(\varepsilon_{i+(K-1)}^j - \varepsilon_{i-(2i-K+1)}^j) + \dots + c_{i+1}(\varepsilon_{i+(i+1)}^j - \varepsilon_{i-(i-1)}^j) + \\
 &+ c_i(\varepsilon_{i+i}^j - \varepsilon_{i-i}^j) + \dots + c_1(\varepsilon_{i+1}^j + \varepsilon_{i-1}^j) + c_0 \varepsilon_i^j + O(h^4)
 \end{aligned} \tag{3.3.28}$$

Since all the coefficients in (3.3.22) are positive, we can take the absolute values in (3.3.28), obtaining

$$\begin{aligned}
 |\hat{\varepsilon}_i^{j+1}| &= \left| \int_0^{\Delta T} (\Delta T - s) \frac{\partial^2 u}{\partial \xi^2}(a^j + s, t^n + s, x_i) ds \right| + |c_K(\varepsilon_{i+K}^j - \varepsilon_{i-(2i-K)}^j)| + \\
 &\quad + |c_{K-1}(\varepsilon_{i+(K-1)}^j - \varepsilon_{i-(2i-K+1)}^j)| + \dots + |c_{i+1}(\varepsilon_{i+(i+1)}^j - \varepsilon_{i-(i-1)}^j)| + \\
 &\quad + |c_i(\varepsilon_{i+i}^j - \varepsilon_{i-i}^j)| + \dots + |c_1(\varepsilon_{i+1}^j + \varepsilon_{i-1}^j)| + |c_0 \varepsilon_i^j| + O(h^4) \leq \\
 &\leq \left| \int_0^{\Delta T} (\Delta T - s) \frac{\partial^2 u}{\partial \xi^2}(a^j + s, t^n + s, x_i) ds \right| + |c_K(\varepsilon_{i+K}^j + \varepsilon_{i-(2i-K)}^j)| + \\
 &\quad + |c_{K-1}(\varepsilon_{i+(K-1)}^j + \varepsilon_{i-(2i-K+1)}^j)| + \dots + |c_{i+1}(\varepsilon_{i+(i+1)}^j + \varepsilon_{i-(i-1)}^j)| + \\
 &\quad + |c_i(\varepsilon_{i+i}^j + \varepsilon_{i-i}^j)| + \dots + |c_1(\varepsilon_{i+1}^j + \varepsilon_{i-1}^j)| + |c_0 \varepsilon_i^j| + O(h^4)
 \end{aligned}$$

The rest of the proof is identical to the way we proceeded in case 1) (see 3.3.13) and that's why we shall omit it.

2b) If $K > 2i$

The way we proceed in this case is analogous to case 2a, adopting all notations. We present the modified STS scheme at time level t^{n+1} in the following form

$$\begin{aligned}
 \hat{U}_i^{j+1} &= c_K(U_{i+K}^j - U_{i-(2i-K)}^j) + c_{K-1}(U_{i+(K-1)}^j - U_{i-(2i-K+1)}^j) + \dots + c_{2i}(U_{i+(2i)}^j - U_{i+0}^j) + \\
 &\quad + c_{2i-1}(U_{i+(2i-1)}^j - U_{i-(1)}^j) + \dots + c_{i+1}(U_{i+(i+1)}^j - U_{i-(i-1)}^j) + c_i(U_{i+i}^j - U_{i-i}^j) + \\
 &\quad + c_{i-1}(U_{i+(i-1)}^j + U_{i-(i-1)}^j) + \dots + c_1(U_{i+1}^j + U_{i-1}^j) + c_0(U_i^j), \\
 &\quad i = 1, \dots, M-1, j = 0, \dots, N_s-1
 \end{aligned} \tag{3.3.29}$$

Repeating the same steps as in case 2a, we obtain for $i = 1, \dots, M-1, j = 0, \dots, N_s-1, n = 0, \dots, N_t-1$ an error equation, similar to equation (3.3.24) with the consequent difference in ε_2 term

$$\begin{aligned}
 \varepsilon_2 &= c_K(u_{i+K}^j - u_{i-(2i-K)}^j) + c_{K-1}(u_{i+(K-1)}^j - u_{i-(2i-K+1)}^j) + \dots + c_{2i}(u_{i+(2i)}^j - u_{i+0}^j) + \\
 &\quad + c_{2i-1}(u_{i+(2i-1)}^j - u_{i-(1)}^j) + \dots + c_{i+1}(u_{i+(i+1)}^j - u_{i-(i-1)}^j) + c_i(u_{i+i}^j - u_{i-i}^j) + \dots \\
 &\quad + c_1(u_{i+1}^j + u_{i-1}^j) + c_0 u_i^j
 \end{aligned} \tag{3.3.30}$$

Using Taylor expansions and simplifying afterwards, we yield

$$\begin{aligned}
 \varepsilon_2 = & u_i^j [c_0 + 2c_1 + \dots + 2c_i] + 2ih \frac{\partial u_i^j}{\partial x_i} [c_{i+1} + c_{i+2} + \dots + c_K] + h^2 \frac{\partial^2 u_i^j}{\partial x_i^2} [c_1 + 2^2 c_2 + \dots + i^2 c_i] + \\
 & + 2ih^2 \frac{\partial^2 u_i^j}{\partial x_i^2} [1c_{i+1} + 2c_{i+2} + \dots + (i-1)c_{2i-1} + ic_{2i} + \dots + (K-i)c_K] + \\
 & + \frac{2i^3 h^3}{3!} \frac{\partial^3 u_i^j}{\partial x_i^3} [c_{i+1} + c_{i+2} + \dots + c_{2i-1} + c_{2i} + \dots + c_K] + \\
 & + ih^3 \frac{\partial^3 u_i^j}{\partial x_i^3} [1^2 c_{i+1} + 2^2 c_{i+2} + \dots + (i-1)^2 c_{2i-1} + i^2 c_{2i} + \dots + (K-i)^2 c_K] + O(h^4)
 \end{aligned}$$

We add and subtract the expression $2u_i^j[c_{i+1} + c_{i+2} + \dots + c_K]$ and using the fact that the solution of (3.1.1) (Dirichlet boundary conditions) is identically 0 at the boundary points $x = 0$ and $x = 1$, we only add $2u_0^j[c_{i+1} + c_{i+2} + \dots + c_K]$.

We also use the formulas:

$$\begin{aligned}
 \bullet \quad & 2u_0^j[c_{i+1} + c_{i+2} + \dots + c_K] = \\
 & = 2[c_{i+1} + c_{i+2} + \dots + c_K] \left[u_i^j - ih \frac{\partial u_i^j}{\partial x_i} + \frac{i^2 h^2}{2!} \frac{\partial^2 u_i^j}{\partial x_i^2} - \frac{i^3 h^3}{3!} \frac{\partial^3 u_i^j}{\partial x_i^3} + O(h^4) \right]
 \end{aligned}$$

$$\bullet \quad u_i^j[c_0 + 2c_1 + \dots + 2c_i] + 2u_i^j[c_{i+1} + c_{i+2} + \dots + c_K] = u_i^j \quad (\text{see Proposition 1})$$

Thus, we arrive to the following result

$$\begin{aligned}
\varepsilon_2 &= u_i^j - 2u_i^j[c_{i+1} + c_{i+2} + \dots + c_K] + \\
&\quad + 2[c_{i+1} + c_{i+2} + \dots + c_K] \left[u_i^j - ih \frac{\partial u_i^j}{\partial x_i} + \frac{i^2 h^2}{2!} \frac{\partial^2 u_i^j}{\partial x_i^2} - \frac{i^3 h^3}{3!} \frac{\partial^3 u_i^j}{\partial x_i^3} \right] + \\
&\quad + 2ih \frac{\partial u_i^j}{\partial x_i} [c_{i+1} + c_{i+2} + \dots + c_K] + h^2 \frac{\partial^2 u_i^j}{\partial x_i^2} [c_1 + 2^2 c_2 + \dots + i^2 c_i] + \\
&\quad + 2ih^2 \frac{\partial^2 u_i^j}{\partial x_i^2} [1c_{i+1} + 2c_{i+2} + \dots + (K-i)c_K] + \\
&\quad + \frac{2i^3 h^3}{3!} \frac{\partial^3 u_i^j}{\partial x_i^3} [c_{i+1} + c_{i+2} + \dots + c_{2i-1} + c_{2i} + \dots + c_K] + \\
&\quad + ih^3 \frac{\partial^3 u_i^j}{\partial x_i^3} [1^2 c_{i+1} + 2^2 c_{i+2} + \dots + (i-1)^2 c_{2i-1} + i^2 c_{2i} + \dots + (K-i)^2 c_K] + O(h^4) = \\
&= u_i^j + h^2 \frac{\partial^2 u_i^j}{\partial x_i^2} [c_1 + 2^2 c_2 + \dots + i^2 c_i + (i+1)^2 c_{i+1} + \dots + K^2 c_K] - \\
&\quad - h^2 \frac{\partial^2 u_i^j}{\partial x_i^2} [1^2 c_{i+1} + 2^2 c_{i+2} + \dots + (K-i)^2 c_K] + \\
&\quad + ih^3 \frac{\partial^3 u_i^j}{\partial x_i^3} [1^2 c_{i+1} + 2^2 c_{i+2} + \dots + (K-i)^2 c_K] + O(h^4) = \\
&= u_i^j + D\Delta T \frac{\partial^2 u_i^j}{\partial x_i^2} - h^2 [1^2 c_{i+1} + 2^2 c_{i+2} + \dots + (K-i)^2 c_K] \left[\frac{\partial^2 u_0^j}{\partial x_0^2} + ih \frac{\partial^3 u_0^j}{\partial x_0^3} + O(h^2) \right] + \\
&\quad + ih^3 [1^2 c_{i+1} + 2^2 c_{i+2} + \dots + (K-i)^2 c_K] \left[\frac{\partial^3 u_0^j}{\partial x_0^3} + O(h) \right] + O(h^4) = \\
&= u_i^j + D\Delta T \frac{\partial^2 u_i^j}{\partial x_i^2} + O(h^4),
\end{aligned}$$

which is exactly what we obtained in the case $i \leq K \leq 2i$ (see equation 3.3.27) and consequently we skip the details for the rest of the proof. \square

3.4. Performance on Test Problems

In this section we investigate the performance of the modified super-time-stepping scheme on three exactly solvable test problems. Relying on the stability results given in Section 3.3, we believe the algorithm will work well also in the case of Neumann boundary conditions and we demonstrate this empirically. We choose the parameter ν as a random number in the interval $(0, 1)$ and we perform a large number of experiments. In each case we compare modified STS with schemes of the same or higher order, namely the explicit, fully implicit and Crank-Nicolson standard schemes, in terms of numerical efficiency and approximation. For the implementation of the implicit schemes we use either direct or iterative methods for solving the resulting system. Since SOR iterations and Thomas' algorithm showed best results, we list comparisons

only with them. In the modified super-time-stepping scheme we vary the parameter ν and the number of sub-steps we do, while in the implicit schemes we increase the number of steps in time. Moreover, when applying SOR iterations we report the value of ω (found by trial) which gives the best approximation and we use a tolerance of 10^{-6} for convergence.

3.4.1 Problem 1 - Diffusion in Lotka-McKendrick's Model

We consider a population with a finite age and for simplicity we take the maximum age of the individuals $a_+ = 1$. The mortality and the survival probability are $\mu(a) = \frac{1}{1-a}$, $\pi(a) = 1-a$ respectively. We choose the following initial conditions:

$$p_0(a, x) = e^{-\alpha^* a}(1-a)\sin(\pi x), \text{ for Dirichlet boundary conditions} \quad (3.4.1)$$

$$p_0(a, x) = e^{-\alpha^* a}(1-a)(2 + \cos(\pi x)), \text{ for Neumann boundary conditions} \quad (3.4.2)$$

where α^* is the intrinsic Malthusian parameter which determines the population growth via the birth rate $B(t, x)$. We assume the fertility $\beta(a) = \beta$ and by choosing an appropriate value of $\alpha^* = 2$, we calculate it by formula (1.3.3), which provides continuity of the solution $p(a, t, x)$. The solution of system (1.3.1) is given by:

$$p(a, t, x) = e^{\alpha^*(t-a)}(1-a)e^{-\pi^2 D t} \sin(\pi x), \quad (3.4.3)$$

and the one of problem (1.3.2)

$$p(a, t, x) = e^{\alpha^*(t-a)}(1-a)[2 + e^{-\pi^2 D t} \cos(\pi x)], \quad (3.4.4)$$

We assume the diffusion constant $D = 1$ for simplicity. In order to satisfy the CFL condition $\tau \leq \frac{h^2}{2D}$ for the explicit scheme, we choose $\tau = 0.00125$ and $h = 0.05$. In the other schemes we fix $M = 20$ and we vary the number of steps in time. All calculations in the first three tables are done for $T=3$ (since the solution (3.4.1) of (1.3.1) does not grow in time). In case of Neumann conditions on the boundary, the solution grows fast and we give results only for $T=1$.

In the tables below we use the following notations:

t_{steps} - total number of steps in time; **a_{steps}** - total number of steps in age;

N_f - number of calculations of the birth integral; **N_{STS}** - total number of super-steps;

K - number of intermediate steps per one super-step; **iter** - number of iterations;

ω - factor, used in SOR iterations; **CPU** - time (in seconds), needed for computations;

E_{abs} - the max L^∞ error; **E_{L1}** - the max L^1 error; **E_{rel}** - the max relative error;

COMMON - common parameters; **IS** - pure implicit scheme; **CN** - Crank-Nicolson scheme

a) Dirichlet boundary conditions: $T=3$

Table 8: MODIFIED SUPER - TIME - STEPPING								
ν	N_{STS}	K	t_{steps}	a_{steps}	N_f	E_{abs}	E_{L^1}	CPU
0.00	2400	1	2400	36480000	45600	3.07E-3	6.10E-4	24.18
0.0003	66	6	396	159258	1254	1.16E-1	2.36E-2	0.07
0.0006	150	4	600	561450	2850	4.93E-2	9.89E-3	0.24
0.001	99	5	495	302841	1881	7.63E-2	1.54E-2	0.14
0.001	27	10	270	41553	513	3.82E-1	7.94E-2	0.01
0.004	279	3	837	1468377	5301	2.62E-2	5.23E-3	0.48
0.006	168	4	672	705432	3192	4.24E-2	8.50E-3	0.31
0.006	114	5	570	402876	2166	6.15E-2	1.24E-2	0.19
0.009	177	4	708	783579	3363	3.92E-2	7.86E-3	0.28
0.02	150	5	750	701100	2850	3.88E-2	7.81E-3	0.30
0.07	126	10	1260	983934	2394	1.50E-2	3.13E-3	0.25
0.07	48	25	1200	342912	912	8.34E-3	2.67E-3	0.08
0.095	48	30	1440	411312	912	5.81E-3	1.87E-3	0.09
0.20	69	30	2070	866571	1311	2.66E-3	8.41E-4	0.18

Table 9: COMMON			IS + THOMAS' ALGORITHM			IS + SOR ITERATIONS				
t_{steps}	N_f	a_{steps}	E_{abs}	E_{L^1}	CPU	ω	iter	E_{abs}	E_{L^1}	CPU
450	8550	1282500	2.59E-2	5.14E-3	1.09	1.57	597	2.46E-2	4.89E-3	1.11
600	11400	2280000	1.99E-2	3.94E-3	1.76	1.46	778	2.42E-2	4.81E-3	1.88
1200	22800	9120000	1.07E-2	2.13E-3	6.85	1.35	1389	1.91E-2	3.78E-3	7.25
1800	34200	20520000	7.66E-3	1.52E-3	15.12	1.27	2030	1.49E-2	2.96E-3	15.87
2400	45600	36480000	6.13E-3	1.22E-3	26.37	1.22	2641	1.42E-2	2.90E-3	26.55

Table 10: COMMON			CN + THOMAS' ALGORITHM			CN + SOR ITERATIONS				
t_{steps}	N_f	a_{steps}	E_{abs}	E_{L^1}	CPU	ω	iter	E_{abs}	E_{L^1}	CPU
300	5700	570000	1.19E-3	2.12E-4	0.61	1.1	667	3.62E-2	5.20E-3	1.05
450	8550	1282500	1.38E-3	2.63E-4	1.24	1.17	913	2.33E-2	4.62E-3	1.26
600	11400	2280000	1.45E-3	2.82E-4	2.01	1.14	1109	1.07E-2	2.13E-3	2.04
1200	22800	9120000	1.51E-3	2.99E-4	6.83	1.36	1687	1.70E-3	3.38E-4	7.32
1800	34200	20520000	1.53E-3	3.02E-4	15.43	1.22	2327	1.09E-3	2.16E-4	16.28

b) Neumann boundary conditions: $T=1$

Table 11: MODIFIED SUPER - TIME - STEPPING									
ν	N_{STS}	K	t_{steps}	a_{steps}	N_f	E_{abs}	E_{L^1}	E_{rel}	CPU
0.00	800	1	800	13440000	16800	1.12E-2	1.85E-3	9.66E-4	8.54
0.0001	22	6	132	58674	462	1.22E-1	2.63E-2	4.12E-2	0.03
0.0005	50	4	200	206850	1050	5.04E-2	1.00E-2	1.64E-2	0.09
0.0009	32	5	160	104832	672	7.87E-2	1.56E-2	2.58E-2	0.05
0.006	38	5	190	148428	798	6.31E-2	1.25E-2	2.07E-2	0.07
0.008	58	4	232	278922	1218	4.09E-2	8.13E-3	1.31E-2	0.15
0.03	58	5	290	348348	1218	3.09E-2	6.14E-3	9.83E-3	0.15
0.08	56	8	448	518616	1176	1.42E-2	2.83E-3	4.47E-3	0.17
0.08	75	6	450	700875	9450	4.79E-2	1.01E-2	9.78E-3	0.24
0.1	50	10	500	515550	1050	1.13E-2	2.24E-3	3.55E-3	0.16
0.22	34	22	748	519078	714	1.15E-2	1.92E-3	1.52E-3	0.13

Table 12a: IS + THOMAS' ALGORITHM						
t_{steps}	N_f	a_{steps}	E_{abs}	E_{L^1}	E_{rel}	CPU
150	3150	472500	3.11E-1	5.14E-2	7.86E-3	0.47
200	4200	840000	1.76E-1	2.91E-2	6.06E-3	0.72
400	8400	3360000	4.45E-2	7.39E-3	3.29E-3	2.76
600	12600	7560000	2.01E-2	3.35E-3	2.37E-3	6.17
800	16800	13440000	1.15E-2	1.93E-3	1.89E-3	10.82

Table 12b: IS + SOR ITERATIONS								
t_{steps}	N_f	a_{steps}	ω	iter	E_{abs}	E_{L^1}	E_{rel}	CPU
150	3150	472500	1.5	1492	2.35E-1	3.64E-2	7.83E-3	0.92
200	4200	840000	1.2	2838	1.66E-1	3.88E-2	6.28E-3	1.75
400	8400	3360000	1.36	2533	1.55E-2	2.41E-3	3.25E-3	3.96
600	12600	7560000	1.3	3096	1.57E-2	3.77E-3	2.28E-3	8.41
800	16800	13440000	1.6	6258	1.00E-2	1.84E-3	2.10E-3	15.81

Table 13a: CN + THOMAS' ALGORITHM

t_{steps}	N_f	a_{steps}	E_{abs}	E_{L^1}	E_{rel}	CPU
100	2100	210000	1.31E-3	1.85E-4	2.89E-4	0.33
150	3150	472500	1.27E-3	2.52E-4	3.94E-4	0.54
200	4200	840000	1.38E-3	2.75E-4	4.29E-4	0.79
400	8400	3360000	1.49E-3	2.97E-4	4.65E-4	2.92
600	12600	7560000	1.52E-3	3.02E-4	4.72E-4	6.54

Table 13b: CN + SOR ITERATIONS

t_{steps}	N_f	a_{steps}	ω	iter	E_{abs}	E_{L^1}	E_{rel}	CPU
100	2100	210000	1.57	820	3.30E-2	6.55E-3	6.94E-3	0.44
150	3150	472500	1.5	914	1.73E-2	3.44E-3	1.10E-3	0.65
200	4200	840000	1.45	1089	7.74E-3	1.15E-3	7.28E-4	1.12
400	8400	3360000	1.48	2320	3.72E-3	7.39E-4	4.84E-4	3.98
600	12600	7560000	1.15	3403	3.17E-3	7.28E-4	4.72E-4	8.84

From the data reported in the first table, we can see that smaller ν is, larger the errors are, but the computations are fast performed. One way to improve accuracy is by increasing the damping factor. Thus the duration ΔT of the super-step decreases and the errors we get are with better accuracy, but the cost goes up. One can see that when decreasing the number of intermediate steps we also obtain better accuracy (compare results for $\nu = 0.0003$, $K = 6$ and $\nu = 0.0006$, $K = 4$ or $\nu = 0.001$, $K = 10$ and $\nu = 0.001$, $K = 5$ in Table 8), but computational time increases sensitively. Similar behavior can be observed in Table 11.

Since the upper bound of the parameter ν in case of Dirichlet b.c. is approximately 0.006 ($\frac{\lambda_{min}}{\lambda_{max}} \approx 0.00619$), we increased the damping factor to 0.004 and 0.006 and we obtained an error comparable to the error given by the fully implicit scheme + Thomas' algorithm and to the one of the fully implicit scheme + SOR, but modified STS appeared to be much more effective (see Tables 8, 9 and 10). Furthermore, relying on the fact that in practice computations work far beyond the theoretical limits, we tried the modified STS algorithm with larger values of ν and the results show that it behaves extremely well. It follows that the analytical restriction $\nu \in (0, \frac{\lambda_{min}}{\lambda_{max}}]$ is too strong and we can choose the values of ν in the interval (0,1) randomly. Doing so, we could decrease the number of super-steps N_{STS} and consequently the number of computations of the boundary condition N_f too. Thus, for $\nu \approx 0.2$ (also in case of Neumann b.c., Table 11) we obtained accuracy comparable to the accuracy of the explicit scheme (note that for $\nu = 0$ and $K = 1$, we have exactly the explicit scheme itself) and to that one of the second order Crank-Nicolson scheme (see Table 10). Regarding the CPU time, one can see that

the speed up given by the modified STS is enormous.

In case of Neumann boundary conditions, the excessive restrictiveness of the theoretical condition imposed on ν is even more obvious (since $\lambda_{min} = 0$) and it is proved empirically (see Table 11) that the scheme works for $\nu \in (0, 1)$. It implies, we can also apply the modified STS to problems (for example nonlinear problems) where the eigenvalues of the matrix A in (3.2.4) are not known. This fact is confirmed by our experiments done for the nonlinear model (1.1.10) and listed below.

The results obtained in case of Neumann b.c. are similar to these for Dirichlet b.c. In addition to the absolute and L^1 errors, we show also the relative error. It seems that in both cases for smaller values of ν we achieve best accuracy for smaller number of inner steps, which corresponds to number of super-steps between 30 and 60 per unit time. By increasing ν , we yield better results as we increased the number of the inner steps as well (compare error values for $\nu = 0.07$, $K = 10$ and $K = 25$ in Table 8 and $\nu = 0.08$, $K = 6$ or $K = 8$ in Table 11). Another interesting observation is that while the implicit scheme combined with Thomas' algorithm is as exact and efficient as the implicit scheme combined with SOR iterations in case of Dirichlet b.c. (Table 9), in the other case the implicit scheme with SOR iterations, appears to be much slower with respect to the implicit scheme with Thomas' algorithm (see Tables 12a and 12b). Concerning the Crank-Nicolson scheme in both cases its combination with Thomas' algorithm is better (as error values and time consumption) than the combination with SOR iterations (compare results from Tables 10, 13a and 13b). Moreover, in case of Neumann b.c. SOR iterations are more expensive than Thomas' algorithm (Tables 12a and 12b; 13a and 13b).

3.4.2 Problem 2 - Diffusion in the Model with the Profile

Here we consider the same values for the fertility and mortality as in the linear case and our initial conditions are the following

$$w_0(a, x) = \frac{\beta e^{-\alpha^* a} (1 - a) (2 + \cos(\pi x))}{2}, \quad (3.4.5)$$

where we assume α^* is again equal to 2.

The solution of system (1.3.5) is given by

$$w(a, t, x) = \frac{\beta e^{\alpha^*(t-a)} (1 - a) (2 + e^{-\pi^2 D t} \cos(\pi x))}{2 e^{\alpha^* t}}, \quad (3.4.6)$$

where the exact value of the total population (1.1.11) is

$$P(t) = \frac{2 e^{\alpha^* t}}{\beta} \quad (3.4.7)$$

In order to obtain stability for the explicit scheme we keep the values of N and M as in the previous case, i.e. $N = 800$ and $M = 20$ and we use the same notations.

We underline that since the solution of (1.3.5) is bounded, it implies the errors remain stable in time and we present results only for $T=1$.

Table 14: MODIFIED SUPER - TIME - STEPPING - NONLINEAR CASE									
ν	N_{STS}	K	t_{steps}	a_{steps}	N_f	E_{abs}	E_{L^1}	E_{rel}	CPU
0.00	800	1	800	13440000	16800	2.24E-2	4.46E-3	3.31E-3	10.13
0.0005	50	4	200	206850	462	2.40E-1	4.96E-2	3.61E-2	0.14
0.004	26	6	156	82446	546	4.37E-1	9.40E-2	6.75E-2	0.05
0.004	54	4	216	241542	1134	2.14E-1	4.43E-2	3.23E-2	0.16
0.008	58	4	232	278922	1218	1.91E-1	3.94E-2	2.87E-2	0.19
0.03	58	5	290	348348	1218	1.29E-1	2.70E-2	1.96E-2	0.18
0.08	64	7	448	594048	1344	5.17E-2	9.99E-3	1.05E-2	0.30
0.1	50	10	500	515550	1050	5.09E-2	8.82E-3	9.91E-3	0.22
0.20	59	12	708	863583	1239	3.05E-2	5.11E-3	5.76E-3	0.28
0.22	57	13	741	872613	1197	2.97E-2	4.88E-3	5.54E-3	0.26
0.24	55	14	770	874335	1155	2.92E-2	4.71E-3	5.38E-3	0.24

Table 15a: IS + THOMAS' ALGORITHM - NONLINEAR CASE							
t_{steps}	N_f	a_{steps}	iter	E_{abs}	E_{L^1}	E_{rel}	CPU
150	3150	472500	309	1.32E-1	2.60E-2	1.94E-2	0.65
200	4200	840000	396	9.97E-2	1.97E-2	1.46E-2	0.97
400	8400	3360000	634	5.11E-2	1.01E-2	7.44E-3	3.48
600	12600	7560000	918	3.48E-2	6.90E-3	5.06E-3	7.51
800	16800	13440000	1137	2.67E-2	5.29E-3	3.86E-3	12.65

Table 15b: IS + SOR ITERATIONS - NONLINEAR CASE								
t_{steps}	N_f	a_{steps}	ω	iter	E_{abs}	E_{L^1}	E_{rel}	CPU
150	3150	472500	1.5	442	1.24E-1	2.45E-2	1.49E-2	0.52
200	4200	840000	1.45	667	9.89E-2	1.95E-2	1.49E-2	0.90
400	8400	3360000	1.35	1026	5.07E-2	1.00E-2	7.39E-3	3.22
600	12600	7560000	1.25	1198	3.46E-2	6.86E-3	4.97E-3	6.48
800	16800	13440000	1.2	1297	2.53E-2	5.03E-3	3.79E-3	10.65

Table 16a: CN + THOMAS' ALGORITHM - NONLINEAR CASE

t_{steps}	N_f	a_{steps}	iter	E_{abs}	E_{L^1}	E_{rel}	CPU
100	2100	210000	189	2.50E-3	7.24E-4	2.17E-3	0.39
150	3150	472500	282	1.85E-3	4.07E-4	9.68E-4	0.67
200	4200	840000	361	2.06E-3	3.89E-4	5.45E-4	1.18
400	8400	3360000	616	2.28E-3	4.47E-4	4.51E-4	3.82
600	12600	7560000	810	2.33E-3	4.59E-4	4.66E-4	7.58

Table 16b: CN + SOR ITERATIONS - NONLINEAR CASE

t_{steps}	N_f	a_{steps}	ω	iter	E_{abs}	E_{L^1}	E_{rel}	CPU
100	2100	210000	1.5	377	5.84E-3	1.16E-3	6.94E-4	0.34
150	3150	472500	1.3	448	5.35E-3	1.06E-3	8.65E-4	0.61
200	4200	840000	1.25	528	3.71E-3	7.37E-4	5.97E-4	1.12
400	8400	3360000	1.3	917	2.29E-3	4.55E-4	4.61E-4	3.57
600	12600	7560000	1.18	1101	1.50E-3	2.99E-4	3.12E-4	7.47

What we see from Table 14 is that the behavior of the modified STS we observed in the linear models, does not change here - the method remains very accurate and efficient also in the nonlinear case. For small ν it is fast, but the accuracy is poor. In order to achieve accuracy we have to proceed as before, i.e. taking larger values of ν which increases sensitively the computational time. The best performance of the modified STS here (as CPU time) was obtained for $\nu = 0.004$ and $N_{STS} = 26$ with absolute error ≈ 0.437 , L^1 error ≈ 0.094 and relative error ≈ 0.0675 . Increasing the damping factor up to 0.22 and 0.24 we obtained errors similar to the errors of the explicit scheme but with much less costs.

We have to remark that in the nonlinear case the both implicit schemes (and especially the fully implicit scheme) combined with SOR iterations are more efficient than their combination with Thomas' algorithm (compare Tables 15a and 16a with 15b and 16b respectively). Moreover they are more efficient even than the implicit schemes with SOR iterations in the linear case (see Tables 15b and 12b; Tables 16b and 13b). It seems that the integral term in the leading equation of model (1.3.5) enables the fast convergence of these schemes. The fully implicit scheme with Thomas' algorithm shows results (as error values) similar to these of the fully implicit scheme with SOR iterations (see Tables 15a and 15b). The same is valid for the Crank-Nicolson method (Tables 16a and 16b). As CPU time, the worst result of the modified STS (CPU=0.30) is better than the best result for Crank-Nicolson + SOR iterations (CPU=0.34). As errors, the best values are obtained by Crank-Nicolson scheme (Tables 16a and 16b). Although the errors of the modified STS are of the same range as these of the fully implicit scheme (compare Tables 14, 15a and 15b), their computational times are vastly different.

3.5. Comparison of Different Approaches

Proceeding as in the case without diffusion, we want to compare different ways of approximating the solution of the linear model (1.3.2) and the model with the profile (1.3.5). In other words we are concerned with the question if the direct solving of the problem with $p(a, t, x)$ and then the computation of the profile $w(a, t, x)$ or the approximation of the problem for the profile itself and vice versa, is better. In the case without diffusion (Section 2.5: Tables 4a, 4b and 5) it is shown that the indirect ways - via the integral equation and via the age profile, work better than the direct approach of the linear model. In the diffusion dependent case we observe different behavior and since all the schemes showed similar results we present results only for one of them, namely the fully implicit scheme with Thomas' algorithm.

Let us introduce the following notations:

- \mathbf{E}_{absp} - the maximum absolute error for $p(a, x, t)$;
- \mathbf{E}_{absw} - the maximum absolute error for $w(a, x, t)$;
- \mathbf{E}_{relp} - the maximum relative error for $p(a, x, t)$;
- \mathbf{E}_{relw} - the maximum relative error for $w(a, x, t)$

Table 17: IS + THOMAS' ALGORITHM - via $p(a, x, t)$						
T	N	M	E_{absp}	E_{absw}	E_{relp}	E_{relw}
1	200	20	1.76E-1	3.01E-2	6.06E-3	6.06E-3
1	600	20	2.01E-2	1.18E-2	2.37E-3	2.37E-3
1	400	200	4.44E-2	1.43E-2	2.83E-3	2.83E-3
1	1000	100	7.33E-3	5.77E-3	1.16E-3	1.16E-3

Table 18: IS + THOMAS' ALGORITHM - via $w(a, x, t)$						
T	N	M	E_{absp}	E_{absw}	E_{relp}	E_{relw}
1	200	20	3.745	9.97E-2	1.46E-2	1.46E-2
1	600	20	1.236	3.48E-2	5.06E-3	5.06E-3
1	400	200	1.858	4.89E-2	7.16E-3	7.16E-3
1	1000	100	7.40E-1	1.97E-2	2.87E-3	2.87E-3

From Table 17 and Table 18 it is obvious that in the case with diffusion the better way to obtain $p(a, x, t)$ is the direct treatment of the linear model (1.3.2). Moreover it seems that finding $w(a, x, t)$ by $p(a, x, t)$ is better (as accuracy) than obtaining it directly from the nonlinear system.

3.6. Final Remarks

Since the nature of the problems discussed above is somehow unusual, we have to design special numerical algorithms for them. In this Chapter we introduced a new acceleration method (for explicit finite difference schemes) that can be applied on models containing both - age and diffusion. In order to construct the method we took advantage from an already existing numerical scheme for parabolic problems (STS) and we adapted it to the age-structured models with spatial diffusion we deal with. The analysis and computations presented show that modified Super-Time-Stepping is very effective and accurate method in case of age-dependence and diffusion. It is applicable and simple to employ in an existing explicit code for such problems. Its features, fastness, accuracy and more easiness to implement than implicit schemes, make it preferable also for higher-dimensional and nonlinear problems.

CHAPTER 4

HANDLING NONLINEAR AGE-DEPENDENT MODELS

Some characteristics of organisms change with their age, for instance their birth and death rates vary as the time passes. Since such changes occur, individual organisms may affect growth of the whole population differently. Consequently, a mathematical model that accurately accounts for these changes must keep track on the dependence of the vital rates not only on age, but also on the population size. The linear age-structured model (1.1.1) fails in incorporating this important feature, i.e. in it we see demographic rates depending only on the age of the species. The first authors who understood the need of more refined assumptions and included into their model (1.2.1 with $i=1$ and $\gamma(a) = 1$) fertility and mortality functions depending also on the total population size, were Gurtin and MacCamy (1974). This fact opened a vast field of uninvestigated problems, on one hand because of the much more complex analysis it demanded and on the other hand, because of its various applications in demography, epidemiology, cellular biology, etc. This explains the vivid interest of many authors and the growing number of papers on this problem that have been published after 1974 (for example [28], [41], [44], [49], [94]). Using as a base the Gurtin-MacCamy's model, highly realistic models can be constructed. Unfortunately they all include nonlinear terms and the classical instruments for their analytical treatment are not sufficient. Thus, it seems that their analysis will rely on numerical solution techniques. Hence, it is desirable to have robust schemes which can produce many qualitative and quantitative properties of the solution of the differential problem. Our aim is to give a review on the numerical methods developed for Gurtin-MacCamy's equation and to give an insight on other possibilities to solve numerically this and other similar problems. We deal with models describing some types of intraspecies interactions introduced in Section 1.2. We analyze both approaches - direct numerical treatment of the models of Logistic Growth and Cannibalism 1.2.5 and 1.2.7 respectively as hyperbolic equations with nonlocal boundary condition and indirect

approximation of the solution of Logistic Growth model via its integral reformulation 1.2.6. We want to pursue the both avenues and to compare them in terms of accuracy and efficiency.

4.1. State-of-the-Art of Numerical Methods for Gurtin-MacCamy's Model

During the last 20 years, many numerical methods for the approximation of the solution of Gurtin-MacCamy equation have been proposed. A typical way to solve this model numerically is the finite difference discretization of the partial derivatives along the characteristic lines using the same or different age and time discretization parameters. Other methods are based on a theoretical representation of the solution, obtained by integration along characteristics. In the following we shall give a review on the numerical methods (from both categories) considered for the numerical approximation of Gurtin-MacCamy's model or its modifications.

The first contribution to the design of algorithms for the numerical treatment of linear/nonlinear age/size-dependent models was due to de Roos, Tanya Kostova and Fabio Milner. De Roos [89] introduced a semi-discrete scheme called The Escalator Boxcar Train. The idea of the method was to approximate certain momenta (in terms of integrals) of the original density function (which have biological meaning) over moving domains instead of approximating the density function itself at the nodal-point values. He made no assumptions about the smoothness of the density function, even allowing it to be a delta-function. The method was derived for the linear case (however, the coefficient functions were allowed to be time-dependent), but the author noted (and explained) that its extension to the nonlinear case was straightforward. No convergence analysis was provided.

The article of Milner, written together with Jim Douglas [26] is considered to be the first published work in which a numerical approximation of simplified versions of Gurtin-MacCamy's model were concerned. These authors first dealt with a nonlinear model in which the mortality function depended only on the total population - $\mu(P(t))$ and the condition on the boundary was of Dirichlet's type (the birth law was given explicitly, i.e. $p(0, t) = g(t)$, where $g(t)$ was a known, nonnegative function and $g(0)=p_0(0)$). Later on they studied a problem with nonlocal, linear boundary condition (they considered the birth rate depending on the age and time). They proposed numerical methods of first order which were a finite difference version of the method of characteristics over a uniform age-time mesh. A convergence analysis was carried out but no numerical results were presented. Kostova [57] introduced a first order method based on the method of lines. She discretized the time variable (with an interval of discretization h) obtaining an ordinary differential equation which she solved analytically yielding an integral expression and she applied the trapezoidal rule to the integral terms. The method appeared to

be nonapplicable in case of nonlocal boundary conditions. It was shown that for sake of convergence the steps of discretization σ and h along the age and time axes respectively should satisfy the condition $\sigma = O(h^2)$ which was a very restrictive condition. The convergence analysis was confirmed by numerical experiments.

In 1989 Kannan and Ortega [51] studied the same simplified model and they established existence and uniqueness of its solution. A first order finite difference scheme was employed and even though its convergence was established, no numerical results were presented. In the same year, Kostova and Martcheva [61] published a paper in which they presented a numerical method for the original Gurtin-MacCamy's problem, i.e. they designed a finite difference scheme for the case in which the birth and death moduli depended on both - the age and the total population (it is considered that this work was the first one which treated the Gurtin-MacCamy's problem itself). They demonstrated positivity and boundedness of the discrete solution and they proved the scheme was convergent with rate $O(h)$. No numerical results were given.

One year later Kostova [58] considered a more general case of Gurtin-MacCamy's model and used the same numerical method presented in [61] in order to approximate it (and in 1991, in [64] this method was applied to solve a system of two coupled equations for an intramolluscan trematode population dynamics). The rate of convergence of the method in this case was shown to be $O(h)$, but no numerical results were given. In the same year Chichia Chiu published two articles. Taking advantage from the theoretical representation of the solution of Gurtin MacCamy's equation given by

$$p_{i+1}^{n+1} = p_i^n \exp \left(- \int_0^h \mu(a + \tau, P(t^n + \tau)) d\tau \right) \quad (4.1.1)$$

a first order numerical scheme was introduced. She proposed and analyzed an explicit method by approximating the exponential function $\exp(x)$ by its Taylor polynomial $(1+x)$ for nonnegative x and by using the composite midpoint rule for the integral terms. In the first work [24] the mortality function was assumed depending on age and on the total population and thus the numerical scheme was the following

$$\begin{aligned} p_i^0 &= p_i, P^0 = 2h \sum_{i=0}^M p_{2i+1} \\ p_{i+1}^{n+1} &= \frac{p_i^n}{1 + \mu(a_i, P^n)h} \\ P^n &= 2h \sum_{i=0}^M p_{2i+1}^n \\ p_0^{n+1} &= 2h \sum_{i=0}^M \beta(a_{2i+1}, P^n) p_{2i+1}^n, \end{aligned} \quad (4.1.2)$$

where we have used the notations introduced in Section 2.1 and by P^n we have denoted the total population number $P(t)$ at time $t = nh$. First order convergence was proved:

$$2h \sum_{i=0}^M \{|p(a_i, t^n) - p_i^n|\} \leq C(h + \frac{\varepsilon}{h}), 0 \leq n \leq N,$$

where $\varepsilon > 0$ is a given value, such that, if $T > 0$ is fixed, there exist $a^* > 0$ and $\sigma > 0$:

$\int_{a^*}^{\infty} p(a, t) da \leq \varepsilon$ and $K \geq P(t) \geq \sigma > 0$, $0 \leq t \leq T$. A numerical example to test the algorithm was reported, but in it the fertility was independent of the total population.

In a second paper published during the same year [25], a model in which the mortality depended on the age and time variables but not on the $P(t)$ was studied. The author assumed that "in a modern peaceful society, most deaths are due to natural causes, disease, and accident, which are being reduced over time as science and technology develop." Even though the mortality rate was linear, she considered a nonlinear fertility function depending on the age and the total population, since "the newborn population has to be controlled by the size of the population (i.e. by $P(t)$) in order to let the population stay stable." For sake of simplicity both $\mu(a, t)$ and $\beta(a, P(t))$ were assumed to be variable separable, i.e.

$$\mu(a, t) = \mu_1(a)\mu_2(t) \quad \text{and} \quad \beta(a, P(t)) = \beta_1(a)\beta_2(P(t))$$

Applying the algorithm developed in [24] some computational results showing first order convergence rate were reported (which was in agreement with the theoretical results carried in [24]). In 1991 Lopez-Marcos [69] presented a first order upwind finite-difference scheme for the numerical approximation of a nonlinear hyperbolic equation with integral boundary condition. He applied the method on a more general version of Gurtin-MacCamy's model replacing each of the partial derivatives by a finite difference quotient with different denominator (namely the denominators were the step size in time h and in age k , where $k = \frac{a_+}{M}$ and $M \in \mathbb{N}$) and the integrals by the end-point rule, obtaining:

$$\begin{aligned} \frac{p_i^{n-1} - p_{i-1}^{n-1}}{h} + \frac{p_i^n - p_i^{n-1}}{k} &= -\mu(a_i, P^{n-1})p_i^{n-1} \\ p_0^n &= k \sum_{i=1}^M g(\beta(a_i, P^n)p_i^n) \\ P^n &= k \sum_{i=1}^M p_i^n \end{aligned} \tag{4.1.3}$$

It was proved that if $k = rh$ and $0 \leq r \leq 1$, the following error estimate held:

$$\max_{0 \leq n \leq N} \left(\sum_{i=1}^M |p(a_i, t^n) - p_i^n|^2 \right)^{\frac{1}{2}} + \left[\frac{k}{2} (|p(0, 0) - p_0^0|^2 + |p(0, t^N) - p_0^N|) + k \sum_{n=1}^{N-1} |p(0, t^n) - p_0^n|^2 \right]^{\frac{1}{2}} \leq Ch$$

Numerical results were provided and it was shown that the effective rate of convergence of the method for $0 \leq r < 1$ coincided with the theoretical one.

In 1991 Lopez-Marcos and Fairweather [29] presented and analyzed a first second order method for nonlinear integro-differential equations with nonlocal boundary conditions. This was the so called Box method that we used in Section 2.3 in order to approximate the equation with the Age profile (2.3.3). The difference with the previous method consisted in the fact that the Box method was implicit when μ depended on $P(t)$ and that's why some iterations were needed to be done. The authors proved theoretically its second order of convergence with the following error bounds:

$$\begin{aligned} h \left(\sum_{i=1}^M |p(a_{i-\frac{1}{2}}, t^n) - p_{i-\frac{1}{2}}^n|^2 \right)^{\frac{1}{2}} + \left[\frac{k}{2} (|p(0, 0) - p_0^0|^2 + |p(0, t^N) - p_0^N|) + k \sum_{n=1}^{N-1} |p(0, t^n) - p_0^n|^2 \right]^{\frac{1}{2}} \leq \\ \leq \left[O(h^2)^2 + O(h^2 + k^2) \right]^{\frac{1}{2}} \end{aligned}$$

The numerical experiments confirmed the second order of convergence of the algorithm and the authors concluded that for fixed k the approximation was better as they decreased h , while for fixed h the approximations could be improved as k decreased only for small h .

An extrapolated version of the Box method was proposed by the same authors (Fairweather and Lopez-Marcos [30]) in 1994. They considered an explicit, second order method for the same (more general) problem, where an extrapolation in the nonlinear terms was employed. Its second order accuracy was demonstrated analytically and numerically. A treatment of the integral terms with different high order quadrature rules was done. The authors pointed out the importance of the use of higher order rules in practical situations where the data of the problem are only known on a fixed discrete set of points in the age interval.

One year later an extrapolated version of the Lopez-Marcos' upwind scheme was proposed by Kim and Park in [55]. They studied the long time behavior of the numerical solution of the Gurtin-MacCamy's model. While in [69] nonnegativity of the numerical solutions was preserved only for small mesh sizes, for the extrapolated upwind method it was proved that the numerical solutions were always nonnegative. The modification of the scheme was as follows $0 \leq i \leq M-1, 0 \leq n \leq N$:

$$\begin{aligned} \frac{p_i^n - p_i^{n-1}}{k} + \frac{p_i^{n-1} - p_{i-1}^{n-1}}{\frac{k}{h} p_{M-1}^{n-1}} &= -\mu(a_i, P^{n-1}) p_i^{n-1} \\ p_M^n &= \frac{\frac{k}{h} p_{M-1}^{n-1}}{1 + k\mu(a_M, P^{n-1})} \\ p_0^n &= h \sum_{i=1}^M \beta(a_i, P^n) p_i^n \\ P^n &= h \sum_{i=1}^M p_i^n \end{aligned} \tag{4.1.4}$$

The authors obtained first-order convergence of the method by means of Taylor expansions:

$$\max_{0 \leq n \leq N} \max_{0 \leq i \leq M} |p(a_i, t^n) - p_i^n| \leq Ch$$

Numerical results were provided and first order effective order of convergence in case of finite or infinite maximum age a_+ was demonstrated.

Before the extrapolated versions of the upwind and Box schemes to appear, in 1992 Milner and Rabbio [84] considered and analyzed a second order method for a nonlinear model in which the birth rate was dependent on a , but independent of the population. They initialized the method by an Euler scheme combined with the trapezoidal rule:

$$\begin{aligned} p_i^0 &= p_0(a_i), \quad 0 \leq i \leq M; \quad P^0 = \frac{h}{2}(p_0^0 + p_M^0) + h \sum_{i=1}^{M-1} p_i^0 \\ \frac{p_i^1 - p_{i-1}^0}{h} &= -\mu(a_{i-1}, P^0) p_{i-1}^0, \quad i \geq 1 \\ p_0^1 &= \frac{h}{2}(\beta_0 p_0^1 + \beta_M p_M^1) + h \sum_{i=1}^{M-1} \beta_i p_i^1 \\ P^1 &= \frac{h}{2}(p_0^1 + p_M^1) + h \sum_{i=1}^{M-1} p_i^1 \end{aligned} \tag{4.1.5}$$

Then, they advanced in age and time for $2 \leq i \leq M$ and $2 \leq n \leq N$ by an explicit, three level finite difference method:

$$\begin{aligned} \frac{p_i^n - p_{i-2}^{n-2}}{2h} &= -\mu(a_{i-1}, P^{n-1}) \frac{p_i^n + p_{i-2}^{n-2}}{2} \\ \frac{p_1^n - p_0^{n-1}}{h} &= -\mu(a_0, P^{n-1}) p_0^{n-1}, \quad n \geq 2 \\ p_0^n &= \frac{h}{2}(\beta_0 p_0^n + \beta_M p_M^n) + h \sum_{i=1}^{M-1} \beta_i p_i^n, \quad n \geq 2 \\ P^n &= \frac{h}{2}(p_0^n + p_M^n) + h \sum_{i=1}^{M-1} p_i^n, \quad n \geq 2 \end{aligned} \tag{4.1.6}$$

The authors showed the method was second order accurate, proving

$$\|\varepsilon\|_{l^\infty(l^\infty)} \leq Ch^2,$$

where $\varepsilon_i^n = |p(a_i, t^n) - p_i^n|$ for $0 \leq i \leq M$, $0 \leq n \leq N$. In the same paper the authors treated a two-sex model formulated by Hoppensteadt in [41]. They adapted the scheme given above to this model and demonstrated its second order convergence. The analytical results were supported by numerical experiments.

In 1993 Milner [82] considered a modification of the Gurtin-MacCamy model, where the birth and death rates depended on a time integral of the solution rather than on an age integral. In

this way the influence of past history in the time dependence of the death and birth moduli was modeled. He proposed a first order finite difference method along characteristics and its convergence was proved:

$$\max_{0 \leq n \leq N} \max_{0 \leq i \leq M} |p(a_i, t^n) - p_i^n| \leq Ch$$

Some numerical examples were given.

During the same year Deborah Sulsky [93] made a comparison of different methods for the Gurtin-MacCamy's equation. Two different schemes were used: a second order finite difference scheme for first-order hyperbolic partial differential equations (the so called Lax-Wendroff method) and a TVD (Total Variation Diminishing) method for homogeneous conservation equations (derived by Harten and Osher [40] in 1987), adapted to the population model she dealt with. The Lax-Wendroff is a fractional-step method, defined first at intermediate levels $t^{n+\frac{1}{2}} = (n + \frac{1}{2})h$ and $a_{i+\frac{1}{2}} = (i + \frac{1}{2})k$ (h and k are the step-sizes in time and age respectively) and then at the full time and age levels for $1 \leq i \leq M$, $0 \leq n \leq N$ as follows:

$$\begin{aligned} p_{i+\frac{1}{2}}^{n+\frac{1}{2}} &= \left[1 - \frac{h}{2}\mu(a_{i+\frac{1}{2}}, P^n)\right] \frac{p_{i+1}^n + p_i^n}{2} - \frac{h}{2k}(p_{i+1}^n - p_i^n) \\ p_i^{n+1} &= p_i^n - \frac{h}{2}\mu(a_i, P^{n+\frac{1}{2}}) \left(p_{i+\frac{1}{2}}^{n+\frac{1}{2}} + p_{i-\frac{1}{2}}^{n+\frac{1}{2}}\right) - \frac{h}{k} \left(p_{i+\frac{1}{2}}^{n+\frac{1}{2}} - p_{i-\frac{1}{2}}^{n+\frac{1}{2}}\right) \end{aligned} \quad (4.1.7)$$

For the approximation of the total population size at full time-levels (as well as for the birth integral) the composite trapezoidal rule was used and for its approximation at half-time levels, the composite midpoint rule respectively:

$$\begin{aligned} P^n &= \frac{k}{2}(p_0^n + p_M^n) + k \sum_{i=1}^{M-1} p_i^n, \quad P^{n+\frac{1}{2}} = k \sum_{i=0}^{M-1} p_{i+\frac{1}{2}}^{n+\frac{1}{2}} \\ p_0^n &= \frac{k}{2}(\beta(a_0, P^n)p_0^n + \beta(a_M, P^n)p_M^n) + k \sum_{i=1}^{M-1} \beta(a_i, P^n)p_i^n \end{aligned} \quad (4.1.8)$$

Even though the author did not provide convergence results for neither of the methods (Lax-Wendroff and TVD), the author pointed out that the Lax-Wendroff scheme was second order accurate in h and k and the CFL condition $\frac{h}{k} < 1$ should be satisfied for stability reason. Both methods were tested with different test examples (including real data problems) and their performance was discussed. The numerical results indicated convergence.

Again in 1993 another two authors Kwon and Cho [64] published a paper in which a finite difference method along characteristics was introduced. The method was second order accurate and it was very similar to the one proposed by Milner and Rabbio (4.1.5, 4.1.6). The difference consisted in the term $\frac{p_i^n + p_{i-2}^{n-2}}{2}$ (see 4.1.6) replaced by p_{i-1}^{n-1} . The new scheme was tested on two

different cases $\mu(P(t))$, $p(0, t) = g(t)$ and $\mu(a, t, P(t))$, $p(0, t) = \int_0^{t+M} \beta(a, t)p(a, t)da$, $0 \leq a \leq t + M$. Kwon and Cho compared their scheme (in both cases) with two other algorithms - the

first order method given by Kostova [57] and the second-order scheme of Milner and Rabbiole discussed above. The convergence was discussed, providing the following estimate:

$$\sup_{0 \leq n \leq N} \sup_{0 \leq i \leq M} |p(a_i, t^n) - p_i^n| \leq Ch^2$$

In 1995 Abia and Lopez-Marcos [2] proposed difference schemes based on Runge-Kutta (RK) methods of arbitrary high order. They studied a more general version of Gurtin-MacCamy's model. Their work could be considered as a generalization of the work of Milner and Rabbiole [84] in which an explicit forth-order Runge-Kutta scheme (combined with the composite Simpson rule) for the linear problem (see 2.1.2) was given. The authors designed explicit and implicit RK methods of order $n \geq 2$ and they studied in details their consistency, stability and convergence. Lots of numerical experiments confirming the good performance of the methods were reported. The following convergence estimate was derived:

$$\max_{0 \leq n \leq N} \max_{0 \leq i \leq M} |p(a_i, t^n) - p_i^n| \leq C \left(h^s + \sum_{l=0}^s \max_{0 \leq i \leq M} |p(a_i, t^l) - p_i^l| \right)$$

Two years later, in 1997 Iannelli, Kim and Park [45] published an article in which a backward finite difference method along the characteristics was proposed. They assumed individuals with a finite life span, which was the more biologically significant case but much more difficult to deal with. They considered the Gurtin MacCamy's model, where the mortality function was given as: $\mu(a, P(t)) = m(a) + M(a, P(t))$. The function m was called the natural mortality and M was called the external mortality (i.e. a mortality, caused by an external force). The algorithm they proposed was a first-order, explicit method (where by \tilde{f} were denoted the approximations of the respective functions), given by:

$$\begin{aligned} p_i^0 &= p_0(a_i), \quad P^0 = h \sum_{i=0}^M p_i^n \\ \frac{p_i^{n-\frac{1}{2}} + p_{i-1}^{n-1}}{h} + \tilde{m}_i p_i^{n-\frac{1}{2}} &= 0, \quad n > 1, 1 \leq i \leq M \\ \frac{p_i^n + p_{i-1}^{n-\frac{1}{2}}}{h} + \tilde{M}(a_i, P^{n-1}) p_i^n &= 0, \quad n > 1, 1 \leq i \leq M \\ p_0^n &= h \sum_{i=0}^M b_i \beta(a_i, P^{n-1}) p_i^n \\ P^n &= h \sum_{i=0}^M c_i p_i^n, \end{aligned} \tag{4.1.9}$$

where c_i and b_i are weights for numerical quadrature rules (trapezoidal rule or Riemann sum). The authors showed first order of convergence, providing:

$$\max_{0 \leq n \leq N} \max_{0 \leq i \leq M} |p(a_i, t^n) - p_i^n| \leq Ch$$

They adapted the scheme above to a SIS model and confirmed their analytical results by various numerical experiments.

The same year, Abia and Lopez-Marcos [3] following the ideas of Chiu [24] proposed second order implicit finite difference schemes based on Padé rational approximations for a more general version of Gurtin-MacCamy's model. Using the theoretical representation formula (4.1.1) of the solution of Gurtin-MacCamy's equation, they designed a family of such schemes in the following way - they approximated the integral terms with quadrature rules and the exponential function $\exp(x)$ in terms of Padé(m, n) rational approximation $R(x) = \frac{P_m(x)}{Q_n(x)}$. The polynomials P and Q were, respectively of degrees m and n and such that:

$$|\exp(x) - R(x)| = O(x^3), \quad x \rightarrow 0$$

The methods defined in that paper were the following:

$$\begin{aligned} p_{i+1}^{n+1} &= p_i^n R\left(-\frac{h}{2}[\mu(a_i, P^n) + \mu(a_{i+1}, P^{n+1})]\right), \quad 0 \leq n \leq N-1, \quad 0 \leq i \leq M-1 \\ p_0^n &= \frac{h}{2}\left(\beta(a_0, P^n, t^n)p_0^n + \beta(a_M, P^n, t^n)p_M^n\right) + h \sum_{i=1}^{M-1} \beta(a_i, P^n, t^n)p_i^n, \quad 0 \leq n \leq N-1 \\ P^n &= \frac{h}{2}(p_0^n + p_M^n) + h \sum_{i=1}^{M-1} p_i^n, \quad 0 \leq n \leq N \end{aligned} \tag{4.1.10}$$

In order to approximate the integrals the authors used the composite trapezoidal rule (see the scheme above) which resulted in an implicit method that required the use of iterations at each time step. Full stability and convergence analysis was provided, as well as a variety of numerical experiments. To test their algorithm the authors chose Padé(1, 1), Padé(0, 2), Padé(2, 0) and Padé(2, 2) rational approximations to the function $\exp(x)$, given respectively by:

$$\frac{2+x}{2-x}, \quad \frac{1}{1-x+\frac{x^2}{2}}, \quad 1+x+\frac{x^2}{2}, \quad \frac{12+6x+x^2}{12-6x+x^2}$$

Comparison with another second order (Runge-Kutta) method proposed in [2] was done. Even though the family of schemes above used as an approximation rule the trapezoidal rule, the authors tested the method also with the Simpson's rule. Finally, they pointed out that the discrete equations (4.1.10) can be made explicit if a quadrature rule other than the trapezoidal rule was used to approximate the integral inside the exponential in (4.1.1) that only required data from previous time levels.

In 1999 the same authors [4] described and analyzed an alternative (to the one formulated in 1997) explicit second order method for the numerical integration of nonlinear age-dependent models. The scheme was again designed by means of a representation formula for the theoretical

solution of the discussed model (4.1.1) joint with an open quadrature formula for the numerical approximation of the nonlocal terms. The method was initialized by

$$\begin{aligned} p_{i+\frac{1}{2}}^{\frac{1}{2}} &= p_{i+\frac{1}{2}}^0 \exp\left(-\frac{h}{2}\mu(a_{i+\frac{1}{2}}, P^0, t^0)\right), \quad 0 \leq i \leq M-1 \\ p_{\frac{1}{2}}^{\frac{1}{2}} &= p_0^0 \exp\left(-\frac{h}{2}\mu(a_0, P^0, t^0)\right) \\ p_0^{\frac{1}{2}} &= h\beta(a_{\frac{1}{2}}, P^{\frac{1}{2}}, t^{\frac{1}{2}})p_{\frac{1}{2}}^{\frac{1}{2}} + h \sum_{i=1}^{M''} \beta(a_i, P^{\frac{1}{2}}, t^{\frac{1}{2}})p_i^{\frac{1}{2}}, \end{aligned} \quad (4.1.11)$$

where the double prime in the summation means that the first and the last terms are halved and we have used the notation introduced above for the half age and time levels. Furthermore, the stepping in age and time for $0 \leq n \leq N-1$ was done in the following way

$$\begin{aligned} p_{i+\frac{1}{2}}^n &= p_{i-\frac{1}{2}}^{n-1} \exp\left(-h\mu(a_i, P^{n-\frac{1}{2}}, t^{n-\frac{1}{2}})\right), \quad 1 \leq i \leq M-1 \\ p_{\frac{1}{2}}^n &= p_0^{n-\frac{1}{2}} \exp\left(-\frac{h}{2}\mu(a_{\frac{1}{4}}, \frac{3}{2}P^{n-\frac{1}{2}} - \frac{1}{2}P^{n-1}, t^{n-\frac{1}{4}})\right) \\ p_0^n &= h \sum_{i=1}^{M-1} \beta(a_{i+\frac{1}{2}}, P^n, t^n)p_{i+\frac{1}{2}}^n \end{aligned} \quad (4.1.12)$$

and also

$$\begin{aligned} p_{i+\frac{1}{2}}^{n+\frac{1}{2}} &= p_i^{n-\frac{1}{2}} \exp\left(-h\mu(a_{i+\frac{1}{2}}, P^n, t^n)\right), \quad 0 \leq i \leq M-1 \\ p_{\frac{1}{2}}^{n+\frac{1}{2}} &= p_0^n \exp\left(-\frac{h}{2}\mu(a_{\frac{1}{4}}, \frac{3}{2}P^n - \frac{1}{2}P^{n-\frac{1}{2}}, t^{n+\frac{1}{4}})\right) \\ p_0^{n+\frac{1}{2}} &= h\beta(a_{i+\frac{1}{2}}, P^{n+\frac{1}{2}}, t^{n+\frac{1}{2}})p_{\frac{1}{2}}^{n+\frac{1}{2}} + h \sum_{i=1}^{M''} \beta(a_i, P^{n+\frac{1}{2}}, t^{n+\frac{1}{2}})p_i^{n+\frac{1}{2}} \end{aligned} \quad (4.1.13)$$

Finally, for the approximation of the total population size at full and half time levels, the authors proceeded in the following way: they used the composite trapezoidal rule at the full time levels

$$P^n = \frac{h}{2}(p_0^n + p_M^n) + h \sum_{i=1}^{M-1} p_i^n$$

and a composite rule for the half time levels, which consisted of the midpoint rule in the first subinterval and the trapezoidal rule in the rest of the subintervals:

$$P^{n+\frac{1}{2}} = hp_{\frac{1}{2}}^{n+\frac{1}{2}} + \frac{h}{2} \sum_{i=1}^M (p_{i-1}^{n+\frac{1}{2}} + p_i^{n+\frac{1}{2}})$$

The consistency, stability and existence of the discrete solutions were established and with this choice of the quadrature rules second order convergence was proved:

$$\begin{aligned} \max_{0 \leq n \leq N} |p(a_0, t^n) - p_0^n| &\leq Ch^2 \\ \left\{ \max_{0 \leq n \leq N-1} |p(a_{\frac{1}{2}}, t^{n+\frac{1}{2}}) - p_{\frac{1}{2}}^{n+\frac{1}{2}}|, \max_{1 \leq i \leq M} |p(a_i, t^{n+\frac{1}{2}}) - p_i^{n+\frac{1}{2}}| \right\} &\leq Ch^2 \\ \max_{0 \leq n \leq N} \max_{1 \leq i \leq M-1} |p(a_{i+\frac{1}{2}}, t^n) - p_{i+\frac{1}{2}}^n| &\leq Ch^2 \end{aligned} \quad (4.1.14)$$

In this paper the authors made an important statement about the dominant error in the numerical integration of problems like Gurtin-MacCamy's model. They underlined and proved that the error due to the integration of the nonlocal terms was the dominant error in such cases. They stressed on the fact that the use of higher order quadrature rules could improve the numerical approximation and they proposed various high order special quadrature rules. Their statement was later confirmed by the numerical experiments. Thus, an important conclusion could be done: in order to obtain better accuracy the quadrature rules used for the numerical integration of the nonlocal terms should be of order equal or preferably greater than the order of the difference scheme.

In 2002 Kim and Kwon [53] proposed and analyzed a collocation method for the Gurtin-MacCamy's equation. They assumed the maximum age a_+ of the species was finite (i.e the more realistic case) which brought new problems to deal with. For such kind of problems the reader is referred to [48] for a complete discussion. The method of Kim and Kwon was a forth order implicit Runge-Kutta method of two stages for the integration of the ODE along characteristics whose collocation points were zeros of Legendre monic polynomial. For $3 \leq n \leq N-1$, $0 \leq i \leq M-2$ the scheme was defined as follows:

$$\begin{aligned} \gamma_1 &= p_i^n - h \left\{ \frac{1}{4} \mu(a_i + c_1, P^{n+c_1}) \gamma_1 + \left(\frac{1}{4} - \frac{\sqrt{3}}{6} \right) \mu(a_i + c_2, P^{n+c_2}) \gamma_2 \right\} \\ \gamma_2 &= p_i^n - h \left\{ \left(\frac{1}{4} - \frac{\sqrt{3}}{6} \right) \mu(a_i + c_1, P^{n+c_1}) \gamma_1 + \frac{1}{4} \mu(a_i + c_2, P^{n+c_2}) \gamma_2 \right\} \\ p_{i+1}^{n+1} &= p_i^n - \frac{1}{2} \left\{ \mu(a_i + c_1, P^{n+c_1}) \gamma_1 + \mu(a_i + c_2, P^{n+c_2}) \gamma_2 \right\}, \end{aligned} \quad (4.1.15)$$

where $c_1 = \frac{1}{2} - \frac{\sqrt{3}}{6}$ and $c_2 = \frac{1}{2} + \frac{\sqrt{3}}{6}$,

$$P^{n+c_1} = \left\{ \frac{55}{24} - \frac{107\sqrt{3}}{216} \right\} P^n - \left\{ \frac{59}{24} - \frac{71\sqrt{3}}{72} \right\} P^{n-1} + \left\{ \frac{37}{24} - \frac{47\sqrt{3}}{72} \right\} P^{n-2} - \left\{ \frac{3}{8} + \frac{35\sqrt{3}}{216} \right\} P^{n-3}$$

and

$$P^{n+c_2} = \left\{ \frac{55}{24} + \frac{107\sqrt{3}}{216} \right\} P^n - \left\{ \frac{59}{24} + \frac{71\sqrt{3}}{72} \right\} P^{n-1} + \left\{ \frac{37}{24} + \frac{47\sqrt{3}}{72} \right\} P^{n-2} - \left\{ \frac{3}{8} - \frac{35\sqrt{3}}{216} \right\} P^{n-3}$$

For the approximation of the nonlocal terms they used the Simpson's rule as follows:

$$\begin{aligned} p_0^{n+1} &= \frac{h}{3 - h\beta(a_0, P^{n+1})} \left[4\beta(a_1, P^{n+1})p_1^{n+1} + \beta(a_2, P^{n+1})p_2^{n+1} + \right. \\ &\quad \left. + \sum_{k=1}^{\frac{M}{2}-1} (\beta(a_{2k}, P^{n+1})p_{2k}^{n+1} + 4\beta(a_{2k+1}, P^{n+1})p_{2k+1}^{n+1} + \beta(a_{2k+2}, P^{n+1})p_{2k+2}^{n+1}) \right] \quad (4.1.16) \\ P^{n+1} &= \frac{h}{3} \left\{ p_0^{n+1} + 4p_1^{n+1} + p_2^{n+1} + \sum_{k=1}^{\frac{M}{2}-1} (p_{2k}^{n+1} + 4p_{2k+1}^{n+1} + p_{2k+2}^{n+1}) \right\} \end{aligned}$$

For the initialization of the algorithm the authors used a second order implicit Runge-Kutta method together with Richardson extrapolation, but they could use some of the schemes based on the method of characteristics that were described above. It should be noted that since equations (4.1.16) were nonlinear an iteration procedure was done. The convergence was established by deriving the following estimate:

$$\sup_{0 \leq n \leq N} \sup_{0 \leq i \leq M} |p(a_i, t^n) - p_i^n| \leq Ch^4$$

The method was compared with another second-order scheme (given in an article [56] that was never published) and the numerical computations showed the expected forth order of convergence.

Very similar models (to the Gurtin-MacCamy problem) arise when size-structured populations are considered. Their numerical treatment is also similar to the one of the age-structured models. Mostly concerned with size-structured populations are Luis-Maria Abia, Oscar Angulo and Lopez-Marcos who published several papers on that topic and proposed some new numerical techniques. The reader is referred to [1], [7], [8] and [9] for a comprehensive study of numerical methods for size-structured population and to [59] for a very interesting explicit third order scheme for such problems.

4.2. Numerical Approximation of a Model of Logistic Growth

In this Section we deal with the Model of Logistic Growth (1.2.5) introduced in Chapter 1. Our aim is to present a comparative study about the numerical methods and their performance for both - the partial differential equation itself (1.2.5) and its integral reformulation (1.2.6). Taking advantage from the variety of schemes described above (see Section 4.1), we choose some of them (or their modification) in order to solve numerically (1.2.5). Wishing to give an insight on other possibilities to approximate the Logistic Growth equation and to see whether it makes sense to use its integral reformulation as an indirect way for its approximation, we discuss and compare the accuracy and the efficiency of the schemes based on several test examples we propose. Some of the results presented in this and in the next sections were obtained in collaboration with Mimmo Iannelli, Giuseppe Izzo, Eleonora Messina, Elvira Russo and Antonella Vecchio [88]. We leave the stability and convergence analysis to future studies.

Let us first rewrite (1.2.5) in the following simplified form

$$\begin{cases} \frac{\partial u(a, t)}{\partial t} + \frac{\partial u(a, t)}{\partial a} = 0, & a, t > 0 \\ u(0, t) = R_0 \phi(S(t)) \int_0^{a_+} \beta_0(a) \pi_0(a) u(a, t) da, & t > 0 \\ u(a, 0) = \frac{p_0(a)}{\pi_0(a)}, & a > 0 \\ S(t) = \int_0^{a_+} \gamma(a) \pi_0(a) u(a, t) da, \end{cases} \quad (4.2.1)$$

where we have substituted: $u(a, t) = \frac{p(a, t)}{\pi_0(a)}$. We assume that $\phi \in C^1(0, \infty)$, μ_0, β_0 and γ are either smooth or piecewise smooth functions on $[0, a_+]$. We also suppose that

$$\int_0^{a_+} \beta_0(a) \pi_0(a) da = 1 \quad (4.2.2)$$

and that the compatibility condition (1.1.4) is satisfied. Under these assumptions it is proved [44] that if $R_0 \leq 1$ there exists only one equilibrium and it is the trivial one which is *stable*, while if $R_0 > 1$, there exists one and only one nontrivial equilibrium and the trivial one is *unstable*. It is shown that if the function $\gamma(a) \pi_0(a)$ is non increasing and convex, then the nontrivial equilibrium is *stable* for all $R_0 > 1$. But in some situations the stationary state can loose its stability, i.e if at certain values of some varying parameter, a couple of roots of the respective characteristic equation (see 4.2.6 for a special case) cross the imaginary axis to the right, then a *periodic solution* is generated and we have a Hopf bifurcation for our model. Since a complete analytical treatment of this matter is very difficult we need to approach these phenomena by numerical analysis' tools. We shall establish the value of R_0 at which the bifurcation occurs.

Such an investigation has already been done in [18] by applying pseudospectral differencing methods for the characteristic roots of the same age-structured model. It is shown that for certain values of some of the parameters a bifurcation occurs. In the following we want to study the existence of periodic solutions numerically, by treating both the partial differential equation (1.2.5) and its integral equivalent (1.2.6).

Firstly we want to study and compare the behavior of both methods - the second order trapezoidal rule for the integral equation (1.2.6) and a first order finite difference scheme combined with the trapezoidal rule for the hyperbolic equation (4.2.1). We shall investigate these methods in several aspects to see whether the numerical solution produced by the respective method, mimics the behavior of the analytical one, i.e. if we can trust the qualitative information provided by the numerical algorithm when simulating real problems; we shall be concerned with the efficiency of the schemes. We introduce the following notations:

$$K(a) = \beta_0(a)\pi_0(a) \quad \text{and} \quad H(a) = \gamma(a)\pi_0(a), \quad a \in [0, a_+] \quad (4.2.3)$$

The application of the methods we shall use for both models will depend on the continuity of these functions. We shall consider examples with continuous and piecewise defined (discontinuous) kernels.

When the initial data are smooth, we shall proceed in a trivial way:

- for the leading equation in (4.2.1) we use a direct integration along the characteristic lines obtaining: $u_{i+1}^{n+1} = u_i^n$ (see Figure 3.1 and (2.1.1)), while for the boundary condition we use the composite trapezoidal rule and an iterative procedure because of its nonlinearity.
- for the integral reformulation of the same model (1.2.6) we apply the composite trapezoidal rule to the integral terms $S(t)$ and $B(t)$ and we again use an iterative procedure. The functions $F(t)$ and $G(t)$ are in general known functions.

When we have discontinuous kernels (4.2.3), the situation is different. The point of discontinuity should be taken as a node of the discretization mesh. Let us assume that we have discontinuous kernels $K(a)$ and $H(a)$, defined as follows

$$K(a) = \begin{cases} K_1(a), & a \in [0, a^*] \\ K_2(a), & a \in [a^*, a_+] \end{cases} \quad (4.2.4)$$

$$H(a) = \begin{cases} H_1(a), & a \in [0, a^*] \\ H_2(a), & a \in [a^*, a_+], \end{cases} \quad (4.2.5)$$

where a^* is the maturation age of the individuals. Then the integral equation (1.2.6) takes the form:

$$\begin{aligned} t &\leq a^* \\ S(t) &= G(t) + \int_0^t H_1(t-s)B(s)ds \\ B(t) &= R_0\phi(S(t))[F(t) + \int_0^t K_1(t-s)B(s)ds] \end{aligned}$$

$$\begin{aligned} t &\geq a^* \quad \text{and} \quad t \leq a_+ \\ S(t) &= G(t) + \int_0^t K(t-s)B(s)ds = G(t) + \int_{t-a^*}^t H_1(t-s)B(s)ds + \int_0^{t-a^*} H_2(t-s)B(s)ds \\ B(t) &= R_0\phi(S(t))[F(t) + \int_0^t K(t-s)B(s)ds] = \\ &= R_0\phi(S(t))[F(t) + \int_{t-a^*}^t K_1(t-s)B(s)ds + \int_0^{t-a^*} K_2(t-s)B(s)ds] \end{aligned}$$

$$\begin{aligned} t &> a_+ \\ S(t) &= \int_{t-a_+}^t H(t-s)B(s)ds = \int_{t-a^*}^t H_1(t-s)B(s)ds + \int_{t-a_+}^{t-a^*} H_2(t-s)B(s)ds \\ B(t) &= R_0\phi(S(t)) \int_{t-a_+}^t K(t-s)B(s)ds = \\ &= R_0\phi(S(t)) \left[\int_{t-a^*}^t K_1(t-s)B(s)ds + \int_{t-a_+}^{t-a^*} K_2(t-s)B(s)ds \right], \end{aligned}$$

Thus, if we consider the same partition of the interval $[0, T]$ as in Section 2.2.1 (see Figure 2.2) and the same discretization parameter h , a direct application of the trapezoidal rule on the equations above yields

$$\begin{aligned} n &\leq n^* \\ S^n &= G^n + \frac{h}{2} \left(H_1(hn)B^0 + H_1(0)B^n \right) + h \sum_{i=1}^{n-1} H_1(h(n-i))B^i \\ B^n &= R_0\phi(S^n) \left[F^n + \frac{h}{2} \left(K_1(hn)B^0 + K_1(0)B^n \right) + h \sum_{i=1}^{n-1} K_1(h(n-i))B^i \right] \end{aligned}$$

$$n \geq n^* \quad \text{and} \quad n \leq N$$

$$\begin{aligned} S^n &= G^n + \frac{h}{2} \left(H_1(hn^*) + H_2(hn^*) \right) B^{n-n^*} + \frac{h}{2} H_1(0) B^n + h \sum_{i=n-n^*+1}^{n-1} H_1(h(n-i)) B^i + \\ &\quad + \frac{h}{2} H_2(hn) B^0 + h \sum_{i=1}^{n-n^*-1} H_2(h(n-i)) B^i \\ B^n &= R_0 \phi(S^n) \left[F^n + \frac{h}{2} \left(K_1(hn^*) + K_2(hn^*) \right) B^{n-n^*} + \frac{h}{2} K_1(0) B^n + h \sum_{i=n-n^*+1}^{n-1} K_1(h(n-i)) B^i + \right. \\ &\quad \left. + \frac{h}{2} K_2(hn) B^0 + h \sum_{i=1}^{n-n^*-1} K_2(h(n-i)) B^i \right] \end{aligned}$$

$$n > N$$

$$\begin{aligned} S^n &= \frac{h}{2} \left(H_1(h(N-n^*)) + H_2(h(N-n^*)) \right) B^{n^{**}} + \frac{h}{2} H_1(0) B^n + h \sum_{i=n^{**}+1}^{n-1} H_1(h(n-i)) B^i + \\ &\quad + \frac{h}{2} H_2(hN) B^{n-N} + h \sum_{i=n-N+1}^{n^{**}-1} H_2(h(n-i)) B^i \\ B^n &= R_0 \phi(S^n) \left[\frac{h}{2} \left(K_1(h(N-n^*)) + K_2(h(N-n^*)) \right) B^{n^{**}} + h \sum_{i=n^{**}+1}^{n-1} K_1(h(n-i)) B^i + \right. \\ &\quad \left. + \frac{h}{2} K_1(0) B^n + \frac{h}{2} K_2(hN) B^{n-N} + h \sum_{i=n-N+1}^{n^{**}-1} K_2(h(n-i)) B^i \right] \end{aligned}$$

where we have used the notation $n^{**} = n - N + n^*$; S^n and B^n are the approximations of the functions $S(t)$ and $B(t)$ respectively at the point mesh t^n and $n^* = \frac{a^*}{h}$.

In order to solve this system of integral equations we should use an iterative procedure.

Concerning equation (4.2.1), the way we split the integral term at the boundary condition in it is analogous to what we did for the integral equation and we shall omit in details.

Let us now study the behavior of the schemes via several test examples. First of all, we consider a particular case of the characteristic equation of our model given by

$$\hat{K}_0(\lambda) + \tau \hat{K}_1(\lambda) = 1, \quad (4.2.6)$$

where $\tau \in R$; $K_i(\cdot)$, $i = 0, 1 : [0, +\infty) \rightarrow R$ are such that

$$K_i(t) \geq 0, \quad K_i(t) = 0 \quad t > T, \quad \int_0^\infty K_i(t) dt = 1$$

In [44] it is proved that if $\tau > 0$ then equation (4.2.6) has a real positive root. This fact indicates instability of the nontrivial stationary solution $p^*(a)$ of (1.2.5) since $p^*(a)$ is asymptotically stable

when the characteristic equation (4.2.6) has only roots with negative real part. On the other hand it is shown that if the roots of the characteristic equation (4.2.6) have only negative real part for any $\tau < 0$, the following inequality is satisfied:

$$\int_0^\infty K_1(\sigma) \cos(\omega\sigma) d\sigma \geq 0 \quad \text{for } \forall \omega \in R$$

In such case the stationary solution $p^*(a)$ is asymptotically stable.

If we consider the case $R_0 \geq 1$ and perform linearization at the nontrivial equilibrium $\phi^{-1}(\frac{1}{R_0})$, then we have

$$\tau = \tau(R_0) = R_0 \phi^{-1}(\frac{1}{R_0}) \phi'(\phi^{-1}(\frac{1}{R_0})) \quad (4.2.7)$$

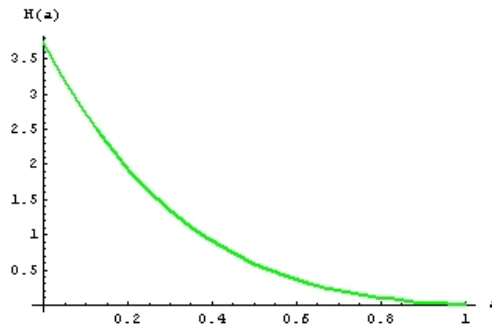
In order to trace the stability of the nontrivial stationary solution for $R_0 > 1$, we will be interested in the values of τ as a function of R_0 as given in the equation above. Moreover, we note that τ is negative and $\tau(1) = 0$. Hence, when R_0 is near to 1 the nontrivial equilibrium is stable and we want to identify where the point (if such a point exists) of crossing of some root through the imaginary axis is. We shall do that considering the following test examples:

Example 1 Let us consider the logistic model (4.2.1) and let us assume that

$$\phi(x) = e^{-x}, \beta_0(a) = \gamma(a) = c_1, \mu_0(a) = \frac{\pi}{2} \tan\left(\frac{\pi}{2}a\right) + c_2, \pi_0(a) = e^{-c_2 a} \cos\left(\frac{\pi}{2}a\right), a_+ = 1,$$

where c_1 and c_2 are positive constants. This choice of the parameters is equivalent to assuming that the total population $S(t)$ is equal to $B(t)$, i.e. we assume that the vital parameters depend on the birth rate. If we calculate the parameter τ by formula (4.2.7), we obtain $\tau(R_0) = -\ln(R_0)$. This means that the nontrivial equilibrium is stable for $R_0 > 1$ (since in such case $\tau(R_0)$ takes only negative values), but R_0 sufficiently close to 1. To draw the graphs below we

have chosen $c_1 = \frac{1 + \frac{\pi^2}{4c_2^2}}{\frac{1}{c_2} + \frac{\pi e^{-c_2}}{2c_2^2}}$ (c_1 was calculated in such a way that the normalization condition (4.3.2) to be satisfied), $c_2 = 3$ and by B^* we have denoted the steady state value.



Remark: We note that since in that case the kernel $H(a)$ is decreasing and convex (see the figure above), we should not expect a bifurcation to occur.

In the following we want to study how the stability of B^* changes when varying R_0 .

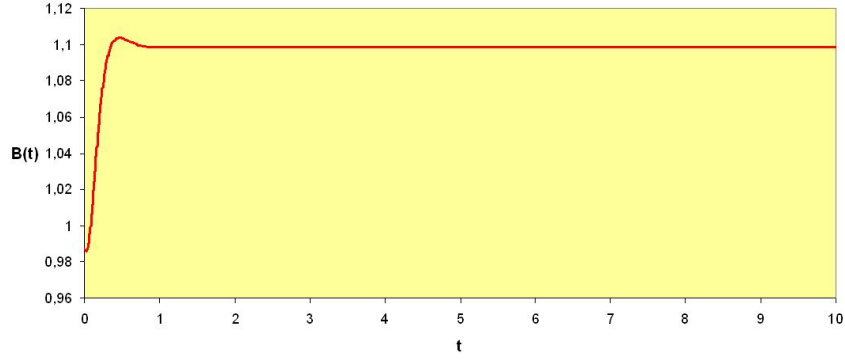


Figure 4.1: $R_0 = 3, B^* = \ln(R_0) \approx 1.09$

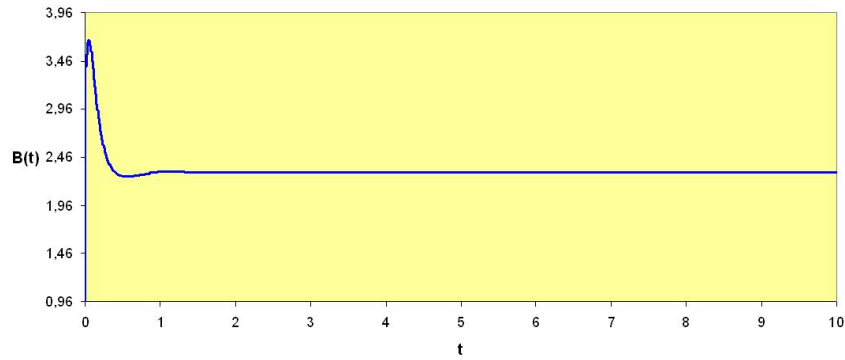


Figure 4.2: $R_0 = 10, B^* = \ln(R_0) \approx 2.30$

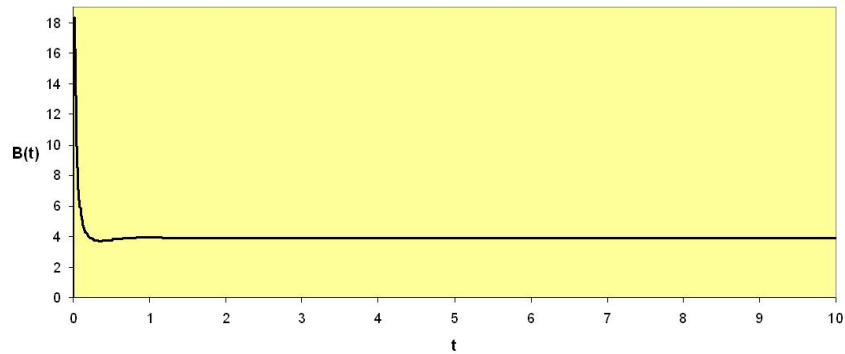


Figure 4.3: $R_0 = 50, B^* = \ln(R_0) \approx 3.91$

Obviously this is the case when the functions $\beta_0(a)$ and $\gamma(a)$ are continuous and thus the application of the trapezoidal rule is trivial. The results from the simulations performed for models (4.2.1) and (1.2.6) were almost equal (as approximate values of $B(t)$) which means that we can consider both algorithms as equally reliable. This presumption is confirmed by the figures above where we can see that the behavior of the approximate solution corresponds to what we expected it to be, i.e. for any $R_0 > 1$ a stable nontrivial equilibrium exists and the approximate solution approaches it. Moreover, when the net reproduction ratio is small we see an exponential growth and stabilization afterwards, while when increasing R_0 we observe a fast exponential growth, a phase of fast decreasing afterwards followed by stabilization. This can probably be explained by the (dramatic) form of the cut-off function $\phi(x)$ in this case.

Example 2 We now consider a similar example, where we change only the function $\phi(x)$

$$\phi(x) = \frac{1}{1+x}, \beta_0(a) = \gamma(a) = c_1, \mu_0(a) = \frac{\pi}{2} \tan\left(\frac{\pi}{2}a\right) + c_2, \pi_0(a) = e^{-c_2 a} \cos\left(\frac{\pi}{2}a\right), a_+ = 1,$$

and c_1, c_2 are the same positive constants as in Example 1. Calculating the value of τ by (4.2.7), we obtain $\tau(R_0) = \frac{1}{R_0} - 1$, which shows stability of the nontrivial steady solution for $R_0 > 1$ and since the function $H(a)$ is the same as in Example 1, no bifurcation should be seen. The situation here is very similar to the previous case. Both algorithms behave good and the approximate solution quickly goes to the stable equilibrium. However, after the exponential growth it comes a deceleration phase and a stabilization afterwards which is due to the more natural form of the function $\phi(x)$.

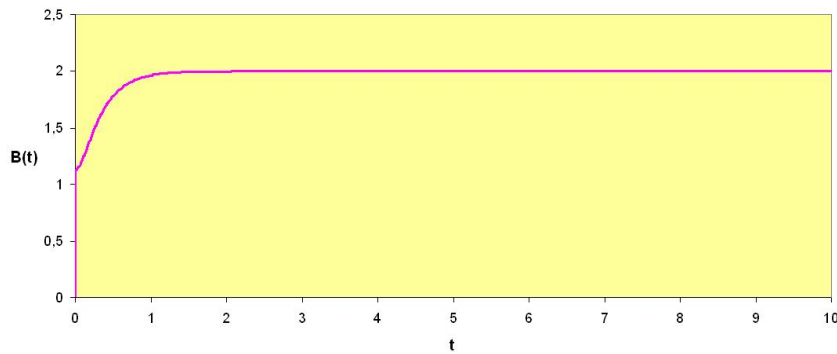


Figure 4.4: $R_0 = 3, B^* = R_0 - 1 = 2$

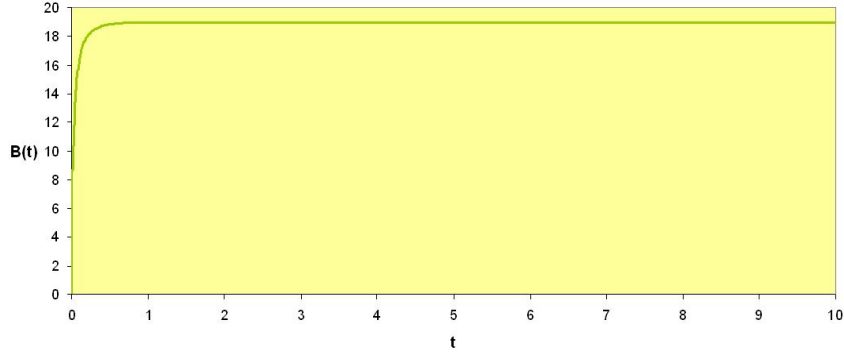


Figure 4.5: $R_0 = 20, B^* = R_0 - 1 = 19$

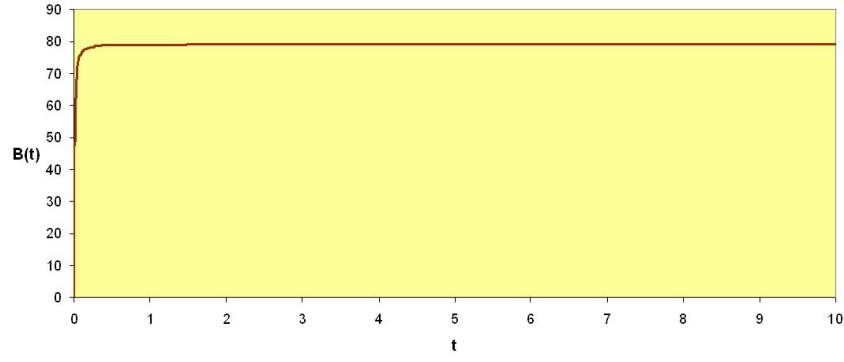


Figure 4.6: $R_0 = 80, B^* = R_0 - 1 = 79$

Example 3 In this example we consider particular vital rates, namely

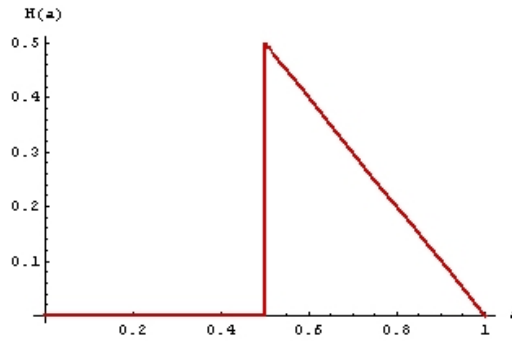
$$\beta_0(a) = \begin{cases} 0, & a \leq a^* \\ 8, & a \geq a^* \end{cases} \quad \gamma(a) = \begin{cases} 0, & a \leq a^* \\ 1, & a \geq a^* \end{cases}$$

$$\phi(x) = e^{-x^\alpha}, \quad \mu_0(a) = \frac{1}{a_+ - a}, \quad \pi_0(a) = a_+ - a,$$

where for simplicity we assume the maximum age $a_+ = 1$ and the maturation age $a^* = \frac{1}{2}$; $\alpha > 0$ is a fixed parameter. Thus, the kernels (4.2.3) take the following form

$$K(a) = 8(1-a)\chi_{[\frac{1}{2},1]}(a), \quad a \in [0,1] \\ H(a) = (1-a)\chi_{[\frac{1}{2},1]}(a), \quad a \in [0,1],$$

where χ_I denotes a characteristic function of the interval $I \subset R$. This means that we consider the mature (adult) population as more important information source than the juveniles. Also, one can see that in this case the kernel $H(a)$ is no more convex.



Obviously the kernels above are discontinuous and hence we are in the more complicated case. In order to use a quadrature rule for the integral terms of models (4.2.1) and (1.2.6), we need to split them as proposed above. When we calculate the value of τ , we obtain $\tau(R_0) = -\alpha \ln(R_0)$, which of course means that the nontrivial equilibrium is stable when R_0 is sufficiently close to 1. However, in [18] the authors study the behavior of the rightmost characteristic roots of (4.2.6) and it is shown that for $\alpha = 1$, "the pure real root λ of (4.2.6) moves towards the left when R_0 increases and it splits into a complex-conjugate pair when $R_0 = e$ and it proceeds to the right towards the imaginary axis for increasing R_0 above e . In particular, when $R_0 \approx 8.772$, a bifurcation occurs." Following this idea and using the algorithms for models (4.2.1) and (1.2.6), we want to check if the bifurcation will occur at the point indicated in [18].

Remark: In this case the birth rate $B(t)$ and the total population $S(t)$ are proportional and that's why we proceed showing graphs for $B(t)$.

a) $\alpha = 1$

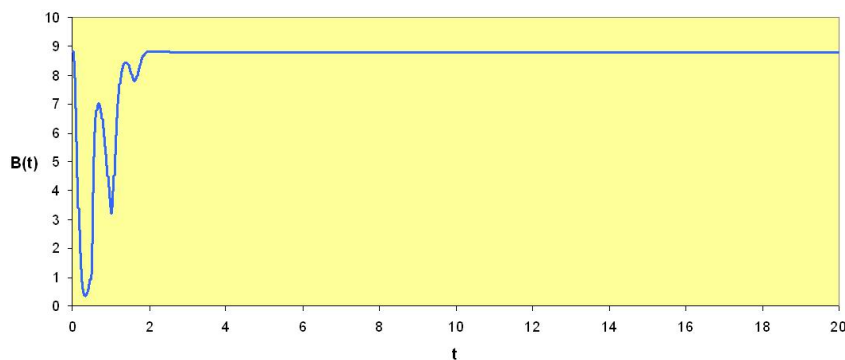
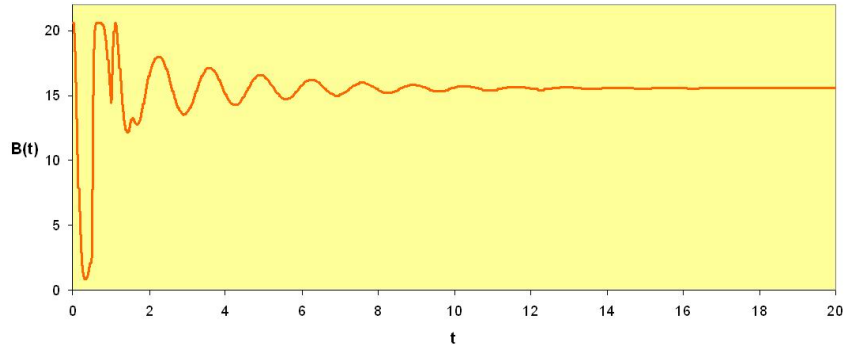
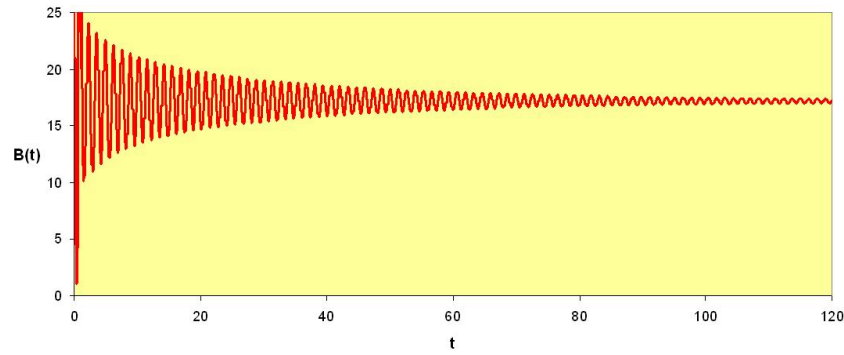
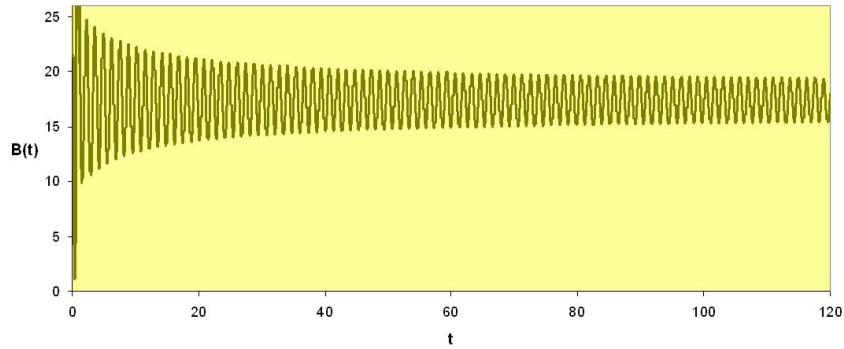


Figure 4.7: $R_0 = 3, B^* = 8 \ln(3) \approx 8.78$

Figure 4.8: $R_0 = 7, B^* = 8 \ln(7) \approx 15.57$ Figure 4.9: $R_0 = 8.6, B^* = 8 \ln(8.6) \approx 17.21$ Figure 4.10: $R_0 = 8.772, B^* = 8 \ln(8.772) \approx 17.37$

What we see from the graphs above is that when R_0 is small ($R_0 = 3$) some oscillations appear in the beginning but they rapidly die out and the nontrivial equilibrium stabilizes. Increasing R_0 to 7 more oscillations occur but they die away for $t \approx 16$. When $R_0 = 8.6$ a clear oscillatory behavior can be observed but the oscillations are damped (their amplitude decreases with time).

However, at point $R_0 \approx 8.772$ (Figure 4.10) a bifurcation occurs. The oscillations of $B(t)$ are very powerful and occurrence of stable periodic solution can be seen. This behavior agrees with the analysis of the characteristic equation (4.2.6) made in [18]. We note that these results were obtained by both schemes, which fact again confirms they are trustworthy.

b) In order to accelerate the occurrence of oscillations we vary the value of the parameter α . In the following we report results for $\alpha = 3$.

The figures below show similar behavior as in the case $\alpha = 1$. The difference is in the bifurcation point, here we see sustained oscillations (and a periodic solution) already for $R_0 = 2.1$. This means that when increasing α , we accelerate the occurrence of bifurcation. This fact is confirmed also by the next example.

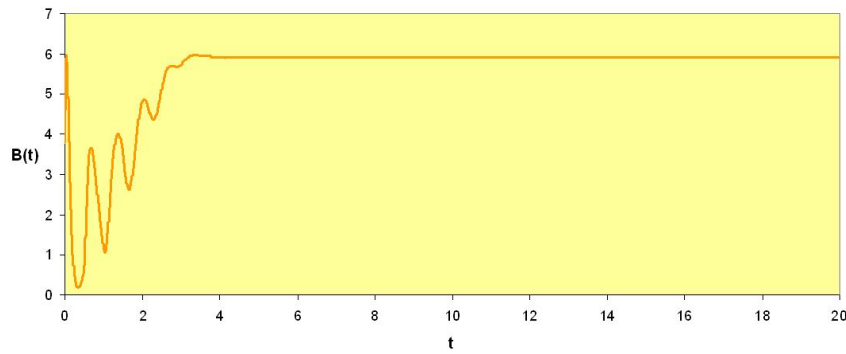


Figure 4.11: $R_0 = 1.5, B^* = 8 \ln(1.5)^{\frac{1}{3}} \approx 5.92$

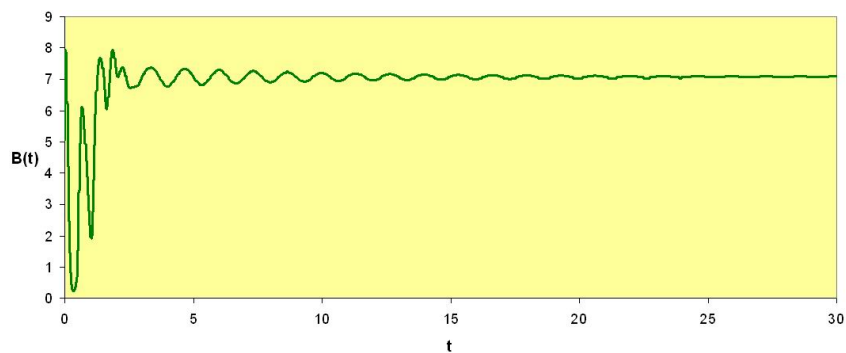


Figure 4.12: $R_0 = 2, B^* = 8 \ln(2)^{\frac{1}{3}} \approx 7.08$

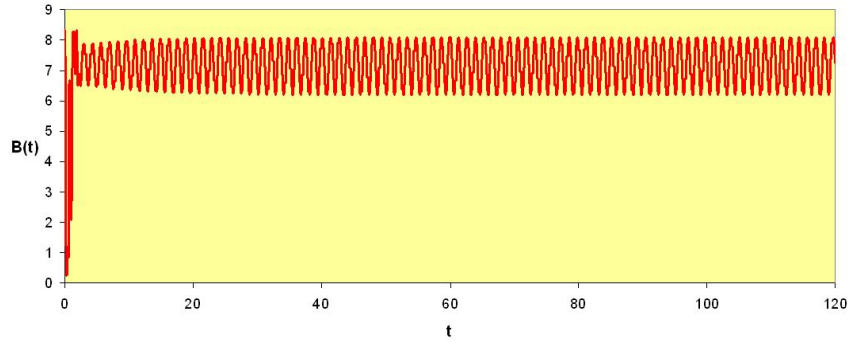


Figure 4.13: $R_0 = 2.1, B^* = 8 \ln(2.1)^{\frac{1}{3}} \approx 7.24$

c) In the following results for $\alpha = 8$ are shown. As we mentioned above taking larger values of α leads to faster occurrence of bifurcations. In this example we see these phenomena already for $R_0 = 1.32$ and for $R_0 = 1.4$ we obtain periodic solution with double-humped peaks (see Figure 4.17). Consequently for this value of R_0 another complex-conjugate pair of roots crosses the imaginary axis and a second peak occurs.

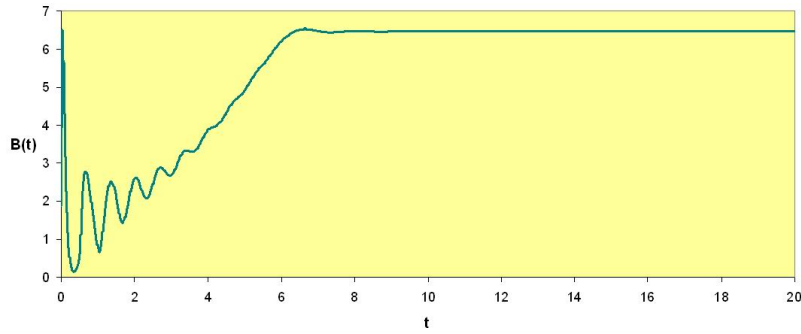


Figure 4.14: $R_0 = 1.2, B^* = 8 \ln(1.2)^{\frac{1}{8}} \approx 6.47$

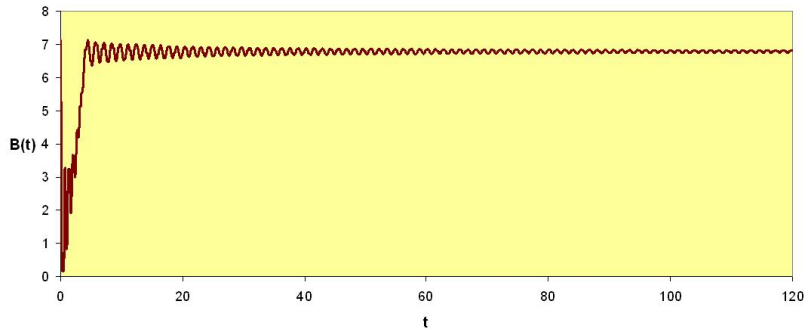
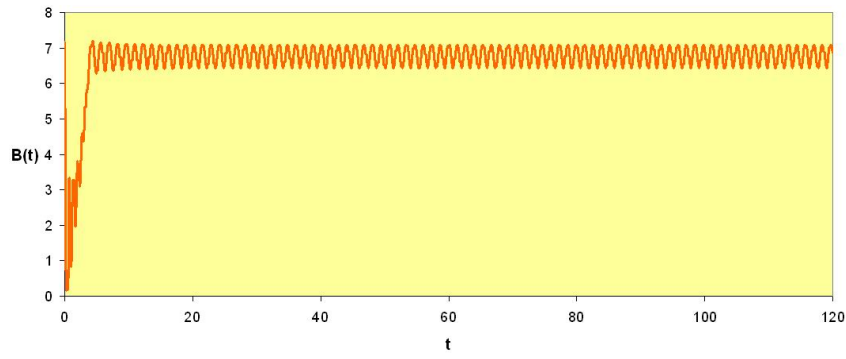
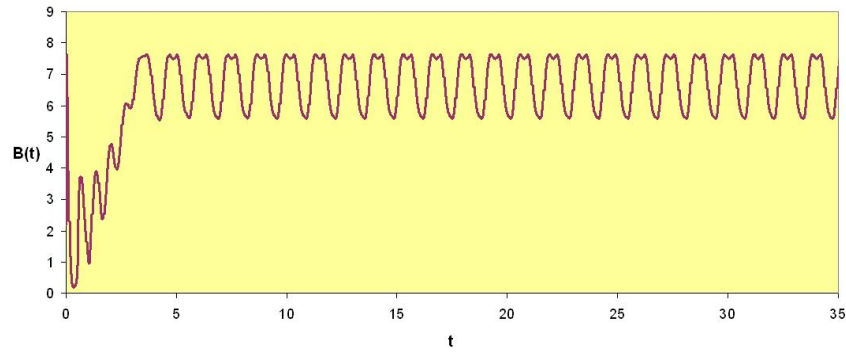


Figure 4.15: $R_0 = 1.31, B^* = 8 \ln(1.31)^{\frac{1}{8}} \approx 6.79$


 Figure 4.16: $R_0 = 1.32, B^* = 8 \ln(1.32)^{\frac{1}{8}} \approx 6.82$

 Figure 4.17: $R_0 = 1.4, B^* = 8 \ln(1.4)^{\frac{1}{8}} \approx 6.98$

The last example we show results for is presented in [44].

Example 4 The following data are given

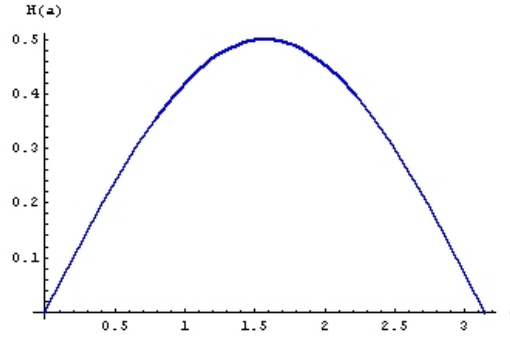
$$\phi(x) = e^{-x^\alpha}, \mu_0(a) = \frac{1}{\pi} - a \Rightarrow \pi_0(a) = \pi - a, \beta_0(a) = \gamma(a) = \frac{\sin(a)}{2(\pi - a)}$$

where the maximum age is $a_+ = \pi$ and the maturation age $a^* = \frac{1}{2}$. Thus, the kernels (4.2.3) take the following form:

$$K(a) = H(a) = \frac{\sin(a)}{2}, \quad a \in [0, \pi]$$

From the figure below one can see that $H(a)$ is concave. Hence, an occurrence of bifurcation could be expected.

In our experiments we consider $\alpha = 8$.



We are again in the case where $B(t) = S(t)$ and the kernels $K(a)$ and $H(a)$ are continuous (i.e. the trivial case, where the application of the numerical algorithms is standard). Obviously the value of τ is the same as in Example 3, i.e. $\tau(R_0) = -\alpha \ln(R_0)$. In [44] it is proved that the bifurcation values of R_0 are given by $R_0^k = e^{\frac{4k^2}{\alpha}}$, $k = 1, 2, \dots$. We want to investigate the behavior of our algorithms, i.e. to check if the bifurcation will occur at the points given above.

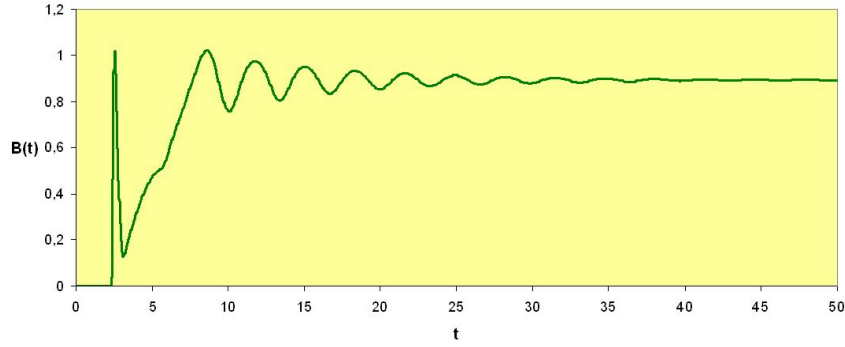


Figure 4.18: $R_0 = 1.5$

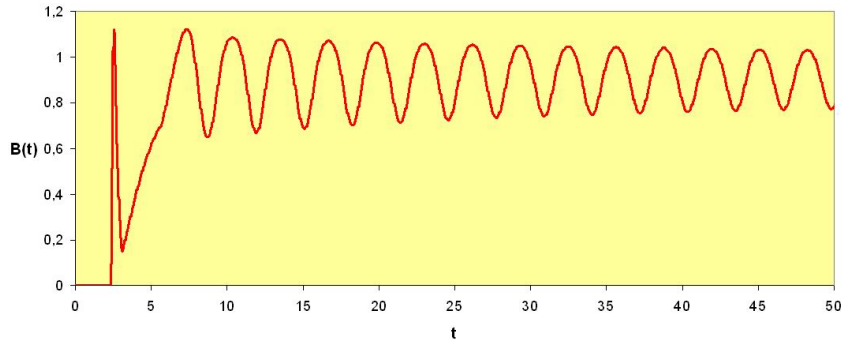


Figure 4.19: $k = 1, R_0^1 = \sqrt{e}$

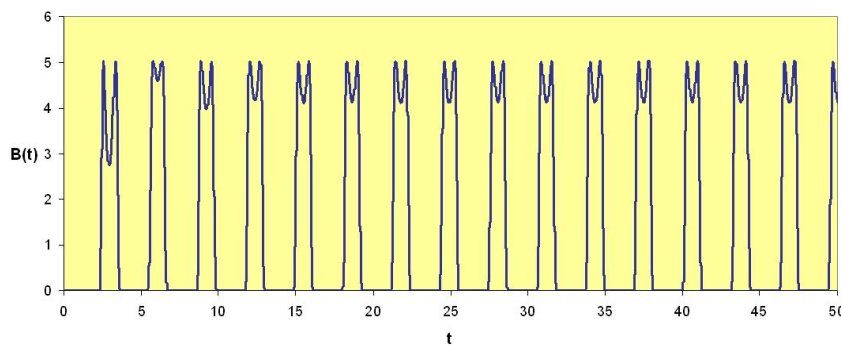


Figure 4.20: $k = 2, R_0^2 = e^2$

The plots above again confirm the good behavior of both algorithms. The bifurcation values given in [44] are accurately reproduced by the numerical approximations and presence of a second root crossing the imaginary axis to the right is shown (see Figure 4.20).

In the following we shall compare the numerical efficiency of both algorithms. We report results for the case with discontinuous kernels. N is the number of mesh nodes in time and we have chosen $\text{tolerance} = 10^{-5}$ for the iterative procedure we use in both schemes. The CPU time is shown in seconds.

Table 19: Efficiency of the schemes; $T=10, R_0 = 2$		
N	$CPU_{\text{Along characteristics}}$	$CPU_{\text{Trapezoidal rule}}$
200	0.034	0.028
400	0.13	0.09
800	0.31	0.21
1000	0.36	0.27

What we can see from Table 19 is that the Trapezoidal rule applied to the integral reformulation (1.2.6) of the Logistic Growth model is a bit faster than the first order method along characteristics. This result is not surprising since the leading equation in (1.2.5) is linear and thus the corresponding system of integral equations is not that complicated (compare (1.2.6) and (1.2.8)), i.e. in (1.2.5) we solve two-variables problem and in (1.2.6), the same problem is rewritten in integral form (which is comparatively simple for numerical approximation) and it is reduced to one-variable problem. Thus, the calculations are performed faster. However, it would be misleading to say that the methods for the integral reformulation of the discussed model are better than the methods along characteristics that can be developed for (1.2.5). Our aim here is not to give a "recipe" for "the best method", but to study the behavior of different schemes and to see how "good" it is. As we already mentioned both algorithms showed very similar behavior which was in a very good agreement with the analytical results. Hence, we can conclude that both schemes are good.

In the model of Logistic Growth discussed above, we considered density independent (but age-dependent) mortality rate and we could observe both - population in equilibrium phase and in fluctuation phase. This is a phenomenon extensively discussed within population theories. Experimental data exhibit oscillations that an ODE model cannot reproduce. The age structured models we have considered show that age structure may provide an explanation of such oscillatory behavior. When a population is part of a community which provides for the recycling and renewal of resources and which exerts density dependent population controls, the result is an S-Curve in which population growth decelerates and establishes an equilibrium related to the carrying capacity of the ecosystem. Point (A) represents the lag phase in which growth proceeds slowly due to the initially small population. As the progeny of those individuals begin to reproduce the population enters the acceleration phase (B) and soon the population growth enters the exponential phase (C). Exponential growth cannot occur for long before environmental resistance takes over and either produces a population crash (F) or the deceleration phase (D), which leads to an equilibrium (E). The equilibrium is the point at which there is a stable balance between the increases to the population from births and the decreases due to deaths. The equilibrium may be only short-lived giving way to repeated fluctuations with changes in birth rates and death rates (G). These fluctuations occur around a carrying capacity. The carrying capacity is the population density which the ecosystem can support.

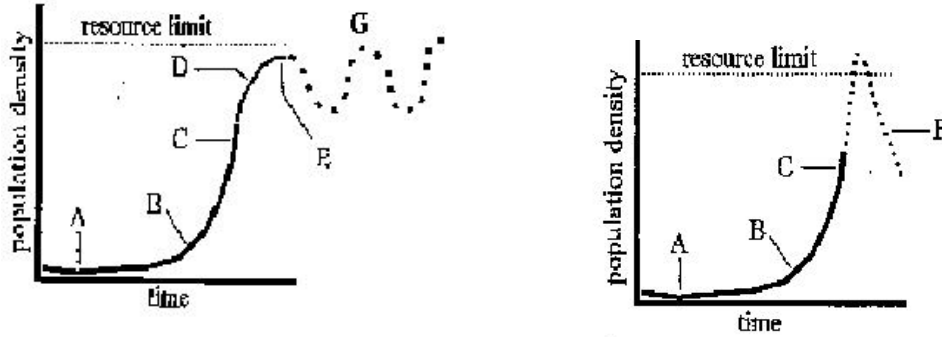


Figure 4.21: S-Curve and J-Curve

We proved experimentally that the approximate solution generated by the algorithms applied to models (4.2.1) and (1.2.6) reproduces accurately the changes in the qualitative behavior of the analytical solution. Our expectations are that these methods will work good also in case of density dependent fertility and mortality functions. We leave the convergence results for the method along the characteristic lines to future development. The reader is referred to [79] and [80], where stability results for a sample Volterra integral equation with double delay is studied and conditions under which the trapezoidal quadrature method is stable are shown.

4.3. Numerical Approximation of a Model of Cannibalism

In this Section we study the model of Cannibalism (1.2.7). We present two numerical methods, namely Runge-Kutta explicit second order method and the Box method which is of same order but implicit. We make an investigation regarding the presence of bifurcations of the nontrivial steady state and we show different results. We do not propose numerical methods for the integral reformulation (1.2.8) of this model since they are subject to further developments. Some of the results presented in the current Section were obtained in collaboration with Mimmo Iannelli, Giuseppe Izzo, Eleonora Messina, Elvira Russo and Antonella Vecchio [88].

We first rewrite (1.2.7) in the following equivalent form

$$\begin{cases} \frac{\partial u(a, t)}{\partial t} + \frac{\partial u(a, t)}{\partial a} + m_1 \chi_{[0, a^*]}(a) A(t) u(a, t) = 0, & a, t > 0 \\ u(0, t) = R_0 \int_0^{a_+} \beta_0(a) \pi_0(a) u(a, t) da, & t > 0 \\ u(a, 0) = \frac{p_0(a)}{\pi_0(a)}, & a > 0 \\ A(t) = \int_{a^*}^{a_+} \pi_0(a) u(a, t) da, \end{cases} \quad (4.3.1)$$

where we made the following substitution $u(a, t) = \frac{p(a, t)}{\pi_0(a)}$. We assume that $\mu_0(a), \beta_0(a)$ and $\pi_0(a)$ are either smooth or piecewise smooth functions on $[0, a_+]$. We want the following condition

$$\int_0^{a_+} \beta_0(a) \pi_0(a) da = 1 \quad (4.3.2)$$

and (1.1.4) to be satisfied. Under these assumptions it is shown in [44] that the bifurcation graph of this model is similar to the one of the Logistic growth, i.e. if $R_0 < 1$ there is only one equilibrium and it is the trivial one, which is stable, while if $R_0 > 1$, there exists a unique nontrivial equilibrium, which stability depends on the roots of the respective characteristic equation, which equation (in case of model of Cannibalism) is not known in an explicit form (see [44] for details) and the trivial steady state is unstable. Since the application of the second order Runge-Kutta method and the Box method that we use in this case is analogous to the application of these methods to the equation with the Age profile (see Section 2.3), we shall omit the details. A more particular case is when the kernel $K(a) = \beta_0(a) \pi_0(a)$ is discontinuous and we should take the point of discontinuity as a mesh node. Then we present the boundary condition as a sum of two integrals, namely $R_0 \int_0^{a_+} \beta_0(a) \pi_0(a) u(a, t) da = R_0 \int_0^{a^*} K_1(a) u(a, t) da + R_0 \int_{a^*}^{a_+} K_2(a) u(a, t) da$, where a^* is the point of discontinuity and we apply for example the composite trapezoidal rule (as its order of convergence is compatible with the one of the Runge-Kutta and Box methods)

to both integrals.

Let us now discuss the following example:

Example 1 We consider specific vital rates, namely

$$\beta_0(a) = \begin{cases} 0, & a \leq a^* \\ 8, & a \geq a^* \end{cases} \quad \mu_0(a) = \frac{1}{a_+ - a} \Rightarrow \pi_0(a) = a_+ - a,$$

where for simplicity we assume the maximum age $a_+ = 1$ and the maturation age $a^* = \frac{1}{2}$. It is clear that in such a way we take into consideration the fact that only mature individuals can reproduce. Thus, the kernel $K(a)$ takes the following form:

$$K(a) = 8(1 - a)\chi_{[\frac{1}{2}, 1]}(a), \quad a \in [0, 1]$$

The respective steady state equation is given by

$$u^*(a) = \begin{cases} \frac{2R_0 \ln(R_0) e^{-\frac{\ln(R_0)a}{a^*}}}{m_1(1 - a^*)^2 a^*}, & a \leq a^* \\ \frac{2 \ln(R_0)}{m_1(1 - a^*)^2 a^*}, & a \geq a^* \end{cases}$$

Remark: We want to underline that from the formula above for $a = 0$ we obtain B^* , which is the stationary solution of equation (1.2.8).

It is clear that for $m_1 > 0$ we have a positive solution only when $R_0 > 1$ and for $R_0 \leq 1$ we have only the trivial solution. We shall study numerically how the birth rate $B(t)$, the adults $A(t)$ and the juveniles $J(t)$ change in time, when we vary the parameters R_0 and m_1 .

We show in figures 4.22, 4.23 and 4.24 how the birth rate $B(t)$ changes when changing the net reproduction ratio. When R_0 is small, $B(t)$ is comparatively small too. The birth rate has an oscillatory behavior but the oscillations die away and it approaches its steady state. Increasing the value of R_0 , $B(t)$ also increases and powerful oscillations occur. However, their amplitude decreases with time and they are dumped (figure 4.23). However, for $R_0 = 20$ we already see sustained oscillations and an occurrence of stable periodic solution.

On the next three figures (4.25, 4.26 and 4.27) we show respectively how the total population $S(t)$, the adults $A(t)$ and the juveniles $J(t)$ "behave" when the net reproduction ratio is equal to 20. We see that the juveniles oscillate in the same way as the total population does while the adults, as the birth rate. The amplitude of the oscillations that appear in the adult population is larger than the amplitude of the oscillations of the juveniles. We also notice that even when the coefficient of attack m_1 is relatively low the adult population is much smaller than the

juvenile population (otherwise the whole population would tend to extinction). The oscillations of the birth rate are around the steady state B^* and we can conjecture that the oscillations of the total, adult and juvenile populations respectively are around their steady states too.

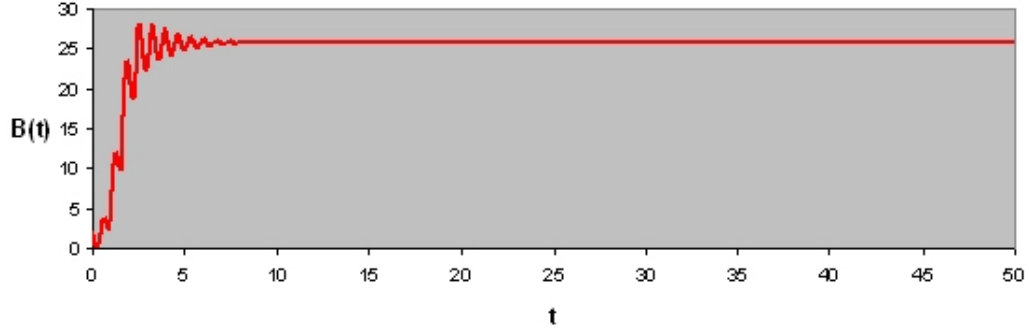


Figure 4.22: $m_1 = 5, R_0 = 5, B^* \approx 25.75$

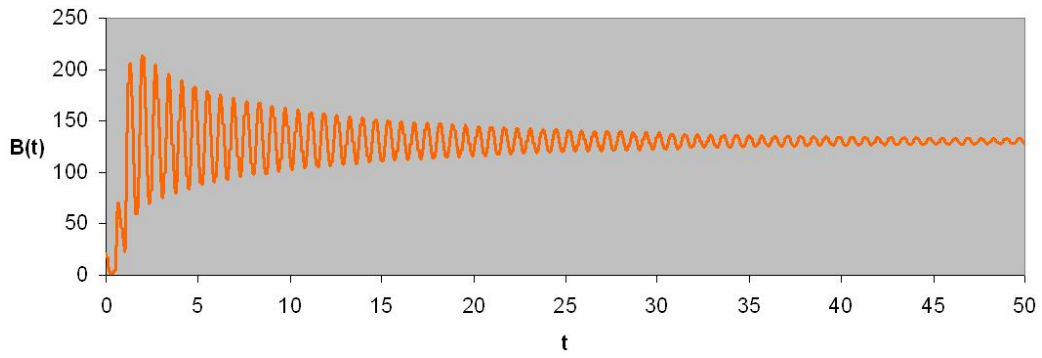


Figure 4.23: $m_1 = 5, R_0 = 15, B^* \approx 129.98$

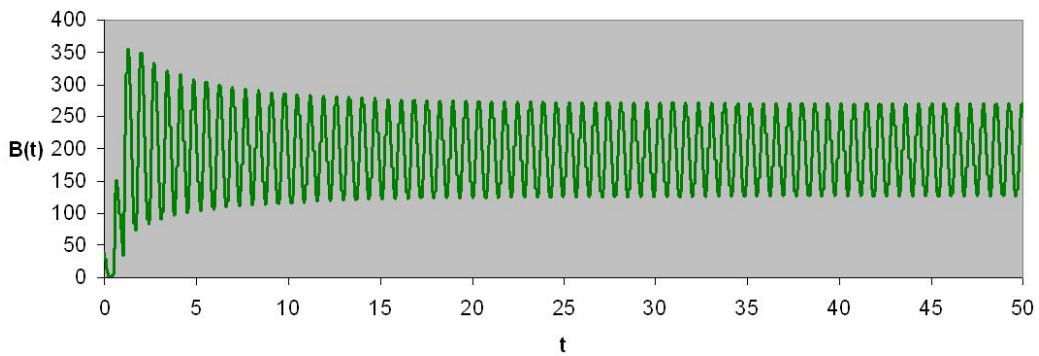
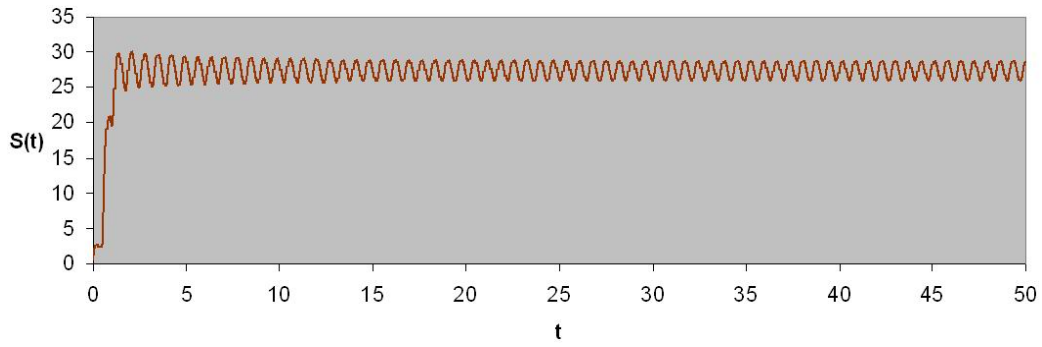
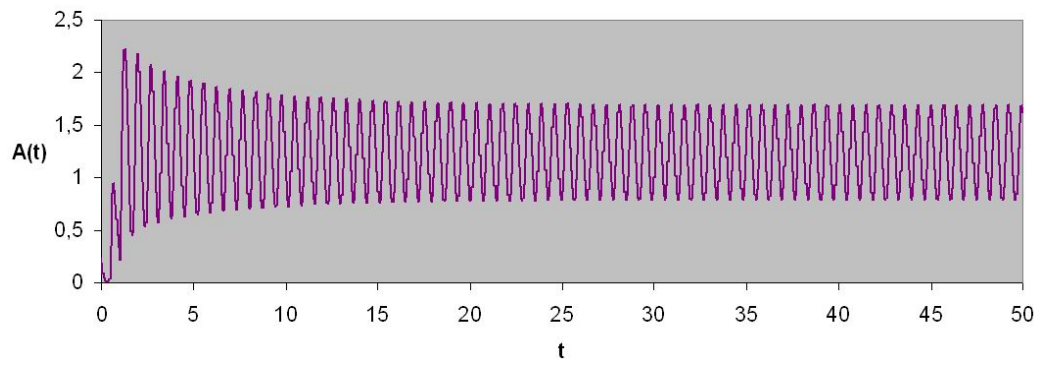
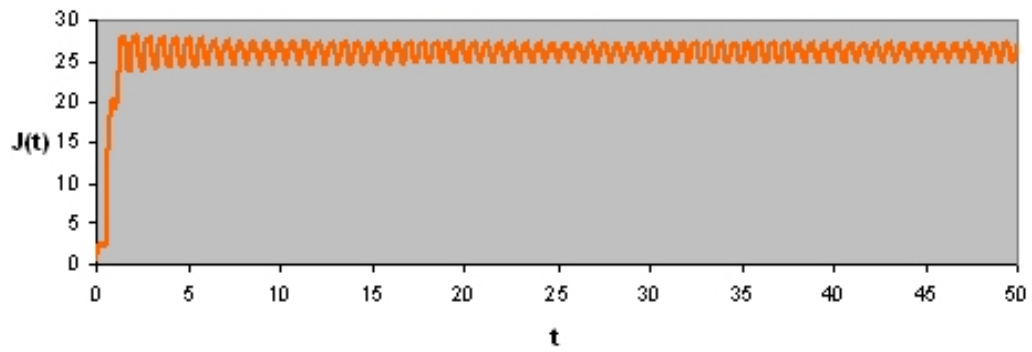


Figure 4.24: $m_1 = 5, R_0 = 20, B^* \approx 191.73$

Figure 4.25: $m_1 = 5, R_0 = 20$ - Total PopulationFigure 4.26: $m_1 = 5, R_0 = 20$ - AdultsFigure 4.27: $m_1 = 5, R_0 = 20$ - Juveniles

Increasing the value of m_1 to 32 and 64, we see that for the same value of R_0 the birth rate decreases (compare figures 4.23 and 4.28; 4.22 and 4.29). We also see that the oscillations for $m_1 = 5, R_0 = 5$ vanish faster than for $m_1 = 64, R_0 = 5$.

When both parameters m_1 and R_0 are large the birth rate is bigger than the corresponding

birth rate for large m_1 and small R_0 (figures 4.29 and 4.30) and it is smaller than the respective birth rate for small m_1 and large R_0 (figures 4.24 and 4.30). In the case when both m_1 and R_0 are large, namely $m_1 = 100$ and $R_0 = 50$, the total population is much smaller than in the case $m_1 = 5$ and $R_0 = 20$, since the coefficient of attack is very high.

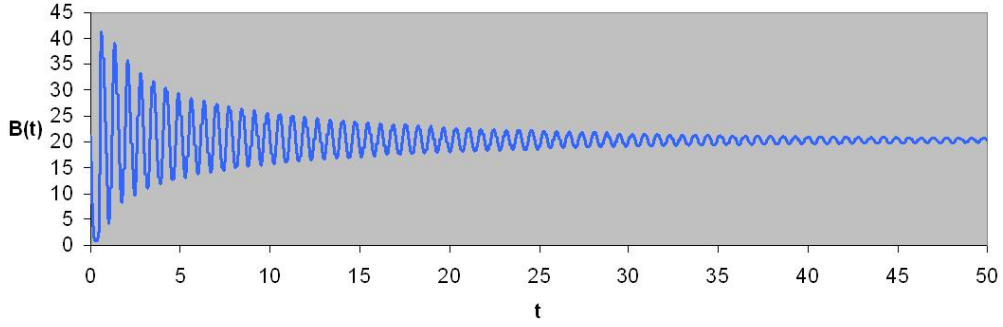


Figure 4.28: $m_1 = 32, R_0 = 15, B^* \approx 20.31$

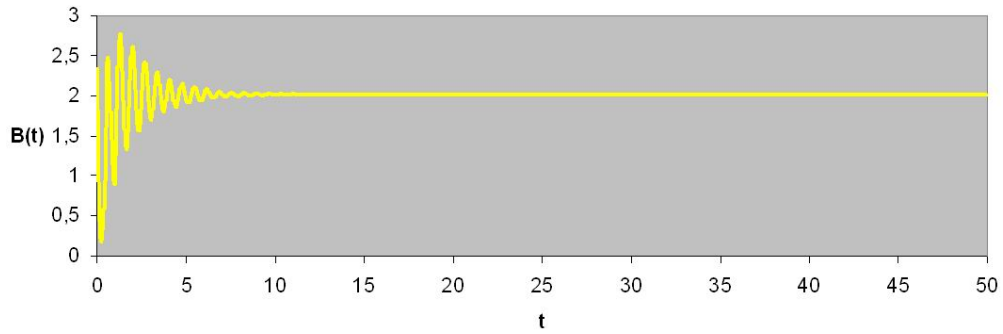


Figure 4.29: $m_1 = 64, R_0 = 5, B^* \approx 2.01$

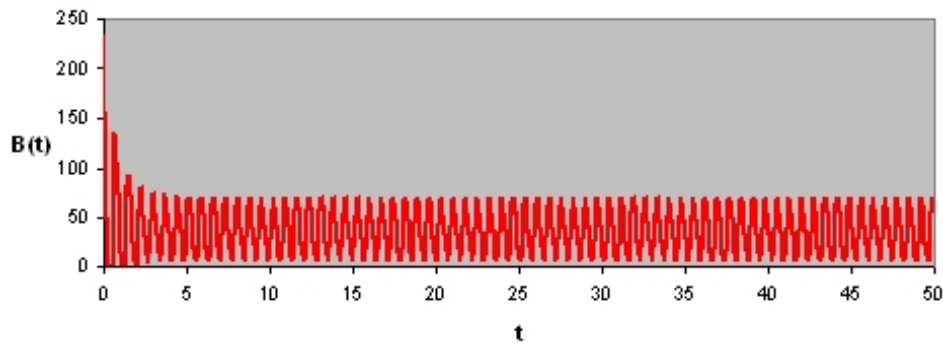
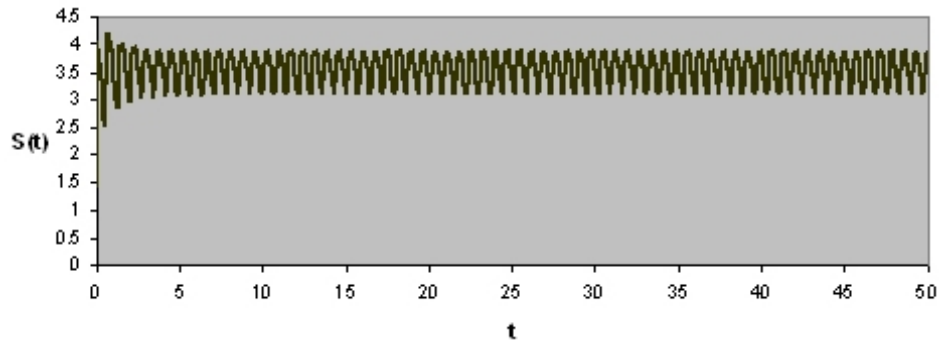
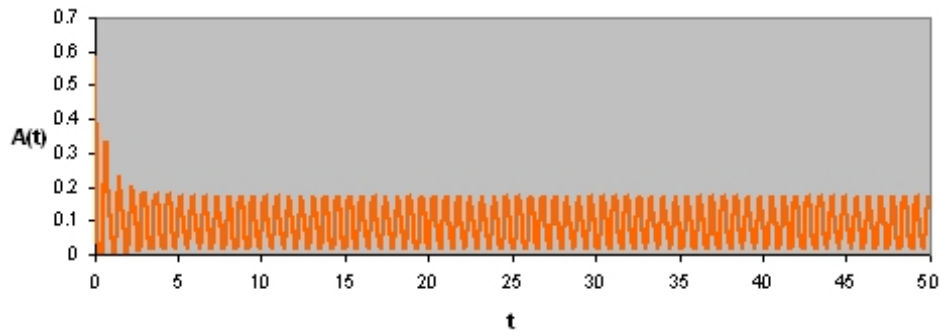
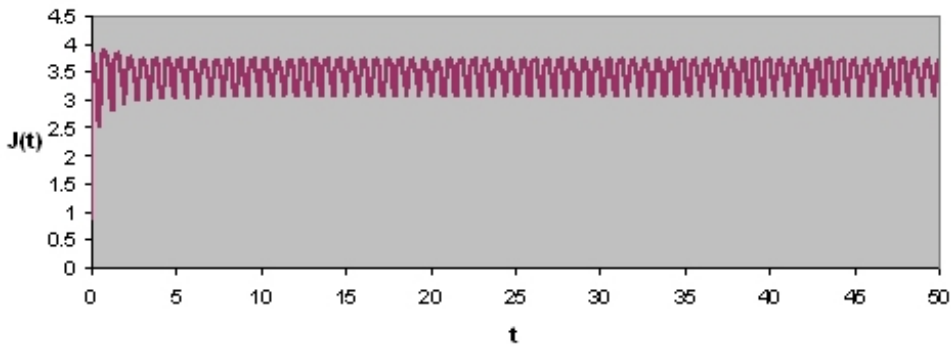


Figure 4.30: $m_1 = 100, R_0 = 50, B^* \approx 31.30$

Figure 4.31: $m_1 = 100, R_0 = 50$ - Total PopulationFigure 4.32: $m_1 = 100, R_0 = 50$ - AdultsFigure 4.33: $m_1 = 100, R_0 = 50$ - Juveniles

Another interesting observation is that in neither of the cases we showed, we could see double-humped oscillations (as in the model of Logistic Growth). The reason for this fact could be that only one root crosses the imaginary axis to the right, but this is a pure conjecture and we cannot be certain since a complete study of the characteristic roots of the model of Cannibalism is not done yet.

CHAPTER 5

FUTURE RESEARCH

In this chapter we show some possible future developments of the present work. We point out several important open issues that are worthy to be investigated and we outline an exemplary plan for their further treatment.

1. **Proving convergence of the Modified STS algorithm for the linear and the nonlinear problems with Neumann boundary conditions.**

Even though a good experimental evidence of the convergence of the method when applied to these models is done, one can use the ideas given in Chapter 2 in order to prove convergence of the method analytically. We have to point out that the models with Neumann conditions on the boundary are much more natural than the model with Dirichlet boundary conditions and hence, it is worthy more attention to be paid to them.

2. **Considering models with age and/or time dependent coefficient of diffusion.**

Since we deal with age-structured populations and we are interested how these populations develop in time, it is apparent that the age and the time variables should be taken into account when considering the diffusion coefficient. Hence, more realistic models could be proposed and treated.

3. **Considering diffusion in Gurtin-MacCamy's equation and its special cases.**

As it was mentioned above our aim is to study realistic models, which accurately describe the behavior of a given population. This means that we have to deal with nonlinear models, since the linear ones do not show correctly the growth of the population in a long time interval. Since the motion (spreading) is inherent property of many living creatures it should properly be included into the nonlinear models we consider. The Modified STS scheme could successfully be used for such models since it is a first order scheme and it is

rapidly converging.

4. Trying to accelerate the numerical schemes for the integral equations in the nonlinear case.

An interesting problem would be to try accelerating the numerical schemes for the integral equations in the nonlinear case. If we compare the Volterra integral equation obtained by integrating the Lotka-McKendrick's equation along the characteristic lines and the integral reformulations of the models of Logistic Growth, Cannibalism and Competition respectively, we see that in the linear case we deal with a single integral equation and in the nonlinear one, we obtain a system of integral equations. This system of equations normally results in an algorithm that is more complex to implement and more time consuming (than the respective schemes along the characteristic lines). Thus, it would be a challenge to create stable and fast converging algorithms for such systems of integral equations.

5. Providing a complete investigation of the model of Competition - searching for multiple equilibria and periodic solutions.

In the present work no results were given for the model of Juvenile-Adult competition. Since it is a model that takes account of both - density dependent fertility and mortality, it should be carefully investigated. Moreover, as an analytical evidence of multiple equilibria and existence of periodic solution is already given, it is necessary to study this phenomenon also numerically (as it was done for the models of Logistic Growth and Cannibalism). Such study can be done by using some of methods we applied to the other nonlinear models.

Bibliography

- [1] L.M. ABIA, O. ANGULO AND J.C. LOPEZ-MARCOS: Size-structured population dynamics models and their numerical solutions, *Discrete Contin. Dyn. Syst.*, **B4** (4), (2004), 1203-1222.
- [2] L.M. ABIA AND J.C. LOPEZ-MARCOS: Runge-Kutta methods for age-structured population models, *Appl. Num. Math.*, **17** (1995), 1-17.
- [3] L.M. ABIA AND J.C. LOPEZ-MARCOS: Second order schemes for age-structured population equations, *J. Biolog. Sys.*, **5** (1997), 1-16.
- [4] L.M. ABIA AND J.C. LOPEZ-MARCOS: On the numerical integration of non-local terms for age-structured population models, *Math. Biosc.*, **157** (1999), 147-167.
- [5] V. ALEXIADES: Overcoming the stability restriction of explicit schemes via super-time-stepping, *2nd International Conference on Dynamic Systems and Applications*, (1995), Atlanta.
- [6] V. ALEXIADES, G. AMIEZ AND P-A. GREMAUD: Super-Time-Stepping acceleration of explicit schemes for parabolic problems, *Communications in numerical methods in engineering*, **12** (1996), 31-42.
- [7] O. ANGULO AND J.C. LOPEZ-MARCOS: Numerical schemes for size-structured population equations, *Math. Biosc.*, **157** (1999), 169-188.
- [8] O. ANGULO AND J.C. LOPEZ-MARCOS: Numerical integration of autonomous and nonautonomous nonlinear size-structured population models, *Math. Biosc.*, **177-178** (2002), 39-71.
- [9] O. ANGULO AND J.C. LOPEZ-MARCOS: Numerical integration of fully nonlinear size-structured models, *Appl. Numer. Math.*, **50** (2004), 291-327.
- [10] T. ARBOGAST AND F.A. MILNER: A finite difference method for a two-sex model of population dynamics, *SIAM Num. Anal.*, **26** (1989), 1474-1486.

BIBLIOGRAPHY

- [11] B. AYATI: A variable time step method for an age-dependent population model with nonlinear diffusion, *Siam Journal of Numerical Analysis*, **37** (5) (2000), 1571-1589.
- [12] N.S. BAHVALOV: Numerical methods I, "Nauka" - Moskow (1973), /in russian/.
- [13] C.T.H. BAKER: Runge-Kutta Methods for Volterra integral equations of the second kind, *Lecture Notes in Mathematics*, **630**, Springer Verlag (1978).
- [14] C.T.H. BAKER: A pererspective on the numerical treatment of Volterra equations, *Journal of Computational and Applied Mathematics*, **125** (2000), 217-249.
- [15] T.H. BARR: Approximation for age-structured population models, using projection methods, *Comp. Math. Applic.*, **21** (5) (1991), 17-40.
- [16] A. BELLEN, Z. JACKIEWICZ, R. VERMIGLIO AND M. ZENNARO: Stability analysis of Runge-Kutta methods for Volterra integral equation of the second kind, *IMA J. Numer. Anal.*, **10** (1990), 103-118.
- [17] G. DI BLASIO: Non-linear age-dependent population diffusion, *Journal of Math. Biology*, **8** (1979), 265-284.
- [18] D. BREDI, C. CUSULIN, M. IANNELLI, S. MASET AND R. VERMIGLIO: Pseudospectral differencing methods for characteristic roots of age-structured population equations, *Research Report UDMI/02/2004/RR*, Dipartimento di Matematica e Informatica, Università degli Studi di Udine, February 2004.
- [19] H. BRUNNER, E. HAIRER AND S.P. NORSETT: Runge-Kutta theory for Volterra integral equations of the second kind, *Mathematics of Computation*, **39**(159) (1982), 147-163.
- [20] H. BRUNNER, P.T. VAN DER HOWEN: The numerical solution of Volterra equations, *Elsevier Science Publishers B.V.* - Amsterdam (1986).
- [21] S. BUSENBERG AND M. IANNELLI: A class of nonlinear diffusion problems in age-dependent population dynamics, *Nonlinear Analysis, Theory, Methods and Applications*, **7** (5) (1983), 501-529.
- [22] S. BUSENBERG AND M. IANNELLI: A degenerated nonlinear diffusion problem in age-structured population dynamics, *Nonlinear Analysis, Theory, Methods and Applications*, **7** (12) (1983), 1411-1429.
- [23] B. CHARLESWORTH: Evolution in age-structured populations, *Cambridge Studies in Mathematical Biology*, 2nd Edition, **14** (1994).

- [24] C. CHIU: A numerical method for nonlinear age dependent population models, *Differential and Integral Equations*, **3** (1990), 767-782.
- [25] C. CHIU: Nonlinear age dependent population models for prediction of population growth, *Mathematical Bioscience*, **99** (1990), 119-133.
- [26] J. DOUGLAS AND F.A. MILNER: Numerical methods for a model of population dynamics, *Calcolo*, **24** (1987), 247-254.
- [27] J.J. DROUX: Three-dimensional numerical simulation of solidification by an improved explicit scheme, *Comput. Methods Appl. Mech. Eng.*, **85** (1991), 57-74.
- [28] R.E. ELDERKIN: Nonlinear globally age-dependent population models: Some basic theory, *J. Math. Anal. Appl.*, **108** (1985), 546-562.
- [29] G. FAIRWEATHER AND J.C. LOPEZ-MARCOS: A box method for a nonlinear equation of population dynamics, *IMA Journal of Numerical Analysis*, **11** (1991), 525-538.
- [30] G. FAIRWEATHER AND J.C. LOPEZ-MARCOS: An explicit extrapolated box scheme for the Gurtin-MacCamy equation, *Computers Math. Applic.*, **27** (1994), 41-53.
- [31] W. FELLER: On the integral equation of renewal theory, *Ann. Math. Statist.*, **12** (1941), 243-267.
- [32] H. VON FOERSTER: Some remarks on changing populations, *Grune and Stratton*, (1959).
- [33] A. FREDERICKSON: A mathematical theory of age structure in sexual populations: Random mating and monogamous marriage models, *Math. Biosci.*, **20** (1971), 117-143.
- [34] W. GENTZSCH AND A. SCHULTER: On one-step methods with cyclic stepsize changes for solving parabolic differential equations, (German), *Z. Angew. Math. Mech.*, **58**, T415-T416 (1978).
- [35] W. GENTZSCH: Numerical solution of linear and non-linear parabolic differential equations by a time-discretisation of third order accuracy, *Proceedings of the Third GAMM-Conference on Numerical Methods in Fluid Mechanics* - Vieweg and Son (1979), 109-117.
- [36] M. GURTIN: A system of equations for age-dependent population diffusion, *Journal of Theoretical Biology*, **40** (1973), 389-392.
- [37] M.E. GURTIN AND R.C. MACCAMY: Nonlinear age-dependent population dynamics, *Arch. Ration. Mech. Anal.*, **54** (1974), 281-300.

BIBLIOGRAPHY

- [38] M.E. GURTIN AND R.C. MACCAMY: Diffusion Models for Age-Structured Populations, *Math. Biosci.*, **54**, no. 1-2 (1981), 49-59.
- [39] M.E. GURTIN AND R.C. MACCAMY: Product Solutions and Asymptotic Bahavir for Age-Dependent, Dispersing Populations, *Math. Biosci.*, **62**, no. 2 (1982), 157-167.
- [40] A. HARTEN AND S. OSHER: Uniformly high-order accurate nonoscillatory schemes, *SIAM J. Numer. Anal.*, **24**, no. 2 (1987), 279-309.
- [41] F. HOPPENSTEADT: Mathematical Theories of Populations: Demographics, Genetics and Epidemics, *SIAM*, Philadelphia (1975).
- [42] P.J. VAN DER HOWEN, P.H.M. WOLKENFELT AND C.T.H. BAKER: Convergence and stability analysis for modified Runge-Kutta methods in the numerical treatment of second kind Volterra equations, *IMA J. Num. Anal.*, **1** (1981), 303-328.
- [43] H. INABA: Weak ergodicity of population evolution process, *Math. Biosc.*, **96** (1989), 195-219.
- [44] M. IANNELLI: Mathematical theory of age-structured population dynamics, *Giardini editory e stampatori* - Pisa (1995).
- [45] M. IANNELLI, M-Y. KIM AND E.J. PARK: Splitting methods for the numerical approximation of some models of age-structured population dynamics and epidemiology, *Appl. Math. Comput.*, **87** (1997), 69-93.
- [46] M. IANNELLI AND M. MARTCHEVA: A semigroup approach to the well posedness of the two-sex population model, *Dynam. Systems. Appl.*, **6** (1997), 353-370.
- [47] M. IANNELLI, M. MARTCHEVA AND F.A. MILNER: Gender-Structured Population Modeling: Mathematical Methods, Numerics, and Simulations, *SIAM Frontiers in Applied Mathematics*, **FR31** (2005).
- [48] M. IANNELLI AND F.A. MILNER: On the approximation of Lotka-McKendrick equation with finite life span, *Journal of Computational and Applied Mathematics* **136** (2001), 245-254.
- [49] M. IANNELLI AND F.A. MILNER: Age-structured populations, (in preparation).
- [50] M.K. JAIN AND K.D. SHARMA: Numerical solutions of linear differential equations and Volterra's integral equation using Lobatto quadrature formula, *The Computer Journal*, **10**(1) (1967), 101-107.

-
- [51] R. KANNAN AND R. ORTEGA: A finite difference approach to the equations of age-dependent population dynamics, *Numer. Methods in PDEs.*, **5** (1989), 157-168.
- [52] M.-Y. KIM: Galerkin methods for a model of population dynamics with nonlinear diffusion, *Numerical methods for partial differential equations*, **12** (1996), 59-73.
- [53] M.-Y. KIM AND Y. KWON: A collocation method for the Gurtin-MacCamy equation with finite life span, *SIAM J. Numer. Anal.*, **39** (6) (2002), 1914-1937.
- [54] M.-Y. KIM AND E.-J. PARK: An upwind scheme for a nonlinear model in age-structured population dynamics, *Computers Math. Applic.*, **30** (8) (1995), 5-17.
- [55] M.-Y. KIM AND E.-J. PARK: Mixed approximation of a population diffusion equation, *Computers Math. Applic.*, **30** (12) (1995), 23-33.
- [56] M.-Y. KIM AND E.-J. PARK: Long-time behavior of numerical solutions to Gurtin-MacCamy equations by method of characteristics, *preprint*.
- [57] T. KOSTOVA: Numerical solutions of a hyperbolic differential-integral equation, *Computers Math. Applic.*, **15** (1988), 427-436.
- [58] T. KOSTOVA: Numerical solutions to equations modelling nonlinearly interacting age-dependent populations, *Computers Math. Applic.*, **19** (1990), 95-103.
- [59] T. KOSTOVA: An Explicit Third-Order Numerical Method For Size-Structured Population Equations, *Numerical Methods for PDEs*, **19** (2003), 1-21.
- [60] T. KOSTOVA AND N. CHIPEV: A model of the dynamics of intramolluscan trematode-populations: some problems concerning oscillatory behavior, *Computers Math. Applic.*, **21** (1991), 1-15.
- [61] T. KOSTOVA AND M. MARCHEVA: Numerical solutions to the Gurtin-MacCamy equation, *Mathematica Balkanica*, **3** (1989), 264-277.
- [62] T. KOSTOVA AND F.A. MILNER: Nonlinear age-dependent population dynamics with constant size, *SIAM J. Math. Anal.*, **22**, no. 1 (1991), 129-137.
- [63] M. KUBO AND M. LANGLAIS: Periodic solutions for a population dynamics problem with age-dependence and spatial structure, *Journal of Math. Biology*, **27** (1991), 363-378.
- [64] Y. KWON AND C. CHO: Second-order accurate difference methods for a one-sex model of population dynamics, *SIAM J. Numer. Anal.*, **30** (1993), 1385-1399.

BIBLIOGRAPHY

- [65] M. LANGLAIS: Large time behavior in a nonlinear age-dependent population dynamics problem with spatial diffusion, *Journal of Math. Biology*, **26** (1988), 319-346.
- [66] R.W. LEWIS, I. MASTERS AND J.T. CROSS: Automatic timestep selection for the super-time stepping acceleration on unstructured grids using object-oriented programming, *Communications in numerical methods in engineering*, **13** (1997), 249-260.
- [67] P. LINZ: Analytical and Numerical methods for Volterra equations, *SIAM Studies in Applied Mathematics* - Philadelphia (1985).
- [68] L. LOPEZ AND D. TRIGIANTE: A hybrid scheme for solving a model of population dynamics, *Calcolo*, **19** (1982), 379-395.
- [69] J.C. LOPEZ-MARCOS: An upwind scheme for a nonlinear hyperbolic integro-differential equation with integral boundary condition, *Computers Math. Applic.*, **22** (1991), 15-28.
- [70] A.J. LOTKA: The stability of the normal age distribution, *Proc. Nat. Acad. Sci. USA*, **8** (1922), 339-345.
- [71] A.J. LOTKA: Elements of Physical Biology, *Williams and Wilkins*, (1925).
- [72] A.J. LOTKA: The structure of a growing population, *Human Biology*, **3** (1931), 459-493.
- [73] A.J. LOTKA: Analytical Theory of Biological Populations, *Plenum Press*, New York, **8** (1998).
- [74] R.C. MACCAMY: A population model with non-linear diffusion, *Journal of Differential Equations*, **39** (1981), 52-72.
- [75] T. MALTHUS: An Essay on the principle of populations - London (1798).
- [76] M. MARTCHEVA AND C. CASTILLO-CHAVEZ: Diseases with chronic stage in a population with varying size, *Mathematical Biosciences*, **182** (2003), 1-25.
- [77] A.G. MCKENDRICK: Applications of mathematics to medical problems, *Proc. Edinb. Math. Soc.*, **44** (1926), 98-130.
- [78] P. MARCATI AND R. SERAFINI: Asymptotic Behaviour in age dependent population dynamics with spatial diffusion, *Bollettino U.M.I.*, **5** (16-B) (1979), 734-753.
- [79] E. MESSINA, E. RUSSO AND A. VECCHIO: A stable numerical method for Volterra Integral Equations with discontinuous kernel, *RT 308/06*, IAC-CNR, (2006), (submitted).

- [80] E. MESSINA, E. RUSSO AND A. VECCHIO: A convolution test equation for double delay integral equations, *Journal of Computational and Applied Mathematics*, (submitted).
- [81] F.A. MILNER: A numerical method for a model of population dynamics with spatial diffusion, *Computers Math. Applic.*, **19**(4) (1990), 31-43.
- [82] F.A. MILNER: Age structured populations with history dependent mortality and natality, *Calcolo*, **30** (1993), 29-39.
- [83] F.A. MILNER AND T. KOSTOVA: Some examples of nonstationary populations of constant size, *Lecture Notes in Biomathematics*, **92**, Springer Verlag (1991), 219-234.
- [84] F.A. MILNER AND G. RABBIOLO: Rapidly converging numerical algorithms for models of population dynamics, *Journal of Mathematical Biology*, **30** (1992), 733-753.
- [85] G. PELOVSKA AND D. BOYADZHIEV: A finite difference acceleration scheme for a diffusion model of population dynamics, *Lecture Notes in Computer Science*, Springer Verlag (2006), (to be published).
- [86] G. PELOVSKA AND M. IANNELLI: Numerical methods for the Lotka-McKendrick's equation, *Journal of Computational and Applied Mathematics*, **197** (2) (2006), 534-557.
- [87] G. PELOVSKA: An improved explicit scheme for age-dependent population models with spatial diffusion, (submitted).
- [88] G. PELOVSKA AND M. IANNELLI: Numerical exploration of oscillatory behaviour in non-linear age-structured population models, (in preparation).
- [89] A.M. DE ROOS: Numerical methods for structured population models: the escalator boxcar train, *Numer. Meth. Partial Differen. Equat.*, **4**, (1988), 173-195.
- [90] A.A. SAMARSKII AND A.V. GULIN: Stability of Difference Schemes, "*Nauka*" - Moscow (1973).
- [91] F.R. SHARPE AND A.J. LOTKA: A problem in age distribution, *Philos. Mag.*, **21** (1911), 435-438.
- [92] G.D. SMITH: Numerical Solution of Partial Differential Equations, *Oxford University Press* (1969).
- [93] D. SULSKY: Numerical solution of structured population models I. Age structure, *J. Math. Biol.*, **31** (1993), 817-839.

BIBLIOGRAPHY

- [94] G.F. WEBB: Theory of nonlinear age-dependent population dynamics, *Pure and Applied Mathematics*, **89**, Marcel Dekker - New York (1985).